THE UNIVERSITY OF MICHIGAN

INDUSTRY PROGRAM OF THE COLLEGE OF ENGINEERING

VAPOR-LIQUID EQUILIBRIUM BEHAVIOR IN METHANE-HYDROCARBON SYSTEMS

Nicholas W. Prodany

A dissertation submitted in partial fulfillment
of the requirements for the degree of
Doctor of Philosophy in the
University of Michigan
Department of Chemical and Metallurgical Engineering
1967

April, 1967

IP-777

DEDICATED TO MY PARENTS

ACKNOWLEDGMENTS

The author wishes to express his sincere appreciation to Professor G. Brymer Williams, under whose guidance this work was conducted, for his interest in me as a student as well as a person. To Professors D.L. Katz, J.J. Martin, J.E. Powers, and R.E. Sonntag, members of his doctoral committee, the author wishes to express appreciation for their suggestions and encouragement throughout the course of this research.

I would like to express thanks to the staff of the Chemical and Metallurgical Engineering Department of the University of Michigan. Special thanks go to Mssrs. Frank Drogosz, Fanny Bolen, Doug Connell, Al Darling, Pete Severn, and John Wurster.

I especially want to thank Mssrs. E.A. Daniels, A.E. Mather, and A.J. Martin for giving so generously of their time. Sincere thanks go to Miss Doris Carr and Miss Helen Walker for their constant encouragement and help in preparing this manuscript. To Donald and Jennifer Dubois I express my deepest appreciation for making life so meaningful throughout my academic career at the University of Michigan.

Finally, the author would like to thank the following corporations for their most generous support:

The Allied Chemical Foundation for awarding me a fellowship;

The Cities Service Research and Development Company for granting me a fellowship;

The Dow Corning Corporation which donated the silicone fluid; and

The Phillips Petroleum Company for furnishing the pentane isomers used in this research.

TABLE OF CONTENTS

TABLE OF CONTENTS (CONT'D)

LIST OF TABLES

LIST OF TABLES (CONT'D)

LIST OF FIGURES

LIST OF FIGURES (CONT'D)

LIST OF FIGURES (CONT'D)

NOMENCLATURE

English Letters

A	Chromatograph peak areas
A,B	Parameters in van Laar and Margules equation for acitivity coefficient
A_o, B_o a,b,c	Parameters in Beattie-Bridgeman equation of state
A_o, B_o, C_o a,b,c,α,γ	Parameters in Benedict-Webb-Rubin equation of state
A_0, A_1, A_2 A_3, A_4, A_5 A_6, A_7, A_8 A_9	Coefficients for Chao-Seader equation for liquid phase fugacity coefficient
A_2, B_2, C_2 A_3, B_3, C_3 A_4, B_4 A_5, B_5, C_5 A_6, B_6 a,b,k	Parameters for modified Martin-Hou equation of state
a,b	Parameters in Van der Waals' equation of state
a,b	Parameters in Redlich-Kwong equation of state
a,b,c,d,e f,g,h,j	Parameters in Redlich-Dunlop equation of state
a_{ij}	Interaction parameters
a	Activity
B	Second virial coefficient
C	Third virial coefficient
C	Number of components in Gibbs phase rule
c,c'	Chromatograph relative response factors
d	Density
E	Energy

English Letters

F	Number of degrees of freedom in Gibbs phase rule
f	Fugacity
G	Gibbs free energy
H	Enthalpy
H	Henry's law constant
K	Equilibrium vaporization ratio
k	Boltzmann constant
m	Mass
n	Moles
P	Pressure
P	Number of phases in Gibbs phase rule
Q	Partition function
q	Effective molar volume in Wohl's equation
R	Universal gas constant
S	Entropy
T	Temperature
V	Volume
x	Mole fraction in liquid phase
y	Mole fraction in vapor phase
Z	Compressibility
Z	Effective volume fraction in Wohl's equation

Greek Letters (cont'd)

α	Coefficient of thermal expansion
α	Interaction parameter
γ	Activity coefficient
δ	Solubility parameter
η	Interaction parameter
λ	Parameter in Wilson equation
Λ	Parameter in Wilson equation
μ	Chemical potential
ν^{o}	Liquid phase fugacity coefficient
ξ	Volume fraction in Flory-Huggins equation
Φ	Effective volume fraction
ϕ	Vapor phase fugacity coefficient
ω	Acentric factor

Superscripts

V	Refers to vapor phase
L	Refers to liquid phase
-	Refers to a partial quantity, except in the case of an intensive property where it refers to a component in a mixture
o	Refers to vapor pressure of a pure component
o	Reference state
E	Excess property

Subscripts

c	Refers to the critical state
i,j,k,l	Refers to enumerated species

Subscripts (cont'd)

r	Refers to the reduced state
T	Infers total sum
-	Refers to an extensive property on a unit mass or mole basis
Δ	Difference, final minus initial

ABSTRACT

The purpose of this research was to investigate the vapor-liquid equilibrium behavior of methane-pentane binary systems and methane-pentane ternary systems throughout the two-phase region.

Phase equilibrium was obtained in a constant-volume cell equipped with an internal stirrer. Phase compositions were determined by withdrawing small samples of each phase and analyzing them using gas chromatography. Vapor-liquid equilibrium data were obtained for the methane-isopentane binary system at pressures from about 500 psia up to the critical region at temperatures of 160° F, 220° F, and 280° F. Data were obtained for the methane-neopentane binary system for pressures from about 300 psia up to the critical region at temperatures of 160° F, 220° F, and 280° F. Data were obtained for the methane-normal pentane binary system at a temperature of 220° F. The phase behavior of the methane-isopentane-normal pentane ternary system was investigated. Vapor and liquid phase compositions were determined at pressures from about 500 psia up to the critical region at temperatures of 160° F, 220° F, and 280° F. Finally data were obtained for the methane-neopentane-normal pentane ternary system at pressures from 500 psia up to the critical region at a temperature of 160° F.

The experimental data obtained are discussed. Diagrams of pressure versus composition are presented for the binary systems. Diagrams of equilibrium vaporization ratio as a function of pressure

are also presented. For the ternary systems, diagrams of equilibrium vaporization ratios versus pressure are presented. In addition, pressure versus composition and triangular compositions diagrams are included.

An analytical correlation which predicts equilibrium vaporization ratios is presented. Calculated equilibrium vaporization ratios are compared with observed equilibrium vaporization ratios. For the total number of points investigated in this research the absolute average deviation of the predicted equilibrium ratios from the observed ratios is within eight percent. The analytical expression, a modified form of the Chao-Seader correlation,[10] incorporates an empirical correction factor. This factor which is based on the phase behavior of methane in isopentane effectively decreases the predicted methane equilibrium ratios by approximately 20 percent in the critical region. The correlation represents the methane-neopentane binary system with an average absolute deviation of approximately 12 percent.

Finally, a review is presented on methods employed in predicting phase equilibrium behavior.

I. INTRODUCTION

In the absence of experimental data, reliable and accurate methods for predicting phase equilibrium behavior of multicomponent mixtures are of prime importance to the engineer concerned with the design of separation equipment. Two methods for predicting equilibrium ratios which have been widely used by the design engineer in the petroleum industry are the NGAA K-Value Charts[36] and the Kellogg Charts.[27] Both methods have been used with a varying degree of success; however, each method is restricted to mixtures of paraffins, olefins, or combinations thereof.

Since the development of the NGAA Charts and the Kellogg Polyco Charts, much effort has been directed toward the formulation of generalized correlations. A primary approach has been to relate the phase behavior of mixtures to experimentally determined properties of pure components and binary systems which comprise the multicomponent mixture. It would be ideal if such correlations could be related to a small number of well-behaved mathematical functions. No matter how complex, these functions could then be solved with the aid of modern, high speed digital computers. The validity of the assumptions made in deriving these functions, however, can only be ascertained by subjecting them to the test of comparison with experimental results.

A number of experimental investigations have been reported on methane and heavier hydrocarbon mixtures. Katz et al.[24] present an excellent bibliography on such systems. Equilibrium ratio data on the methane-pentane systems are incomplete. Methane, normal

pentane, and isopentane are important, naturally occurring compounds in hydrocarbon mixtures. Neopentane, because of its molecular symmetry, is of theoretical interest to the scientist whose ultimate goal is to correlate macroscopic thermodynamic functions to microscopic properties or intermolecular forces.

Boomer, Johnson, and Piercey[5] have determined compositions and densities of the two-phase region at 25°C and pressures ranging from 35 to 135 atmospheres for a system containing impure methane and a mixture of isopentane and normal pentane.

Sage, Reamer, Olds, and Lacey[50] have experimentally determined the specific volumes of six mixtures of methane and normal pentane for seven different temperatures between 100°F and 460°F at pressures up to 5,000 psia. They have, in addition, determined the compositions of the vapor and liquid phases throughout the two-phase region for several temperatures between 100°F and 340°F and pressures from the vapor pressure of normal pentane to the critical pressure of the mixture.

Experimental work on the methane-isopentane binary system has been reported by Amick, Johnson, and Dodge.[1] They report coexisting phase compositions for temperatures ranging from 160°F to 340°F and pressures from 400 psia to 1,000 psia. Their data, however, show considerable scatter.

No experimental information has been found on the methane-neopentane system. Experimental work related to the pure compound neopentane (2,2 dimethyl propane) has been reported by Beattie, Douslin, and Levine[3] and more recently by Heichelheim, Kobe, Silberberg, and

McKetta.[18] Beattie et al. have measured the vapor pressure of neopentane from 50°C to the critical temperature, 160.60°C, and have studied the compressibility of several isotherms around the critical region in order to locate the critical point. Heichelheim et al. have investigated the compressibilities of neopentane using a standard Burnett apparatus. They have determined compressibility factors between one atmosphere and the vapor pressure at 30°C to 150°C and between one atmosphere and 70 atmospheres at 161.5°C, 175°C, and 200°C.

It is the purpose of this research to improve and extend existing equilibrium vaporization ratio data into the critical region on the methane-isopentane binary system and to determine the compositions of both the vapor and liquid phases throughout the two-phase region for the methane-neopentane binary system. Equilibrium ratio data for each component in the methane-isopentane-normal pentane ternary system and the methane-neopentane-normal pentane ternary system are investigated in order to extend our knowledge on more complex systems of methane in mixtures of pentane isomers.

Finally, these experimental data are used to determine the reliability of a generalized correlation for predicting vapor-liquid equilibrium behavior at pressures up to the critical region.

II. THEORETICAL CONSIDERATIONS

There are essentially two methods of evaluating equilibrium ratios or K values. Equilibrium ratios can be determined experimentally and theoretically. Some of the more basic experimental methods of obtaining equilibrium ratios have been reviewed by Katz et al.[24] and Sage and Reamer[49] and will not be discussed in further detail here. Recently Stalkup and Kobayashi[54a] have utilized gas liquid partition chromotography as a means of obtaining phase equlibirium data. The theoretical aspects of phase equilibria will be reviewed in this section. The difficulties encountered in attempting to obtain analytical solutions to the problem of predicting phase equilibrium behavior at high pressures will also be discussed.

At the outset we give the Gibbs Phase Rule. The relationship, first stated by Gibbs,[15] is written symbolically as

$$F + P = C + 2 \qquad (1)$$

where F = degrees of freedom, C = number of components, and P = number of phases.

The derivation of Equation (1) is given by L. O. Case[9] and will not be repeated here. In the present research, the number of phases is always equal to two, namely the liquid and vapor phases. Accordingly, Equation (1) reduces to:

$$F = C \qquad (2)$$

In other words, Equation (2) states that the number of intensive variables needed to completely define the two-phase equilibrium system is equal to the number of components in that system.

For a closed system at equilibrium, Gibbs has shown that the change in free energy at constant temperature and pressure is equal to zero. Expressed in equation form,

$$dG = 0 \qquad \text{at constant } T, P. \tag{3}$$

We can write the free energy relation for each phase as

$$dG^V = -S^V dT + V^V dP + \sum_i \mu_i^V dm_i^V \tag{4a}$$

$$dG^L = -S^L dT + V^L dP + \sum_i \mu_i^L dm_i^L \tag{4b}$$

At constant temperature and pressure, Equations (4) reduce to

$$dG^V = \sum_i \mu_i^V dm_i \tag{5a}$$

$$dG^L = \sum_i \mu_i^L dm_i \tag{5b}$$

where superscripts V and L refer to the vapor and liquid phases, respectively. Since free energy is an extensive property, the total free energy (denoted by G) of the entire system is given by the sum of the free energies of the two constituent phases under consideration. We write this mathematically as:

$$G = G^V + G^L \tag{6}$$

Differentiation of Equation (6) and the condition imposed by Equation (3) yields

$$dG = dG^V + dG^L = 0 \tag{7}$$

Adding Equation (5a) and (5b) and equating the sum to zero, as in Equations (3) and (7), gives

$$\mu_1^V \, dm_1^V + \cdots + \mu_i^V dm_i^V + \cdots + \mu_N^V \, dm_N^V + \mu_1^L \, dm_1^L + \cdots + \mu_i^L \, dm_i^L + \cdots + \mu_N^L \, dm_N^L = 0 \tag{8}$$

Since the system under consideration is a closed system, the total mass of any constituent in the system remains constant, which permits writing

$$dm_i^V + dm_i^L = 0 \tag{9}$$

Equations (8) and (9) imply the necessary and sufficient condition that

$$\bar{\mu}_i^V = \bar{\mu}_i^L \tag{10}$$

where the superscript bar refers to the fact that component i is in a mixture. The verbal formulation of Equation (10) is that the chemical potentials of each constituent are the same in all phases.

The fugacity of a component i in a mixture is defined as:

$$d\bar{\mu}_i = RT \, d \ln \bar{f}_i \tag{11}$$

Integration of Equation (11) and substitution of the result into Equation (10) give the general equation

$$\bar{f}_i^V = \bar{f}_i^L \tag{12}$$

Equation (12) states the fugacity of component i in a multicomponent mixture in the vapor phase equals the fugacity of that same component in the liquid phase at constant temperature and pressure. Equation (12)

is then the basic equation of phase equilibrium thermodynamics. However, this equation cannot be successfully applied unless one knows the following functional relationships:

$$\bar{f}_i^{\,v} = \phi_v\left[P, T, \cdots y_i^{v}, y_j^{v} \cdots\right] \tag{13a}$$

$$\bar{f}_i^{\,L} = \phi_L\left[P, T, \cdots x_i^{L}, x_j^{L} \cdots\right] \tag{13b}$$

That is, for each phase one must express the functional form of the fugacity of component i in a multicomponent mixture in terms of temperature, pressure, and composition.

The ultimate goal of phase equilibrium thermodynamics then is to establish relationships between thermodynamic functions, such as fugacity, and microscopic particle behavior for which the intermolecular forces are unknown quantities. This necessarily suggests the evaluation of the partition function Q, defined as:

$$Q = \sum \exp\left[E_i / kT\right] \tag{14}$$

where E_i equals the energy of each of the possible states of the system. Hirschfelder, Curtiss, and Bird[22] show how the virial equation of state may be developed from the statistical thermodynamical relation between the pressure and the partition function. The range of validity of the virial equation of state is limited, however, by the convergence of the series expansion. The series expansion diverges in the liquid region. The primary value of the virial equation of state lies in the regions of low density gases and gases under moderate pressures.

The problems involved in establishing a model relating macroscopic thermodynamical functions, such as fugacity, that are valid up

to the critical point of a multicomponent mixture to the molecular properties of a system are formidable. In fact, it is unlikely that statistical thermodynamics alone will be used to predict phase behavior for a long time.

In the next section a review is given of the techniques, based on classical thermodynamics, utilized in calculating the fugacities of components in both vapor and liquid phases in equilibrium.

III. METHODS OF PREDICTING PHASE EQUILIBRIA

As stated in Chapter II, the ultimate goal of phase equilibrium thermodynamics is to relate the fugacity of each component in each phase of a multicomponent mixture to the microscopic particle behavior of molecules comprising the system. In view of the level of sophistication required in the treatment of such a problem , engineers have sought solutions to this problem which require a lesser degree of sophistication and, as a natural consequence, have produced solutions which are fruitful but only approximate in light of the necessary and simplifying assumptions.

A realistic goal, however, would be to relate experimental results to some mathematical functions, preferably simple ones, with a small number of constants to allow for the smoothing and interpolation of experimental data. Naturally, these mathematical functions would be based on as much of a theoretical foundation as possible to insure generality. With the aid of modern digital computers, such relations would be desirable from an engineering standpoint because attempts could be made to generalize the experimental results to such a degree that behavior of previously investigated systems, or even new systems which were not previously investigated at all, could be predicted.

The content of subsequent subsections in this chapter is intended to familiarize the reader with some of the methods of predicting vapor-liquid equilibrium behavior. The advantages and limitations of the various methods presented are discussed. The pertinent equations and parameters in conjunction with the correlation used in this work are considered in Chapter IX. Some equations used in Chapter IX are first developed in this chapter.

Early attempts to predict phase behavior were dictated by the immediate needs of the petroleum industry. In the early part of the Twentieth Century, when the petroleum industry first sought methods of predicting equilibrium ratios, the logical solution to the immediate problem was a combination of Raoult's Law and Dalton's Law, which in mathematical formulation is given simply by Equation (15).

$$K_i = \frac{y_i}{x_i} = \frac{P_i^{\circ}}{P} \tag{15}$$

In other words, the equilibrium ratio of component i is a function of the system temperature, pressure, and component identity, but not a function of concentration. Also, Equation (15) neglects the effects of pressure on the behavior of the component in the liquid and vapor phases.

It can readily be shown from classical thermodynamics for a pure component that fugacity is related to pressure, volume, and temperature by the following relationship:

$$\ln \frac{f_i^v}{P} = \int_0^{P_r} \frac{Z-1}{P_r}\, dP_r \tag{16}$$

Graphical integration of the right hand side of Equation (16) at constant temperature yields ratios of fugacity to pressure. Indeed, generalized plots of fugacity-pressure ratios as a function of reduced temperature and pressure have been made. Naturally these plots are as valid as the Z charts on which they are based. For mixtures, the generalized fugacities are combined with the famous Lewis and Randall Rule.[32] For an equilibrium mixture then,

$$K_i = \frac{y_i}{x_i} = \frac{f_i^L}{f_i^v} \tag{17}$$

Note that Equations (15) and (17) are quite similar. The significant difference is that the fugacities partially correct for the deviations of the vapor phase from the ideal-gas law. The most important methods using the generalized fugacity concept were those of Lewis and Luke[31] and Souders, Selheimer, and Brown.[54] These methods are basically the same and differ primarily by the extrapolation methods used in defining the hypothetical standard states. Both methods are an improvement over the Dalton-Raoult Law method in that they partially correct for the pressure effect on the equilibrium ratio; however, the effect of composition is still largely neglected.

In general, the equilibrium vaporization ratio K_i of component i is dependent upon pressure, temperature, and composition of both phases. The dependencies can be calculated if the pressure-volume-temperature (hereafter referred to as P-V-T) behavior is known over the entire concentration range. Because of the great shortage of P-V-T data for mixtures of interest, a great amount of effort has been expended in expressing phase behavior of mixtures in terms of pure component properties.

There have been essentially two approaches to this problem. The first approach has been a purely empirical one based on available experimental results. The second approach is semi-empirical in nature, the main ingredient of which is an equation of state. The primary advantage of empirical methods is the relative simplicity and the mitigation of trial-and-error requirements. The convergence pressure technique is perhaps the most famous example of the empirical approach.

A. Convergence Pressure

The concept of convergence pressure was perhaps first suggested by Brown et al.[54] Katz and Kurata[26] suggested the possiblity of predicting the convergence pressure of a multicomponent mixture from an equivalent binary mixture, and much of the experimental work which led to the NGAA convergence pressure charts has been done by Katz and Hachmuth.[25] The pressure at which the equilibrium ratios of each component in a multicomponent mixture appears to approach unity has come to be known as the convergence pressure. For a binary mixture, the convergence pressure is identical with the critical pressure at that temperature. Correlations using the convergence pressure concept have been published by Hadden;[17] the Natural Gasoline Association of America, now called the Natural Gas Processors Association; Rzasa et al.;[48] Winn;[56] Lenoir and White,[30] and Organick.[37a]

B. Method Using an Equation of State

The substitution of fugacity coefficient for fugacity has been found to be convenient in calculations pertaining to gaseous mixtures. The fugacity coefficient, ϕ_i, of component i is defined by

$$\phi_i = \frac{\bar{f}_i^{\,v}}{y_i P} \tag{18}$$

For gaseous mixtures the fugacity coefficient is given by the relationship

$$\ln \phi_i = \int_0^{P_r} \frac{\bar{Z}_i - 1}{P_r}\, dP_r \tag{19}$$

where $\bar{Z}_i$ is the partial molal compressibility factor. For equations

of state explicit in volume, one can calculate the fugacity coefficient from the following relationship:

$$\ln \phi_i = \frac{1}{RT} \int_0^{P_r} \left[\bar{V}_i - \frac{RT}{P_r} \right] dP_r \qquad (20)$$

For equations of state explicit in pressure

$$\ln \phi_i = \frac{1}{RT} \int_{V=V}^{V=\infty} \left[\left(\frac{\partial P}{\partial n_i} \right)_{T,V,n_j} - \frac{RT}{V} \right] dV - \ln Z \qquad (21)$$

is convenient in form to calculate the fugacity coefficient ϕ_i .

Since no satisfactory equation of state exists for liquid mixtures, the relationship between fugacity and composition is generally expressed in terms of the activity coefficient. Hence, for a multicomponent liquid mixture, the fugacity of component i is related to pressure, temperature, and composition as:

$$\bar{f}_i^L = \gamma_i x_i f_i^\circ \qquad (22)$$

Thus, Equations (12), (18), and (22) present a theoretical basis for predicting phase equilibria. The determination and generalization of the activity and fugacity coefficients require mathematical representation in terms of parameters based on pure component properties and interaction parameters.

C. Equations of State

The requirement of a good equation of state is essential in this second approach to predicting phase behavior of multicomponent mixtures at high pressure.

Perhaps the most famous equation of state is that of Van der Waals. Van der Waals' two-constant equation is simply given as

$$P = \frac{RT}{V-b} - \frac{a}{V^2} \tag{23}$$

where the constant a is a measure of the cohesion between molecules and b is proportional to the volumes of the molecules.

The Beattie-Bridgeman[2] five-constant equation is given as follows:

$$P = \frac{RT}{V} + \frac{RTB_o - A_o - Rc/T^2}{V^2} + \frac{aA_o - RTB_o b - RB_o c/T^2}{V^3} + \frac{RB_o bc}{T^2 V^4} \tag{24}$$

and represents experimental data with good reliability up to two-thirds the critical density. At very high pressures, above 200 atmospheres, the Beattie-Bridgeman equation fails.

In the early 1940's the first real attempt was made to predict phase behavior from an equation of state. At that time, Benedict, Webb, and Rubin[4] published their equation of state. Their equation of state is a modified form of the Beattie-Bridgeman equation. The primary goal in their development was an equation to describe the phase behavior of hydrocarbon mixtures of relatively low molecular weight up to two times the critical density. The equation explicit in pressure is written in the following form:

$$P = \frac{RT}{V} + \frac{B_o RT - A_o - C_o/T^2}{V^3} + \frac{bRT - a}{V^3} + \frac{a\alpha}{V^6} + \frac{\frac{c}{V^3}\left(1 + \frac{\gamma}{V^2}\right)e^{-\frac{\gamma}{V^2}}}{T^2} \tag{25}$$

The eight constants B_o, A_o, C_o, b, a, c, α, and γ are functions of the mixture composition and have been empirically evaluated by the following mixing rules:

$$B_o = \left[\sum_i x_i B_{oi}\right] \tag{26a}$$

$$A_o = \left[\sum_i (x_i A_{oi}^{1/2})\right]^2 \tag{26b}$$

$$C_o = \left[\sum_i (x_i C_{oi}^{1/2})\right]^2 \tag{26c}$$

$$b = \left[\sum_i (x_i b_i^{1/3})\right]^3 \tag{26d}$$

$$a = \left[\sum_i (x_i a_i^{1/3})\right]^3 \tag{26e}$$

$$\alpha = \left[\sum_i (x_i \alpha_i^{1/3})\right]^3 \tag{26f}$$

$$c = \left[\sum_i (x_i c_i^{1/3})\right]^3 \tag{26g}$$

$$\gamma = \left[\sum_i (x_i \gamma^{1/2})\right]^2 \tag{26h}$$

In Equations (26), the symbols with the subscript i , i.e. B_{oi} and A_{oi} , refer to numberical constants for pure components. Benedict and his coworkers evaluated these constants for twelve hydrocarbons.

Martin has recently modified the original Martin-Hou[35] equation. The new sixteen-constant equation describes volumetric behavior of compounds up to two and one-half times the critical density. The equation explicit in pressure is given as:

$$P = \frac{RT}{V-b} + \frac{A_2 + B_2 T + C_2 e^{-kT_r}}{(V-b)^2} + \frac{A_3 + B_3 T + C_3 e^{-kT_r}}{(V-b)^3} + \frac{A_4 + B_4 T}{(V-b)^4} + \frac{A_5 + B_5 T + C_5 e^{-kT_r}}{(V-b)^5} + \frac{A_6 + B_6 T}{e^{\alpha V}} \tag{27}$$

Equation (27) has not as yet been applied to mixtures. However, it has represented experimental data up to twice the critical density for pure components with an average deviation of 0.1 percent for Freon compounds.

Redlich and Kwong published their first equation of state in 1949.[45] The equation is of the form

$$Z = \frac{1}{(1-h)} - \frac{(A^2/B)h}{(1+h)} \tag{28a}$$

$$h = \frac{BP}{Z} = \frac{b}{V} \tag{28b}$$

where $$Z = \frac{PV}{RT} \tag{28c}$$

$$A^2 = \frac{a}{R^2 T^{2.5}} \tag{28d}$$

$$B = \frac{b}{RT} \tag{28e}$$

This equation of state contains only two constants and the authors claim satisfactory results above the critical temperature. The justification of such an equation is the degree of approximation obtained by relatively simple methods.

Having acquired some degree of success, Redlich and Dunlop[44] improved upon the original equation of state by introducing a superposition function which they call the deviation function and a third parameter called the acentric factor. The equation

$$Z = Z' - Z'' \tag{29}$$

is simply the old equation of state where Z' is Z in Equation (28a) and the superimposed deviation function is Z" . The form of the deviation function is

$$Z'' = P_r \Big[a\omega^2 (T_r - 1) + (b - c P_c - d T_c^2) P_r + (e + f/P_c) (T_r - 1)^3 - 10^{-6} g P_c P_r^2 (T_r - 1) \Big] \Big/ \Big[T_r^4 + (h - j T_c) T_c P_r^3 \Big] \tag{30}$$

The numerical values of a, b, c, d, e, f, g, h, and j are given by Redlich and Dunlop in their article and will not be repeated here. The acentric factor is the same as Pitzer et al.,[39] and is defined as

$$\omega = \log\left[P_c/P^{\square}\right] - 1.000 \qquad (31)$$

The acentric factor is determined by the vapor pressure $P^{\square}$ at the reduced temperature $T_r = 0.700$ and the critical pressure P_c. Although Equation (29) represents experimental data better than the original equation, no attempt has been made to extend the applicability of Equation (29) to the critical state or liquid region.

Recently Redlich, Ackerman, Gunn, Jacobson, and Lau[43] have improved upon the Redlich-Dunlop equation and have extended its application to the liquid state and vapor pressures. The equation represents the compressibility factor as the sum of a number of terms.

$$Z = Z_0 + Z_1 + \omega Z_2 + L(Z_3 + \omega Z_4) \qquad (32)$$

where

Z = Root of Equation (28)

ω = the acentric factor

L = 1 for liquids; L = 0 for gases

$Z_1 = Z_1 (P_r, T_r)$

$Z_2 = Z_2 (P_r, T_r)$

$Z_3 = Z_3 (P_r, T_r)$

$Z_4 = Z_4 (P_r, T_r)$

Equation (32) has been compared to available phase equilibrium data for mixtures and pure components. The results show that hydrogen, helium, and water are not satisfactorily represented. Also the critical locus of mixtures is not well described.

The virial equation of state is given by the following series expansion:

$$\frac{PV}{RT} = 1 + \frac{B(T)}{V} + \frac{C(T)}{V^2} + \cdots \tag{33}$$

where the second and third virial coefficients are given by:

$$B = \sum_i \sum_j y_i y_j B_{ij}(T) \tag{34a}$$

$$C = \sum_i \sum_j \sum_k y_i y_j y_k C_{ijk}(T) \tag{34b}$$

Several potential functions are available to evaluate the second and third virial coefficients theoretically. In general, the core model of the Kihara potential[28] does a much better job of representing experimental data than the Lennard-Jones potential,[29] in particular where the molecules differ from spheres in geometry.

In summary, empirical equations of state have been developed to represent experimental data to a high degree of accuracy over a limited range; that is, about twice the critical density. The virial equation of state is limited to moderate pressures well below the critical pressure simply because one cannot readily solve for terms higher than the third virial coefficient and the expansion series diverges on approaching the critical region. At moderate pressures, the virial equation of state can be very useful because it does give exact composition dependence.

The empirical equations of state are more flexible than the virial equation of state and readily lend themselves to computer programming; however, no theory exists for mixing rules. That is, all mixing rules are empirical. It appears unlikely that an empirical equation of state will be developed to predict pressure-volume-temperature and composition effects to greater than three times the critical density that can be used with any degree of facility pertaining to the evaluation of the parameters.

D. Activity Coefficients--Non-Ideal Solutions

To account for the non-ideal behavior of liquid mixtures, it is convenient to introduce a thermodynamic function, activity. The concept of activity has the advantage of relating non-ideal behavior from ideal behavior in one factor called the activity coefficient. The activity and activity coefficient are defined as

$$a_i = \gamma_i x_i = \frac{\bar{f}_i^L}{f_i^o} \tag{35}$$

where f_i^o is the reference fugacity. Many integrated forms of the Gibbs-Duhem equation at constant temperature and pressure exist. This equation at constant temperature and pressure is given as

$$\sum_i x_i \, d \ln \gamma_i = 0 \tag{36}$$

The most famous of these are, perhaps, the van Laar and Margules equations. The Carlson and Colburn[8] form of the van Laar two-constant equations for a binary mixture is given as:

$$\ln \gamma_i = \frac{A}{\left[1 + A x_i / B(1-x_i)\right]^2} \tag{37a}$$

$$\ln \gamma_j = \frac{B}{\left[1 + B(1-x_i)/A x_i\right]^2} \tag{37b}$$

The two-constant Margules equation for a binary mixture (given in the Carlson-Colburn modification) are of polynomial form in concentration.

$$\ln \gamma_j = (2A-B)x_i^2 + 2(B-A)x_i^3 \tag{38a}$$

$$\ln \gamma_i = (2B-A)x_j^2 + 2(A-B)x_j^3 \tag{38b}$$

Wohl[57] expressed the molar Gibbs excess free energy as a polynomial in liquid concentration by the expansion

$$\frac{\Delta G^E / n_T}{RT \sum_i q_i x_i} = \sum_{ij} z_i z_j a_{ij} + \sum_{ijk} z_i z_j z_k a_{ijk} + \sum_{ijkl} z_i z_j z_k z_l a_{ijkl} + \cdots \tag{39a}$$

where q_i , q_j , ... are defined as the effective molar volumes of constituents i , j , ... and z_i , z_j , ... are defined as the effective volume fractions of these constituents. The term n_T denotes the total number of moles in the solution. The effective volume fraction of any component i is defined as

$$z_i = \frac{q_i x_i}{\sum_i q_i x_i} \tag{39b}$$

The constants a_{ij} , a_{ijk} , a_{ijkl} are a measure of the interactions of the various components ij, ijk, ijkl comprising the liquid mixture.

Expressions for activity coefficient can be obtained from the thermodynamically rigorous expression:

$$\left[\frac{\partial \Delta G^E}{\partial n_i}\right]_{T,P,n_j} = RT \ln \gamma_i \qquad (40)$$

The activity coefficients for a binary mixture using the three-suffix form of the Wohl equation are:

$$\ln \gamma_1 = Z_2^2 \left[A + 2\left(\frac{Bq_1}{q_2} - A\right) Z_1\right] \qquad (41a)$$

$$\ln \gamma_2 = Z_1^2 \left[B + 2\left(\frac{Aq_2}{q_1} - B\right) Z_2\right] \qquad (41b)$$

Direct comparisons can be made with Wohl's equations and the previously mentioned expressions for activity coefficients. If $q_1/q_2 = 1$, then it follows from the definition of z_1 and z_2 that $z_1 = x_1$ and $z_2 = x_2$ and

$$\ln \gamma_1 = (2B - A) x_2^2 + 2(A - B) x_2^3 \qquad (42a)$$

$$\ln \gamma_2 = (2A - B) x_1^2 + 2(B - A) x_1^3 \qquad (42b)$$

Equations (42a) and (42b) are then the two-constant Margules equation. Alternately, by taking $q_1/q_2 = a/b$, then Wohl's equation reduces to the well known van Laar equations.

The assumption that $q_1/q_2 = 1$ is useful in treating liquid mixtures whose constituent molecules are similar. The mathematical statement that $q_1/q_2 = A/B$ may perhaps be useful in liquid mixtures with highly dissimilar molecules.

Scatchard and Hamer[53] derived equations for activity coefficients. If the effective molar volumes are replaced by the molar volumes of the pure components $\underline{v}_1$ and $\underline{v}_2$, Equations (41a) and (41b) reduce to those developed by Scatchard and Hamer. Obviously the Wohl

equation would represent experimental data better than the three previously mentioned equations. This would be at the expense, however, of evaluating the additional constant q_1/q_2 .

The term excess free energy was originally introduced by Scatchard[51] and is denoted symbolically as ΔG^E . The excess Gibbs energy consists of two excess quantities--that is, an excess enthalpy and an excess entropy:

$$\Delta G^E = \Delta H^E - T\Delta S^E \qquad (43)$$

The assumption that the excess free energy is equal to zero, that is $\Delta G^E = 0$, leads to the concept of an ideal solution. Other less trivial assumptions would be to set either ΔH^E or $\Delta S^E = 0$. Most equations for activity coefficient were derived from Equation (43) using the assumption that $\Delta S^E = 0$ and ΔH^E could be written as a polynomial expansion in mole fraction or volume fraction. The condition that $\Delta S^E = 0$ leads to the concept of regular solutions.[19] The van Laar, Hildebrand and Wood,[21] and Scatchard[51,52] equations are based on this approach.

The regular solution theory of Hildebrand has been used by Chao and Seader in the development of their correlation.[10] The theory is very good for both qualitative and semi-quantitative predictions for non-polar systems such as mixtures of hydrocarbons. Scatchard made the following basic assumptions in his quantitative development of regular solutions:

1) The mutual energy of two molecules depends only on the distance between them and their relative orientation, and not at all on the nature of the other molecules between or around them or on the temperature.

2) The distribution of the molecules in position and in orientation is random; that is, it is independent of the temperature and of the nature of the other molecules present.

3) The change of volume on mixing at constant pressure is zero.

These assumptions allowed Scatchard to formulate a mathematical expression for the "cohesive energy" of a mole of liquid mixture. The "cohesive energy" of a binary mixture is given as:

$$-E_m = \frac{C_{11} V_1^2 x_1^2 + 2C_{12} V_1 V_2 x_1 x_2 + C_{22} V_2^2 x_2^2}{x_1 V_1 + x_2 V_2} \quad (44)$$

where C_{11} is $-E_1/V_1$ and can be defined as the "cohesive energy density" for pure components. For multicomponent systems, Hildebrand and Scott[20] express activity coefficients in regular solutions by the following relation:

$$RT \ln \gamma_i = V_i \left[\delta_i - \bar{\delta} \right]^2 \quad (45a)$$

where the solubility parameter, δ , is defined as the square root of an energy density

$$\delta \equiv \left[\frac{\Delta E_i}{V_i} \right]^{1/2} \equiv \text{Solubility Parameter} \quad (45b)$$

Hildebrand and Wood[21] derived Equation (45a) by integrating the intermolecular potential energies between pairs throughout the liquid by use of continuous radial distribution functions. Equation (45a) will be discussed further in Chapter IX.

The alternate approach to Equation (43) is to assume $\Delta H^E = 0$; this leads to the concept of athermal solutions. This approach is perhaps best exemplified by Flory[14] and Huggins.[23] The Flory-Huggins equation for athermal mixtures is given by

$$\frac{\Delta G^E}{RT} = \sum_i x_i \ln \frac{\xi_i}{x_i} \quad (46a)$$

where x_i = mole fraction and ξ_i = volume fraction of component i. The relation between mole fraction and volume fraction is given simply as

$$\xi_i = \frac{x_i \underline{V}_i^L}{\sum_i x_i \underline{V}_i^L} \tag{46b}$$

where $\underline{V}_i$ is the molar liquid volume of pure component i in the mixture.

Recently Wilson[55] has developed a new equation to describe the variation of activity coefficient with composition. Wilson's equation is a semi-empirical extension of the Flory-Huggins equation. Wilson expresses the excess free energy at constant temperature as

$$\frac{\Delta G^E}{RT} = -\sum_i x_i \ln\left[1 - \sum_j x_j A_{ji}\right] \tag{47}$$

where A_{ij} and A_{ji} are adjustable parameters. Orye and Prausnitz[38] express the Wilson equation in a slightly different form. They present the Wilson equation for excess free energy as

$$\frac{\Delta G^E}{RT} = -\sum_i x_i \ln\left[\sum_j \Lambda_{ij} x_j\right] \tag{48a}$$

where

$$\Lambda_{ij} = \frac{\underline{V}_j^L}{\underline{V}_i^L} \exp -\left[(\lambda_{ij} - \lambda_{ii})/RT\right] \tag{48b}$$

$$\Lambda_{ji} = \frac{\underline{V}_i^L}{\underline{V}_j^L} \exp -\left[(\lambda_{ji} - \lambda_{jj})/RT\right] \tag{48c}$$

The activity coefficients can be found by differentiating Equation (48a) and using the rigorous expression (Equation (40))

$$RT \ln \gamma_i = \left[\frac{\partial \Delta G^E}{\partial n_i}\right]_{T,P,n_j}$$

The resulting activity coefficient for component k is:

$$\ln \gamma_k = -\ln\left[\sum_i x_i \Lambda_{ki}\right] + 1 - \sum_i \frac{x_i \Lambda_{ik}}{\sum_j x_j \Lambda_{ij}} \qquad (49)$$

For binary systems the activity coefficients are:

$$\ln \gamma_1 = -\ln(x_1 + \Lambda_{12} x_2) + x_2\left[\frac{\Lambda_{12}}{x_1 + \Lambda_{12} x_2} - \frac{\Lambda_{21}}{\Lambda_{21} x_1 + x_2}\right] \qquad (50a)$$

$$\ln \gamma_2 = -\ln(x_2 + \Lambda_{21} x_1) - x_1\left[\frac{\Lambda_{12}}{x_1 + \Lambda_{12} x_2} - \frac{\Lambda_{21}}{\Lambda_{21} x_1 + x_2}\right] \qquad (50b)$$

The Wilson equation has several advantages. First, Equations (48) present only binary constants such as Λ_{kj} and Λ_{jk}. Thus, Wilson's model for multicomponent solutions requires only parameters which can be obtained from binary data which comprise the solution. Orye and Prausnitz[38] have shown the Wilson equation to give good representation of a large variety of mixtures of alcohols in non-polar solvents at low pressures. Second, the parameters Λ_{kj} and Λ_{jk} have a "built-in" temperature dependence, such that one may consider $(\lambda_{ij} - \lambda_{jj})$ and $(\lambda_{ij} - \lambda_{ii})$ to be independent of temperature over moderate temperature intervals.

E. Recent Developments

A generalized correlation for the prediction of equilibrium vaporization ratios has been reported by Chao and Seader.[10] The authors claim their correlation is useful for mixtures of paraffins, olefins, naphthenes, and aromatics. Chao and Seader express the equilibrium vaporization ratio K_i in terms of rigorously defined thermodynamic functions. The expression is conveniently given as:

$$K_i \equiv \frac{y_i}{x_i} \equiv \frac{\nu_i^\circ \gamma_i}{\phi_i} \tag{51}$$

The method for evaluating the liquid phase fugacity coefficient ν_i° is based on the Curl and Pitzer[13] modified form of the principle of corresponding states. The vapor phase fugacity coefficient is determined from the Redlich-Kwong equation of state. Finally, the liquid acitivity coefficient is based on Hildebrand's solubility parameters. Chao and Seader state the correlation has been tested with literature data on mixtures including paraffins, olefins, aromatics, and naphthenes They state the overall deviation from 2,696 data points is 8.7 percent. The correlation has several restrictions on pressure and temperature. These are:

1) For hydrocarbons except methane --

reduced temperature:	0.5 to 1.3 based on the pure component critical temperature.
pressure:	up to about 2,000 psia, but not to exceed about 0.8 of the critical pressure of the system.

2) For the light components (hydrogen and methane) --

temperature:	from -100°F to about 0.93 in pseudo-reduced temperature of the equilibrium liquid mixture, but not to exceed 500°F. The pseudo-reduced temperature is based on the molal average of the critical temperatures of the components.
pressure:	up to about 8,000 psia.

Grayson and Streed[16] have extended the temperature range of the Chao-Seader generalized correlation. From new experimental vapor-liquid equilibria data for high temperature (up to 800°F), high pressure

(3,000 psia) hydrocarbon systems, Grayson and Streed have calculated new constants for the liquid phase fugacity coefficient equation. The authors claim the new equation is useful up to 800°F for hydrogen, methane, and heavy hydrocarbons.

More recently, Prausnitz, Eckert, Orye, and O'Connell[41] have presented a monograph on calculations of multicomponent vapor-liquid equilibria using computers. The vapor phase non-idealities are treated in terms of the virial equation of state truncated after the second virial coefficient. The fugacity for the vapor phase is given by Equation (19) where ϕ_i, the vapor phase fugacity coefficient, is solved in terms of the virial equation of state. Prausnitz et al. relate the liquid phase fugacity in terms of pressure, temperature, and composition with the following equation

$$\bar{f}_i^L = x_i \gamma_i f_i^\circ \exp\left[\frac{P \bar{V}_i}{RT}\right] \qquad (52)$$

where γ_i is the pressure independent activity coefficient. Prausnitz[40] defines the reference fugacity for the light component in a multicomponent mixture by the Henry's Law constant.

$$f_i^\circ = \lim_{x_i \to 0} \frac{\bar{f}_i}{x_i} = H \qquad (53)$$

For the heavy component, Prausnitz adopts the usual convention of defining the reference fugacity to be the fugacity of the pure liquid at the temperature of the solution at some specified pressure. The convention of defining the reference fugacity of the light component by Henry's Law constant offers the advantage of using a reference fugacity which can be derived from real as opposed to imaginary physical data and which is

not ambiguous. The disadvantage of such a convention is that it depends not only on the properties of the light component but also depends on the properties of the heavy component.

In order to satisfy the Gibbs-Duhem equation at constant temperature and pressure, Prausnitz adjusts the activity coefficient

$$\left[\frac{\partial \ln \gamma_i}{\partial P}\right]_{x,T} = \frac{\bar{V}_i}{RT} \tag{54}$$

such that it is a function only of composition.

Using these conventions, Prausnitz defines the activity coefficient for the heavy component as

$$\gamma_1^{(P^\circ)} \equiv \frac{\bar{f}_1^{\,v}}{x_1 f_1^{(P^\circ)}} \exp -\int_{P^\circ}^{P} \frac{\bar{V}_1}{RT}\, dP \tag{55a}$$

And the pressure independent activity coefficient for the light component is defined as

$$\gamma_2^{(P^\circ)} \equiv \frac{\bar{f}_2^{\,v}}{x_2 H^{(P^\circ)}} \exp -\int_{P^\circ}^{P} \frac{\bar{V}_2}{RT}\, dP \tag{55b}$$

where

$$\gamma_1^{(P^\circ)} \rightarrow 1 \quad \text{as} \quad x_1 \rightarrow 1 \tag{55c}$$

$$\gamma_2^{(P^\circ)} \rightarrow 1 \quad \text{as} \quad x_1 \rightarrow 1 \quad (x_2 \rightarrow 0) \tag{55d}$$

Prausnitz states the above definitions facilitate the correlation of equilibrium data.

Chueh, Muirbrook, and Prausnitz[11] have expressed the molar excess Gibbs energy by a power series in the effective volume fraction of the solute

$$\frac{\Delta G^E}{RT(x_1 q_1 + x_2 q_2)} = -\alpha_{22}\Phi_2^2 - \alpha_{222}\Phi_2^3 - \cdots \tag{56a}$$

where

$$\Phi_2 = \frac{q_2 x_2}{q_1 x_1 + q_2 x_2} \tag{56b}$$

They then determine the activity coefficients from the relations

$$\left[\frac{\partial n_T \Delta G^E}{\partial n_1}\right]_{T,P,n_2} = RT \ln \gamma_1^{(P,S)} \tag{57a}$$

$$\left[\frac{\partial n_T \Delta G^E}{\partial n_2}\right]_{T,P,n_1} = RT \ln \gamma_2^{*(P,S)} \tag{57b}$$

In contrast with van Laar's assumption that q_1 and q_2 are independent of composition, Chueh et al. assume that q_1 and q_2 are given by a quadratic function of the effective volume fraction:

$$q_1 = V_1^c \left[1 + \eta_{12} \Phi_2^2\right] \tag{58a}$$

$$q_2 = V_2^c \left[1 + \eta_{12} \Phi_2^2\right] \tag{58b}$$

where the dilation constant η_{ij} is a measure of how the light component swells in the liquid solution. Combining Equations (56), (57), and (58), Chueh et al. express the adjusted activity coefficients for a binary system as

$$\ln \gamma_1^{(P,S)} = A \Phi_2^2 + B \Phi \tag{59a}$$

$$\ln \gamma_2^{*(P,S)} = A\left[\frac{V_2^c}{V_1^c}\right]\left[\Phi_2^2 - 2\Phi_2\right] + B\left[\frac{V_2^c}{V_1^c}\right]\left[\Phi_2^4 - \frac{4}{3}\Phi_2^3\right] \tag{59b}$$

where $A \equiv \alpha_{22} V_1^c$ and $B \equiv 3 \eta_{12} \alpha_{22} V_1^c$

Chueh et al. extend their dilated van Laar model to a ternary system containing two noncondensible and one condensible components. They define the adjusted pressure independent activity coefficient for the third component as

$$\gamma_3^{*(P_1^s)} \equiv \frac{\bar{f}_3^V}{x_3 H_{3,1}(P_1^s)} \exp -\int_{P_1^s}^{P} \frac{\bar{V}_3^L}{RT} dP \qquad (60)$$

Using the molar excess Gibbs energy written as an expansion in terms of effective volume fractions Φ_2 and Φ_3 :

$$\frac{\Delta G^E}{RT(x_1q_1+x_2q_2+x_3q_3)} = -\alpha_{22}\Phi_2^2 - \alpha_{33}\Phi_3^2 - 2\alpha_{23}\Phi_2\Phi_3 - \cdots \qquad (61a)$$

where

$$\Phi_2 = \frac{x_2 q_2}{x_1 q_1 + x_2 q_2 + x_3 q_3} \qquad (61b)$$

and

$$\Phi_3 = \frac{x_3 q_3}{x_1 q_1 + x_2 q_2 + x_3 q_3} \qquad (61c)$$

The parameter q_i is related to the liquid compositions by the relation

$$q_i = V_i^c \left[1 + \eta_{12}\Phi_2^2 + 2\eta_{1,23}\Phi_2\Phi_3 + \eta_{13}\Phi_3^2 \right] \qquad (62)$$

The mixing rules used by Chueh et al. to obtain the interaction coefficients $\eta_{1,23}$ and α_{23} are given as

$$\eta_{1,23} \equiv \left[\eta_{12}\eta_{13} \right]^{1/2} \qquad (63a)$$

$$\alpha_{23} \equiv \left[\alpha_{22}\alpha_{33} \right]^{1/2} \qquad (63b)$$

Using these equations, Chueh et al. report very good agreement between calculated experimental activity coefficients for the nitrogen-oxygen-carbon dioxide ternary system at 0°C and predicted activity coefficients using the above mixing rules.

O'Connell and Prausnitz[37] consider the system composed of one noncondensible constituent and two condensible constituents. In an analogous manner as above, the reference fugacities for the solvents are that of the pure components, and the reference fugacity of the solute is the Henry's Law constant in one of the solvents. By employing the unsymmetric convention for activity coefficients, they transform Wohl's method to predict the properties of a ternary system from information of the binary pairs. They describe the properties of each binary pair by a one-term Margules equation. No comparisons are made to test the validity of their derived equations.

To account for the effect of pressure on the liquid phase activity coefficients, Chueh and Prausnitz[12] have just recently developed a method for predicting partial molar volumes. They first calculate molar volumes of saturated liquid mixtures from a correlation developed by Lyckman, Eckert, and Prausnitz[33] and which is based on the tables presented by Pitzer. Chueh and Prausnitz give their correlation in terms of the reduced saturated volume as

$$\underline{V}_r = \underline{V}_r^{(0)} - \omega \underline{V}_r^{(1)} - \omega^2 \underline{V}_r^{(2)} \qquad (64)$$

where ω is the acentric factor and $\underline{V}_r^{(0)}$, $\underline{V}_r^{(1)}$, and $\underline{V}_r^{(2)}$ are functions of reduced temperature and are tabulated. Chueh and Prausnitz have fitted the tabulated values with an equation. They then calculate

the partial molar volumes from the relation

$$\bar{V}_i = \frac{\left[\partial P/\partial n_i\right]_{T,V,n_j}}{\left[\partial P/\partial V\right]_{T,n_i,n_j}} \tag{65}$$

and the Redlich-Kwong equation of state. The mixing rules, however, are different than those proposed by Redlich and Kwong.

Comparisons between the predicted values of specific volumes of liquid mixtures and partial molar volumes and those based on experimental work are very good.

IV. MATERIALS

The materials used for this study are listed in Table I. The supplier and grade of purity of each component are given. Purity analyses obtained from gas chromatograph scans are also listed.

TABLE I

PURITY OF MATERIALS

Compound	Analysis of Purity	Supplier	Manufacturer's Stated Purity
methane	99.3%	The Matheson Co.	99.1%
normal pentane	99.9%	Phillips Petroleum Co.	99.9%
isopentane	99.9%	Phillips Petroleum Co.	99.9%
neopentane	99.8%	Phillips Petroleum Co.	99.2%

V. DESCRIPTION OF EQUIPMENT

The design of the equipment used in this study has been described by Brainard.[6] The equipment and modifications are described in this section. Figure 1 presents a simplified flow diagram of the apparatus used for this research. Figures 2 and 3 give a more detailed version of the equipment. The entire experimental equipment can be described conveniently in terms of subsystems. These subsystems are: the light and heavy hydrocarbon loading system, the equilibrium system, the sampling system. Also included is a discussion pertinent to the analytical technique for composition determination of the two phases. Finally, some of the safety aspects of the equipment are discussed.

A. Hydrocarbon Loading System

The loading system consists of a high pressure cylinder of methane (3,500 psi) and a stainless steel micro-reaction vessel with a volume of about 140 cubic centimeters. The cylinder of methane has a high pressure regulator manufactured by the Matheson Company (Model No. 6-670). The regulator is provided with 10,000 psi gauges for the inlet and discharge sides, respectively. The lines are all 1/4 inch O.D. by 0.083 inch I.D., 316 stainless steel high pressure tubing. The valves (numbers 2,3,4 in Figure 1) are 30,000 psi items made by Autoclave Engineers, Inc. . These valves will be discussed in more detail in the following section.

B. Equilibrium System

Figure 2 presents a longitudinal section of the equilibrium cell. The cell is a standard Aminco micro-reaction vessel (Catalogue

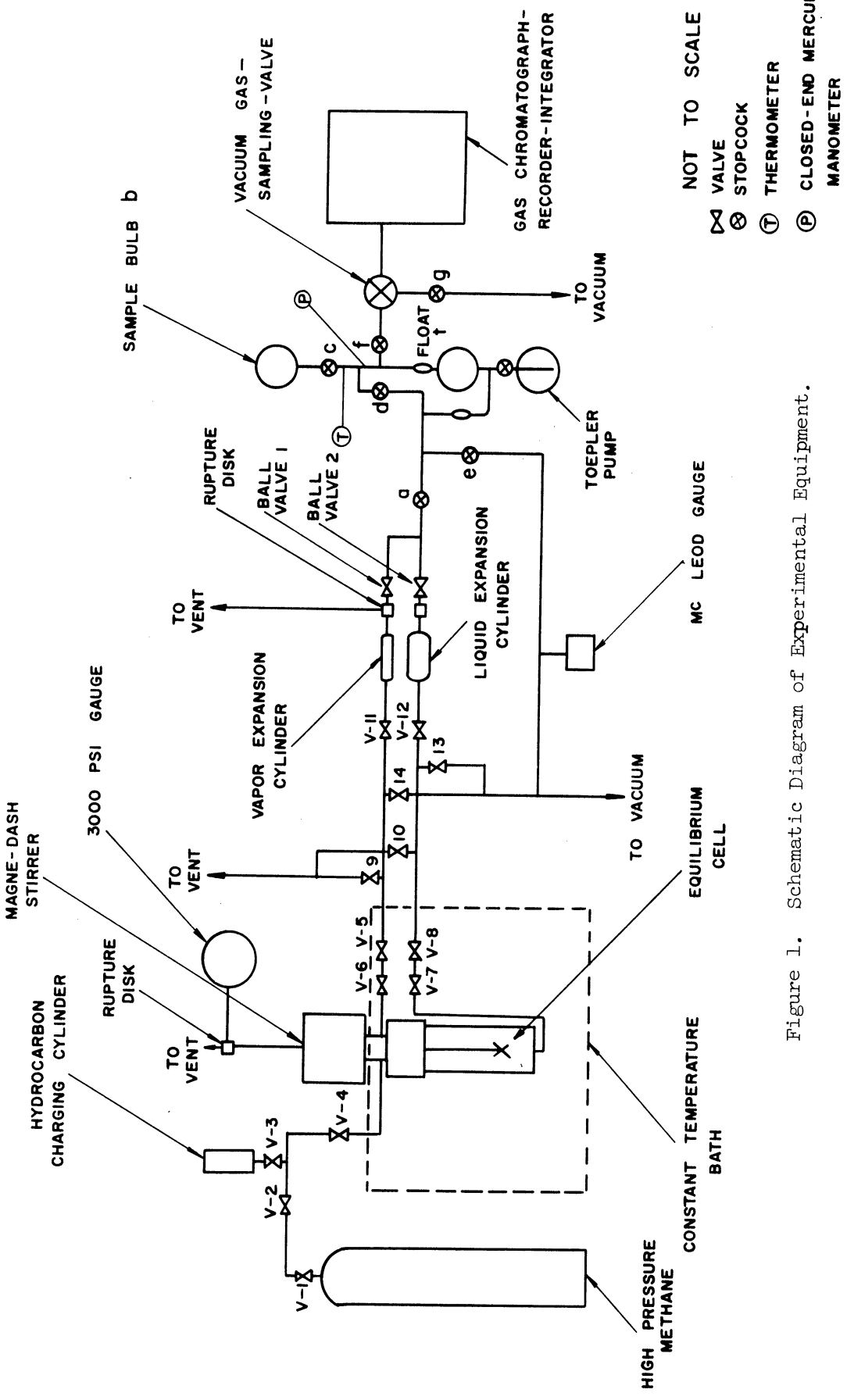

Figure 1. Schematic Diagram of Experimental Equipment.

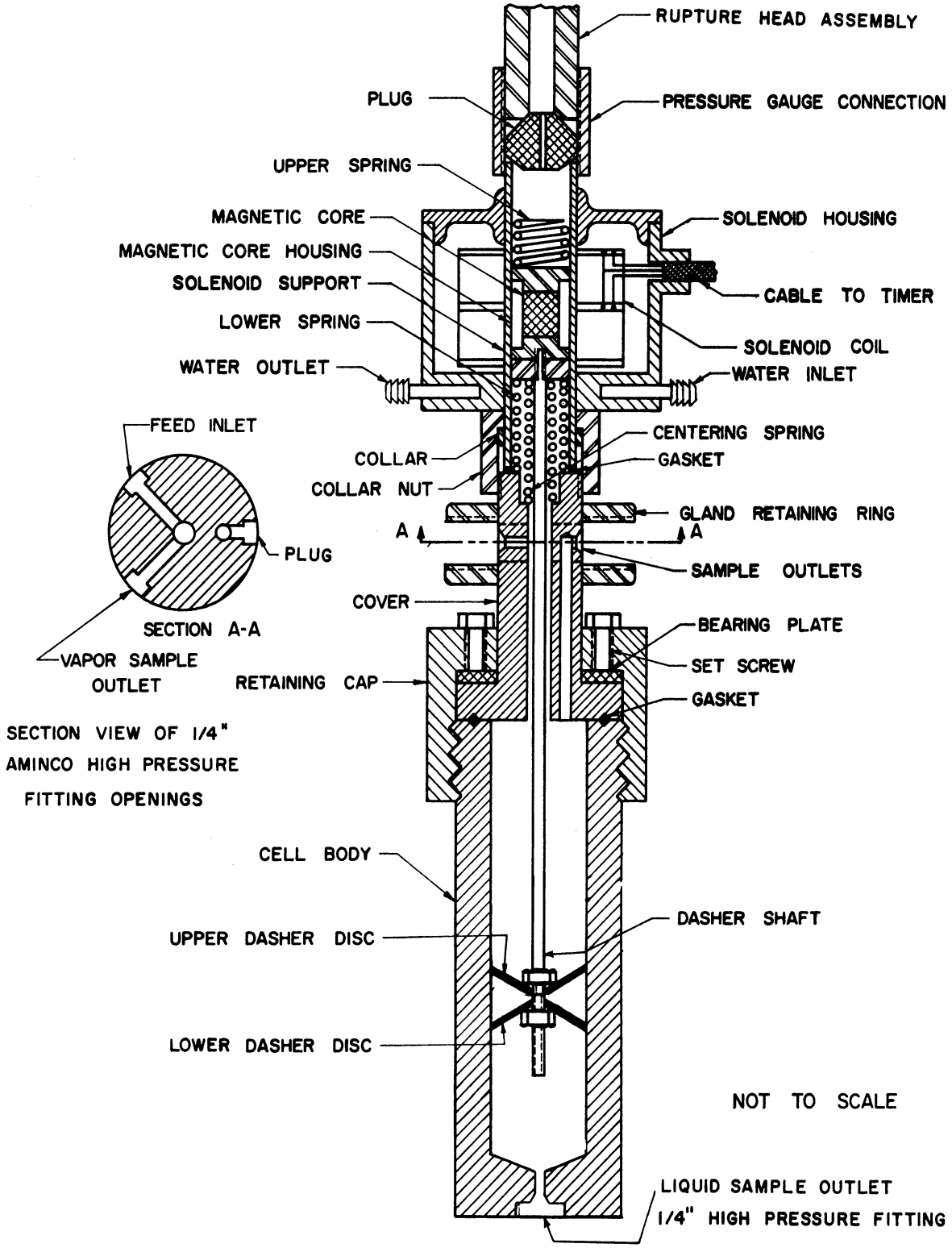

Figure 2. Longitudinal Cross Section of Equilibrium Cell and Magne-Dash Stirrer.

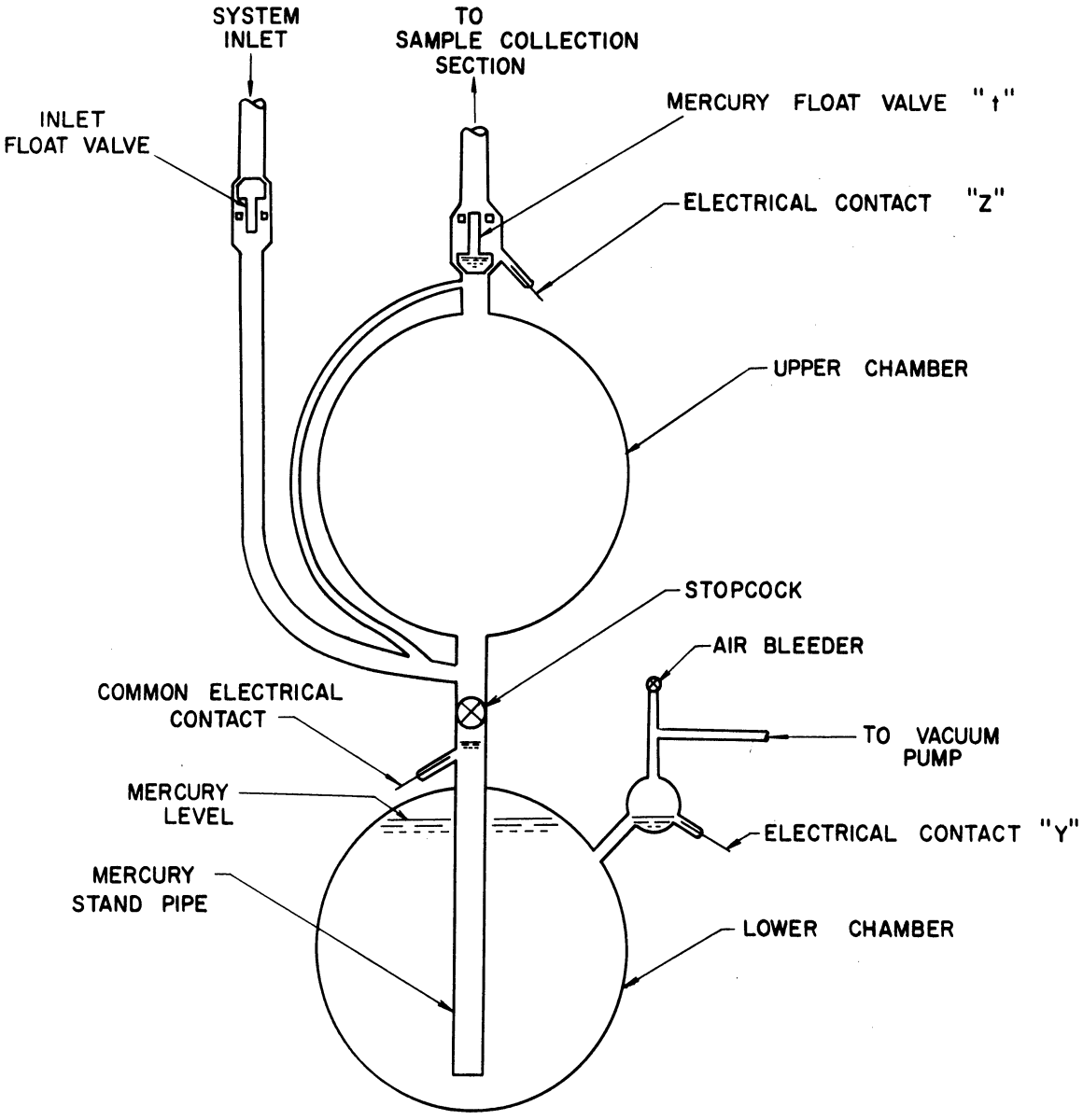

Figure 3. Sketch of Toepler Pump.

No. 41-230). The cell body is made of A.I.S.I. 316 stainless steel, designed for a maximum working pressure of 11,000 psi at 100°F. The wall thickness of the cell is 5/8 inch. The cell has an approximate volume of 200 cubic centimeters and an approximate weight of 20 pounds. The cell was modified in two ways. First, the seating head, at the head gasket, was machined in such a manner that the cell would accommodate the stirring mechanism. Second, a 1/4 inch hole was drilled at the base of the cell and fitted with a 1/4 inch high pressure fitting. This fitting serves as the exit point for the liquid sample.

The rate of attainment of equilibrium in the cell is increased by means of an Autoclave Magne-Dash stirrer. More specifically, agitation of the cell contents is produced by the reciprocating motion of the dasher assembly (see Figure 2). The motion of the dasher is produced by the thrust induced on a magnetic core when the coil surrounding this core is energized electrically. By using two coils, it is possible to give the dasher a positive thrust in both up and down directions. A timer which controls the flow of current to both coils (that is, energizing them alternately) controls the speed of the dasher. The duration of each stroke is then controlled by rheostats in the timer. The frequency of motion can be regulated from about one cycle per 4 seconds to 4 cycles per second. The longitudinal traverse of the dasher is approximately 1-1/2 inches. The upper and lower springs, as shown in Figure 2, act as stops for the core. Finally, the centering spring positions the dasher and supports the weight of the core. The Magne-Dash stirrer is rated for 5,000 psi operation at 650°F. The Magne-Dash stirrer is protected by a rupture disk fabricated from 316 stainless steel and rated at 3,800 psi

at 72°F and 3,078 psi at 400°F.

The equilibrium system, that is the equilibrium cell, is immersed in a constant-temperature bath which is equipped to maintain temperatures ranging from 100°F to 400°F. Heating is provided by six hairpin resistance heaters. Four of the heaters are rated at 1,000 watts each. One of these heaters is electrically in series with a powerstat. The fifth heater is rated at 500 watts. Constant temperatures in the bath are maintained by the sixth heater. This heater, which is rated at 300 watts, is electrically connected to a Fenwal electronic temperature indicating controller (Catalogue No. 56006). A thermistor is used as the temperature sensing probe. The probe is tied into a simple null balance bridge circuit to alternately turn the 300 watt heater off and on. The controller is provided with two modes of operation, namely on-off control operation with completely adjustable differential and proportional control with variable proportional limits. The bath fluid is silicone oil. The oil is produced by the Dow-Corning Corporation and is listed as F-1-0113 type fluid. The fluid has a viscosity of 100 centistokes at 77°F. The fluid (a dimethylpolysiloxane) is usable to 500°F in open air baths.

The bath is a double-walled stainless steel box with a volume of approximately 30 gallons. The oil in the bath is agitated by a mixer which is driven by an electric motor rated at 1/4 horsepower.

The temperature of the constant-temperature bath surrounding the equilibrium cell and both pressure locks is determined with a calibrated mercury-in-glass thermometer (gas-filled type made by the Taylor Instrument Company, Catalogue No. 1704431). Calibration for the thermometer is given in Table XXIX of Appendix C.

The equilibrium pressure is measured with a Heise pressure gauge (Catalogue No. H-42564). The gauge is temperature compensated between -25°F to +125°F and accurate to 0.1 percent of full scale. Calibration of this gauge is given in Table XXVIII of Appendix C.

C. Sampling System

Vapor and liquid samples are removed from the equilibrium cell and contained by means of pressure locks. Each lock is made up of two valves (valves 5,6,7,8 in Figure 1) and a 6 inch nipple, 1/4 inch O.D. by 0.083 inch I.D., type 316 stainless steel. Sixteen gauge chromel A wire was inserted in the 6 inch nipple in order to minimize the dead volume. The valves comprising the pressure lock were a constant source of trouble due to the erosion of the stems. Originally, high temperature Autoclave valves (Catalogue No. 30VM-4071 HT) were used. However, it soon became apparent that these valves leaked after a short period of use. A new set of valves, also manufactured by Autoclave Engineers, Inc. (Catalogue No. 30VM-4071), were tried and found to be ineffectual after several openings and closings. It was finally decided that the erosion of the stems was due to "wire-drawing." A partial solution to the problem was found by using the same type valves but specifying a stellite stem as opposed to 316 stainless steel. The valve packing is glass-impregnated teflon and has proven to be satisfactory. The pressure locks are totally immersed in the constant-temperature bath fluid.

The vapor and liquid phase pressure locks are connected to the vapor and liquid phase expansion cylinders by high pressure 1/4 inch stainless steel tubing. The expansion cylinders used to expand the sample prior to its collection in the glass sample collecting section are gas sampling cylinders manufactured by the Hoke Corporation. The gas sampling cylinders are accommodated with 1/4 inch inlet fittings and 9/16 inch outlet fittings. The catalogue numbers of the vapor phase and liquid phase gas sampling cylinders are 6LD500 and 9LD1000, respectively. Intermediate between the expansion cylinders and the glass sample collecting section are two rupture disks rated at 107 psi at 72°F and two vacuum ball valves (see Figure 1). The ball valves are manufactured by the Jamesbury Corporation (Catalogue No. 1/2" HPV-22-GT) and rated at pressures from 0.01 microns to 4,500 psi. With the ball valves closed, the rupture disks provide a safety feature prior to admitting the sample into the glass section of the equipment if any of the high pressure valves (namely valves 6 and 7) fail.

The vapor and liquid sample lines are coupled together at this point. By means of a Kovar glass seal, the all-metal system previously mentioned is connected to the glass sample collecting system. All stopcocks in the glass section are of the hollow-plug, oblique-bore vacuum type and either 4 millimeters or 8 millimeters in diameter. "Non Aq" stopcock grease distributed by the Fisher Scientific Company is used as the stopcock lubricant. Although "Non Aq" does not possess the best vacuum lubricant properties, it is used in this research to prevent selective adsorption of the samples.

A Toepler pump (see Figure 3) is used to transfer the samples from the sampling lines to the collecting section. The pump is made by the Eck and Krebs Company and has a volume of about 500 cubic centimeters. The glass collection section consists of expansion flasks, a ground glass joint thermometer, and a closed-end mercury manometer. A cathetometer manufactured by the Central Scientific Company is used to measure mercury levels in the closed-end mercury manometer. The cathetometer is capable of discerning distances as small as 50 microns.

D. Composition Determination

A Perkin-Elmer Vapor Fractometer (Model No. 154-D) equipped with a thermal conductivity cell as the sensing device is used for the separation and analysis of the vapor and liquid samples. Essentially, a carrier gas, in this case helium, and the sample pass through a column where the sample components are separated. The column used in all aspects of this research is 14 feet of 1/4 inch tubing packed with squalane (20 percent) on a Chemisorb support. The sample components are swept one by one into the sensing side of the detector. Both sides of the thermal conductivity cell are incorporated into a balanced bridge circuit. When a thermal conductivity change occurs between the reference gas and the sample plus reference gas, a resulting bridge imbalance provides a voltage which drives the pen on a recording potentiometer.

The recorder is a Leeds and Northrup Model G recording potentiometer. The recorder has a one second, full scale balance time and a 5 millivolt nominal span.

The gas sample is introduced into the Fractometer by means of a Perkin-Elmer precision gas sampling valve (Catalogue No. 008-0659). The valve is made of stainless steel and teflon with a sample volume of about 2 cubic centimeters.

A Perkin-Elmer printing integrator (Model No. 194-B) is used to integrate the area under the resultant chromatographic curves. The integrator is a standard velocity, servo-computing arrangement with the input signal produced by a potentiometer installed on the recorder shaft. Within the integrator, an amplifier drives a servo-motor coupled to a tachometer generator and to a printing counter which registers the total number of shaft turns accumulated. The tachometer generator produces an output voltage which is linearly proportional to the speed at which it is driven by the servo-motor. The amplifier compares the tachometer-produced signal to that of the potentiometer in the recorder and continuously regulates the speed of the servo-motor. Each value of the potentiometer input signal corresponds to a definite servo-motor and tachometer speed. Since the rate of rotation of the printing counter is proportional to the recorder pen position, the total number of turns registered in a given time interval is proportional to the integral of the recorder pen position during the same time interval. Hence, it is proportional to the area under the curve produced by the pen. The Perkin-Elmer integrator has a maximum integrating rate of 6,000 counts per minute.

E. Safety

A conscientious attempt was made to incorporate safety features into the design of the experimental equipment. First, the

equilibrium cell and pressure locks were hydrostatically tested to 3,000 psi prior to any experimental runs. A safety shield fabricated of 1/4 inch steel plate surrounds the constant-temperature bath and the equilibrium cell contained therein. A panel was cut out on one of the sides of the barricade such that the valves can be manipulated with a minimum exposure of the operator to the high pressure equipment. As previously mentioned, the Magne-Dash stirrer and sampling lines are provided with rupture disks. Finally, a hood was placed over the equilibrium constant-temperature bath, such that in the case of a rupture disk failure the contents of the cell would be transported out of the room to the exterior of the building.

VI. EXPERIMENTAL PROCEDURES

In the description of the experimental procedure, references to all component equipment identity are made to Figure 1. The initial startup procedure will be discussed in detail.

The entire experimental equipment is evacuated to a pressure of 10 microns or less for a period of not less than 24 hours. With reference to Figure 1, at the outset all stopcocks and valves are open with the exception of valves 2,3,9, and 10. Valve 1 denotes the valve on the high pressure cylinder of methane. The high pressure line between valves 1 and 2 has been flushed several times previously with methane from the cylinder.

Heavy hydrocarbon (pentanes) loading is accomplished by pipetting a prescribed amount, about 90 cubic centimeters, of pentane (normal or iso-) into the charging cylinder. Since neopentane boils at a temperature considerably below room temperature, it is charged into the equilibrium cell directly from the containing cylinder, which is placed on a pan balance. In addition, the equilibrium cell is cooled down by direct contact with solid carbon dioxide. About 50 grams of neopentane are normally administered to the cell. In charging, valves 6 and 7 are closed and valve 3 is then opened to permit the pentane to enter the equilibrium cell by gravity and pressure-induced flow. Valves 3 and 4 are then closed. Valve 6 is opened and closed several times, thereby evacuating any air that is dissolved in the pentane. Closing valve 6, methane is then transferred into the equilibrium cell by setting the pressure regulator at 3,500 psi, opening valve 2, and cracking valve 4.

Upon reaching a pressure (as indicated by the Heise pressure gauge) somewhat less than the desired operating pressure, valve 4 is closed. The Magne-Dash stirrer is then initiated and operated at about 3 cycles per second. The electrical heaters, including the Fenwal temperature controller, are energized and the oil bath agitator is turned on. Having reached the desired operating temperature, the desired operating pressure is obtained by venting some vapor from the cell or pressurizing the cell with methane from the high pressure cylinder. Once the oil bath has reached the desired operating temperature, the heat input into the cell is adjusted by means of a variac and the temperature controller. At this point, the cell and its contents are allowed to physically equilibrate for no less than eight hours. It was found during preliminary runs that a minimum of about four hours was required to attain physical equilibrium, and about eight hours was required to attain equilibrium near the critical region for the cell geometry. During this equilibration time, the stirrer is operated at a frequency of about one cycle per second. The bath thermometer is checked many times to determine the constancy of the temperature indication.

The first step in the vapor sampling procedure is to turn off the stirrer and record the temperature and pressure readings. Valves 5, 13, and 14; both vacuum ball valves; and stopcock "e" are then closed. Valve 6 is opened and closed. In so doing, a vapor sample is transferred from the cell to the previously evacuated pressure lock. Valve 5 is then opened and the vapor sample is allowed to expand into the vapor expansion cylinder. Ball valve 1 is opened and the vapor sample is further expanded into the sample collecting section. At this point, stopcock "d" is closed and the Toepler pump initiated.

The Toepler pump (see Figure 3) operates in such a manner that the sample is transferred from the sampling lines to the sample collecting section. In actual operation, the mercury is in the lower chamber at the outset. With stopcock "d" closed, air is admitted to the lower chamber of the Toepler pump by way of a bleed valve. The air forces the mercury contained therein through a standpipe into the upper chamber. The mercury rises in the upper chamber, forcing the gas sample through the mercury float valve "t" . When the mercury makes contact with electrical contact "Z" , a relay is closed which automatically starts a vacuum pump, thereby evacuating the lower chamber and draining the mercury back into it. The sample, which has been transferred to the sample collection chamber, is now contained by the one-way mercury float valve "t" . As the mercury fills the lower chamber, the gas standpipe is again connected to the upper chamber of the pump. Mercury makes contact at point "Y" and the relay is opened, thereby shutting off the vacuum pump. The cycle starts over again by introducing air by way of the bleed valve into the lower chamber.

Seven to ten cycles of the Toepler pump are found to be sufficient to move the gas sample from the expansion cylinder and the sampling lines into the sample collection chamber. The temperature of the sample is measured with a thermometer, and pressure measurements are performed with the closed-end mercury manometer and the aid of a cathetometer. Normally, the pressure of the sample is maintained at pressure between 10 and 15 centimeters of mercury by using an appropriately sized sample bulb "b" . During all preliminary runs the appropriate volume of sample bulb "b" was determined using the criterion of a maximum pressure of 20 centimeters of mercury. No problems of partial condensation of the samples were encountered in this research.

Analyses of both liquid and vapor samples are carried out in the vapor phase. The analytical procedures involve the introduction of the sample into the gas chromatograph by means of a gas sampling valve. About one hour before the vapor sample is withdrawn from the cell, the gas chromatograph, recorder, and integrator are turned on. The helium carrier-gas flow rate is adjusted to a flow rate of 72 milliliters per minute (at 25°C, 740 millimeters of mercury), as determined by a soap film gas meter. The chromatograph oven temperature was maintained at 80°C. The sample loop is evacuated by means of a vacuum pump. Stopcock "g" is closed and stopcock "f" opened. Once the sample pressure remains constant, the gas sample is introduced into the chromatograph by turning the gas sampling valve, which switches one of the two sample valve tubing loops into the flowing carrier-gas stream. The resulting chromatographic areas are then determined by using the Perkin-Elmer printing integrator.

A minimum of two analyses are made for each sample. In all cases, duplicate samples differed less than .75 percent. The sample loop is evacuated and a new sample is introduced in the same manner as previously described.

During the time that the vapor sample is being transferred from the sample lines to the sample collection chamber by means of the Toepler pump, the liquid sampling line is flushed. This is done to acquire a representative liquid sample from the cell, since preliminary runs showed that the liquid in the liquid drawoff tube was not of the same composition as that in the equilibrium cell. The flushing procedure is accomplished in the following manner. Valves 8, 12, and 14

are closed and valve 10 is opened. A liquid sample is introduced into the liquid pressure lock by opening and closing valve 7. Valve 8 is opened and the liquid sample vented. This procedure of opening and closing valves 7 and 8 is repeated four times. Preliminary runs revealed that the fifth sample was representative of the liquid equilibrium composition in the cell. Geometrically, four flushings are equivalent to about 1.5 times the volume of the liquid drawoff line. Valve 10 is closed and valves 8 and 14 are then opened.

Having analyzed the vapor phase composition, the system is prepared for analysis of the liquid phase composition. A larger sample bulb "b" is inserted into the system after closing stopcocks "c" and "d". For vapor samples, the sample bulb volume ranges from about 25 to 250 cubic centimeters. For liquid samples, the sample bulb volume ranges from approximately 250 to 1000 cubic centimeters. The entire system is then evacuated to a pressure of about 10 microns for a period of about one-half hour.

Liquid samples are withdrawn in the same manner as vapor samples. The valve manipulations in withdrawing and collecting the liquid sample are analogous to those of the vapor sample. In fact, they are symmetrical from the vapor sampling line up to the point where the vapor and liquid sample lines merge. The stopcocks in the glass section are opened and closed in the manner used when analyzing the vapor sample. In collecting the liquid sample, about twice the number of cycles are required to transfer the liquid sample from the sampling lines to the sample collection chamber as compared to the pumping time for the vapor sample. In addition, the liquid sample is allowed to expand, and it is collected again to insure mixing. This mixing process is accomplished in the

folowing manner. After the sample is collected, stopcock "a" is closed and stopcock "d" opened. The sample then expands into the upper chamber of the Toepler pump. Stopcock "d" is closed and the pumping procedure repeated until all of the sample is once again contained in the sample collection chamber.

Analysis of the liquid sample is accomplished in an analogous manner to that for the vapor sample. As with the vapor phase samples, duplicate analyses are run as standard procedure.

The equipment is then prepared for the next run by evacuating the entire system. Methane is administered into the equilibrium cell, thereby increasing the pressure. The Magne-Dash stirrer is reactivated and the equilibrium cell is allowed to re-equilibrate for at least eight hours. For runs near the critical region the cell is allowed to equilibrate for about twelve hours. In the course of this research, experimental data were obtained at three isotherms, namely 160°F, 220°F, and 280°F.

VII. EXPERIMENTAL RESULTS

The experimental data obtained in this research are presented in Tables II through XII and Figures 4 through 22 in the same order as the data were taken chronologically.

The experimental phase equilibrium data for the methane-normal pentane system are given in Table II. Experimental data were taken at one temperature (220°F), and several points were taken at essentially the same pressures to establish the reproducibility of the entire system. The experimental data on this system are compared with those of Sage, Reamer, Olds, and Lacey[50] in Figure 4. As can be seen, agreement between Sage et al. and this work is quite good.

Tables III through V present the experimental phase equilibrium data for the methane-isopentane binary system. Figures 5 through 7 show the pressure composition data at temperatures of 160°F, 220°F, and 280°F, respectively. Included in Figures 5 through 7 are the experimental data reported by Amick, Johnson, and Dodge.[1] Figure 8 is a log-log plot of the equilibrium vaporization ratios, K, of methane and isopentane as a function of pressure. All three isotherms (160°F, 220°F and 280°F) are included in Figure 8. The loci in Figure 8 represent smoothed equilibrium vaporization ratios for methane and isopentane. Smoothed K values were obtained from Figures 5 through 7 and are presented in Tables XIII through XV. The uncertainty of the smoothed values of methane composition is believed to be $\pm$ 0.002 mole fraction. Experimentally determined K values for methane and isopentane are also presented in Figure 8.

Tables VI through VIII present the experimental phase equilibrium data for the methane-isopentane-normal pentane ternary system. The Gibbs Phase Rule states that the number of intensive variables required to specify the system is three for a two-phase system containing three components. The intensive properties selected to determine the ternary system are pressure, temperature, and isopentane concentration to isopentane plus normal pentane concentration in the liquid phase. Figures 9 through 15 graphically present the experimentally determined phase equilibrium behavior of the methane-isopentane-normal pentane ternary system. Figure 9 illustrates the equilibrium ratios for methane, isopentane, and normal pentane as a function of pressure for the three isothermal conditions investigated in this research. Figures 10 through 12 present the pressure-composition diagrams for the methane-isopentane-normal pentane ternary system at the three tempertatures of 160°F, 220°F, and 280°F, respectively. The loci of Figures 9 through 12 are described by a parameter of isopentane concentration to isopentane plus normal pentane concentration. Figures 13 through 15 give the ternary composition diagrams for three pressures. They show the decrease of the two-phase region with increased pressure. They also illustrate the small change of the liquid phase mole fraction parameter with pressure for different isotherms. The data for the methane-normal pentane binary system in Figures 13 through 15 are those of Sage et al.(50)

Tables IX through XI give the experimental phase equilibrium data for the methane-neopentane binary system . Also tabulated are the experimentally determined K values of methane and neopentane. Figures 16 through 18 are the pressure-composition curves for the three isotherms

at which experimental data were obtained. Figure 19 compares smoothed values of the equilibrium vaporization ratios of methane and neopentane with the experimental values as a function of pressure. The loci of the three isotherms presented in Figure 19 represent smoothed data as determined from Figures 16 through 18. These smoothed data are presented in Tables XVI through XVIII. No data have been found in the literature for the methane-neopentane binary system. Hence, no comparisons are made with this work.

Table XII presents the experimental phase equilibrium data for the ternary system of methane-neopentane-normal pentane. Experimental data were obtained for one isotherm, namely 160°F. Figure 20 is a plot of the equilibrium vaporization ratios of methane, neopentane, and normal pentane at 160°F as a function of pressure on logarithmic coordinates. Figure 21 shows the pressure-composition diagram for the methane-neopentane-normal pentane ternary system at 160°F. The locus in Figure 21 is described by a parameter of neopentane concentration to neopentane plus normal pentane concentration in the liquid phase. Finally, Figure 22 presents a ternary composition diagram of this system. It demonstrates the shrinkage of the two-phase region with increased pressure and the relative independence of the heavy components with pressure on a methane-free basis for the liquid phase. Methane-normal pentane data illustrated in Figure 22 are those of Sage et al.[50]

TABLE II

EXPERIMENTAL PHASE EQUILIBRIUM DATA FOR THE METHANE-NORMAL PENTANE BINARY SYSTEM AT 220°F

Run no.	Pressure (psia)	Vapor Phase Composition (mole fraction)		Liquid Phase Composition (mole fraction)		Equilibrium Ratio	
		methane	n-pentane	methane	n-pentane	methane	n-pentane
21	1502	0.808	0.192	0.380	0.620	2.13	0.310
22	1265	0.812	0.188	0.324	0.676	2.50	0.279
23	1231	0.810	0.190	0.306	0.694	2.65	0.273
24	1023	0.806	0.194	0.253	0.747	3.18	0.260
25	1001	0.805	0.195	0.247	0.753	3.26	0.259
26	1999	0.740	0.260	0.532	0.468	1.391	0.556
27	1777	0.788	0.212	0.456	0.544	1.729	0.389
28	1501	0.808	0.192	0.382	0.618	2.11	0.310
29	1260	0.816	0.184	0.310	0.690	2.63	0.267
30	1005	0.814	0.186	0.248	0.752	3.28	0.248

TABLE III

EXPERIMENTAL PHASE EQUILIBRIUM DATA FOR THE METHANE-ISOPENTANE BINARY SYSTEM AT 220°F

Run no.	Pressure (psia)	Vapor Phase Composition (mole fraction)		Liquid Phase Composition (mole fraction)		Equilibrium Ratio	
		methane	i-pentane	methane	i-pentane	methane	i-pentane
31	1256	0.788	0.212	0.331	0.669	2.38	0.317
32	1503	0.774	0.226	0.396	0.604	1.955	0.374
33	1721	0.746	0.254	0.454	0.546	1.645	0.464
34	1899	0.686	0.314	0.566	0.434	1.212	0.724
35	1001	0.791	0.209	0.262	0.738	3.02	0.284
36	759	0.765	0.235	0.192	0.808	3.99	0.290
37	499	0.710	0.290	0.118	0.882	6.01	0.328

TABLE IV

EXPERIMENTAL PHASE EQUILIBRIUM DATA FOR THE METHANE-ISOPENTANE BINARY SYSTEM AT 160°F

Run no.	Pressure (psia)	Vapor Phase Composition (mole fraction)		Liquid Phase Composition (mole fraction)		Equilibrium Ratio	
		methane	i-pentane	methane	i-pentane	methane	i-pentane
38	502	0.841	0.159	0.142	0.858	5.93	0.1856
39	755	0.872	0.128	0.218	0.782	3.99	0.1641
40	1001	0.885	0.115	0.283	0.717	3.13	0.1599
41	1253	0.879	0.121	0.351	0.649	2.50	0.1859
42	1505	0.869	0.131	0.418	0.582	2.08	0.225
43A	1759	0.853	0.147	0.489	0.511	1.744	0.288
44	1992	0.821	0.179	0.545	0.455	1.506	0.394
45	2191	0.741	0.259	0.633	0.367	1.170	0.705

TABLE V

EXPERIMENTAL PHASE EQUILIBRIUM DATA FOR THE METHANE-ISOPENTANE BINARY SYSTEM AT 280°F

Run no.	Pressure (psia)	Vapor Phase Composition (mole fraction)		Liquid Phase Composition (mole fraction)		Equilibrium Ratio	
		methane	i-pentane	methane	i-pentane	methane	i-pentane
46	511	0.520	0.480	0.092	0.908	5.68	0.528
47	759	0.603	0.397	0.161	0.839	3.74	0.473
48	1001	0.636	0.364	0.231	0.769	2.75	0.474
49	1267	0.651	0.349	0.315	0.685	2.07	0.510
49A	1277	0.643	0.357	0.330	0.670	1.948	0.533
50	1517	0.581	0.419	0.488	0.512	1.191	0.818

TABLE VI

EXPERIMENTAL PHASE EQUILIBRIUM DATA

FOR THE METHANE-ISOPENTANE-NORMAL PENTANE TERNARY SYSTEM AT 160°F

Run no.	Pressure (psia)	Vapor Phase Composition (mole fraction)			Liquid Phase Composition (mole fraction)			Equilibrium Ratio		
		methane	isopentane	n-pentane	methane	isopentane	n-pentane	methane	isopentane	n-pentane
51	504	0.871	0.040	0.089	0.138	0.223	0.639	6.29	0.1775	0.1397
52	755	0.894	0.030	0.076	0.211	0.206	0.583	4.23	0.1484	0.1296
53	1003	0.897	0.030	0.073	0.274	0.189	0.537	3.28	0.1567	0.1363
54	1493	0.889	0.031	0.080	0.406	0.153	0.441	2.19	0.200	0.1821
55	1975	0.849	0.040	0.111	0.504	0.129	0.367	1.685	0.314	0.302
55A	1995	0.842	0.042	0.116	0.521	0.123	0.356	1.616	0.343	0.326
58	2268	0.758	0.063	0.178	0.593	0.104	0.303	1.278	0.608	0.589

TABLE VII

EXPERIMENTAL PHASE EQUILIBRIUM DATA
FOR THE METHANE-ISOPENTANE-NORMAL PENTANE TERNARY SYSTEM AT 220°F

Run no.	Pressure (psia)	Vapor Phase Composition (mole fraction)			Liquid Phase Composition (mole fraction)			Equilibrium Ratio		
		methane	isopentane	n-pentane	methane	isopentane	n-pentane	methane	isopentane	n-pentane
59	1765	0.771	0.061	0.168	0.454	0.139	0.407	1.698	0.441	0.413
60	2047	0.747	0.065	0.188	0.555	0.112	0.333	1.346	0.584	0.564
61	1519	0.801	0.053	0.146	0.389	0.154	0.457	2.06	0.342	0.321
62	1263	0.810	0.051	0.139	0.319	0.172	0.509	2.54	0.296	0.273
63	995	0.810	0.051	0.139	0.251	0.188	0.561	3.22	0.272	0.248
64	753	0.788	0.058	0.154	0.186	0.205	0.609	4.22	0.282	0.254
65	507	0.744	0.070	0.185	0.120	0.220	0.660	6.19	0.319	0.281

TABLE VIII

EXPERIMENTAL PHASE EQUILIBRIUM DATE
FOR THE METHANE-ISOPENTANE-NORMAL PENTANE TERNARY SYSTEM AT 280°F

Run no.	Pressure (psia)	Vapor Phase Composition (mole fraction)			Liquid Phase Composition (mole fraction)			Equilibrium Ratio		
		methane	isopentane	n-pentane	methane	isopentane	n-pentane	methane	isopentane	n-pentane
66	539	0.563	0.116	0.320	0.099	0.220	0.681	5.64	0.529	0.471
67	760	0.630	0.097	0.273	0.162	0.202	0.636	3.89	0.479	0.429
68	1001	0.662	0.087	0.251	0.231	0.187	0.582	2.87	0.464	0.431
69	1253	0.674	0.081	0.245	0.306	0.164	0.529	2.20	0.492	0.463
66A	541	0.568	0.120	0.312	0.103	0.232	0.665	5.51	0.516	0.469
67A	757	0.629	0.102	0.269	0.164	0.214	0.622	3.83	0.476	0.432
68A	1031	0.665	0.091	0.244	0.242	0.195	0.563	2.75	0.465	0.434
69A	1255	0.674	0.087	0.238	0.304	0.180	0.516	2.22	0.484	0.462
70B	1565	0.616	0.099	0.285	0.453	0.138	0.408	1.358	0.718	0.698

TABLE IX

EXPERIMENTAL PHASE EQUILIBRIUM DATA FOR THE METHANE-NEOPENTANE BINARY SYSTEM AT 160°F

Run no.	Pressure (psia)	Vapor Phase Composition (mole fraction)		Liquid Phase Composition (mole fraction)		Equilibrium Ratio	
		methane	neopentane	methane	neopentane	methane	neopentane
71	511	0.761	0.239	0.153	0.847	4.96	0.282
72	763	0.797	0.203	0.232	0.768	3.43	0.264
73	1005	0.819	0.181	0.312	0.688	2.63	0.263
74	1273	0.813	0.187	0.391	0.609	2.08	0.306
74A	1281	0.813	0.187	0.398	0.602	2.04	0.311
75A	1521	0.784	0.216	0.482	0.518	1.628	0.416
76B	1709	0.727	0.273	0.560	0.440	1.298	0.620
77	1748	0.685	0.315	0.603	0.397	1.137	0.792
82	310	0.667	0.333	0.085	0.915	7.83	0.364

TABLE X

EXPERIMENTAL PHASE EQUILIBRIUM DATA FOR THE METHANE-NEOPENTANE BINARY SYSTEM AT 220°F

Run no.	Pressure (psia)	Vapor Phase Composition (mole fraction)		Liquid Phase Composition (mole fraction)		Equilibrium Ratio	
		methane	neopentane	methane	neopentane	methane	neopentane
83	308	0.395	0.605	0.051	0.949	7.81	0.637
84	503	0.563	0.437	0.117	0.883	4.82	0.495
85	748	0.639	0.361	0.197	0.803	3.24	0.450
86	1008	0.670	0.330	0.282	0.718	2.38	0.459
87A	1251	0.654	0.346	0.377	0.623	1.735	0.556
88A	1434	0.585	0.415	0.471	0.529	1.242	0.784

TABLE XI

EXPERIMENTAL PHASE EQUILIBRIUM DATA FOR THE METHANE-NEOPENTANE BINARY SYSTEM AT 280°F

Run no.	Pressure (psia)	Vapor Phase Composition (mole fraction)		Liquid Phase Composition (mole fraction)		Equilibrium Ratio	
		methane	neopentane	methane	neopentane	methane	neopentane
91	506	0.280	0.720	0.068	0.932	4.10	0.772
92	755	0.407	0.593	0.163	0.837	2.49	0.709
93B	1004	0.416	0.584	0.281	0.719	1.479	0.813

TABLE XII

EXPERIMENTAL PHASE EQUILIBRIUM DATA
FOR THE METHANE-NEOPENTANE-NORMAL PENTANE TERNARY SYSTEM AT 160°F

Run no.	Pressure (psia)	Vapor Phase Composition (mole fraction)			Liquid Phase Composition (mole fraction)			Equilibrium Ratio		
		methane	neopentane	n-pentane	methane	neopentane	n-pentane	methane	neopentane	n-pentane
95	503	0.845	0.058	0.097	0.141	0.216	0.643	6.01	0.266	0.1512
96	751	0.871	0.046	0.083	0.206	0.200	0.594	4.23	0.230	0.1391
97	1251	0.878	0.040	0.082	0.338	0.164	0.498	2.60	0.246	0.1641
98	1505	0.870	0.041	0.089	0.400	0.148	0.452	2.18	0.276	0.1972
99	1759	0.855	0.043	0.102	0.461	0.131	0.408	1.855	0.327	0.251
100	2013	0.805	0.054	0.141	0.550	0.111	0.339	1.464	0.482	0.417
101	2120	0.775	0.059	0.166	0.602	0.098	0.300	1.288	0.606	0.551
102	1006	0.879	0.040	0.081	0.278	0.176	0.546	3.16	0.231	0.1479

TABLE XIII

SMOOTHED PHASE EQUILIBRIUM DATA FOR THE METHANE-ISOPENTANE BINARY SYSTEM AT 160°F

Pressure (psia)	Vapor Phase Composition (mole fraction)		Liquid Phase Composition (mole fraction)		Equilibrium Ratio	
	methane	i-pentane	methane	i-pentane	methane	i-pentane
500	0.840	0.160	0.139	0.861	6.04	0.186
750	0.872	0.128	0.216	0.784	4.04	0.163
1000	0.884	0.116	0.285	0.715	3.10	0.162
1250	0.880	0.120	0.350	0.650	2.51	0.185
1500	0.874	0.126	0.417	0.583	2.10	0.216
1750	0.853	0.147	0.483	0.517	1.77	0.284
2000	0.817	0.183	0.549	0.451	1.49	0.406
2150	0.768	0.232	0.605	0.395	1.27	0.587
2213	0.688	0.312	0.688	0.312	1.00	1.00

TABLE XIV

SMOOTHED PHASE EQUILIBRIUM DATA FOR THE METHANE-ISOPENTANE BINARY SYSTEM AT 220°F

Pressure (psia)	Vapor Phase Composition (mole fraction)		Liquid Phase Composition (mole fraction)		Equilibrium Ratio	
	methane	i-pentane	methane	i-pentane	methane	i-pentane
500	0.710	0.290	0.119	0.881	5.97	0.329
750	0.766	0.234	0.195	0.805	3.93	0.291
1000	0.790	0.210	0.262	0.738	3.02	0.284
1250	0.789	0.211	0.330	0.670	2.39	0.315
1500	0.774	0.226	0.396	0.604	1.95	0.374
1750	0.742	0.258	0.465	0.535	1.60	0.482
1917	0.638	0.362	0.638	0.362	1.00	1.00

TABLE XV

SMOOTHED PHASE EQUILIBRIUM DATA FOR THE METHANE-ISOPENTANE BINARY SYSTEM AT 280°F

Pressure (psia)	Vapor Phase Composition (mole fraction)		Liquid Phase Composition (mole fraction)		Equilibrium Ratio	
	methane	i-pentane	methane	i-pentane	methane	i-pentane
500	0.513	0.487	0.090	0.910	5.70	0.535
750	0.601	0.399	0.160	0.840	3.76	0.475
1000	0.636	0.364	0.231	0.769	2.75	0.473
1250	0.645	0.355	0.318	0.682	2.03	0.520
1500	0.591	0.409	0.460	0.540	1.28	0.757
1534	0.539	0.461	0.539	0.461	1.00	1.00

TABLE XVI

SMOOTHED PHASE EQUILIBRIUM DATA FOR THE METHANE-NEOPENTANE BINARY SYSTEM AT 160°F

Pressure (psia)	Vapor Phase Composition (mole fraction)		Liquid Phase Composition (mole fraction)		Equilibrium Ratio	
	methane	neopentane	methane	neopentane	methane	neopentane
300	0.656	0.344	0.079	0.921	8.30	0.374
500	0.756	0.244	0.150	0.850	5.04	0.287
750	0.798	0.202	0.230	0.770	3.47	0.262
1000	0.818	0.182	0.311	0.689	2.63	0.264
1250	0.814	0.186	0.388	0.612	2.10	0.304
1500	0.789	0.211	0.475	0.525	1.66	0.402
1755	0.644	0.356	0.644	0.356	1.00	1.00

TABLE XVII

SMOOTHED PHASE EQUILIBRIUM DATA FOR THE METHANE-NEOPENTANE BINARY SYSTEM AT 220°F

Pressure (psia)	Vapor Phase Composition (mole fraction)		Liquid Phase Composition (mole fraction)		Equilibrium Ratio	
	methane	neopentane	methane	neopentane	methane	neopentane
310	0.405	0.595	0.051	0.949	7.96	0.626
500	0.561	0.439	0.116	0.884	4.84	0.497
750	0.641	0.359	0.198	0.802	3.24	0.448
1000	0.670	0.330	0.281	0.719	2.38	0.459
1250	0.654	0.346	0.374	0.626	1.75	0.553
1460	0.528	0.472	0.528	0.472	1.00	1.00

TABLE XVIII

SMOOTHED PHASE EQUILIBRIUM DATA FOR THE METHANE-NEOPENTANE BINARY SYSTEM AT 280°F

Pressure (psia)	Vapor Phase Composition (mole fraction)		Liquid Phase Composition (mole fraction)		Equilibrium Ratio	
	methane	neopentane	methane	neopentane	methane	neopentane
500	0.277	0.723	0.066	0.934	4.20	0.774
750	0.406	0.594	0.160	0.840	2.54	0.707
1035	0.354	0.646	0.354	0.646	1.00	1.00

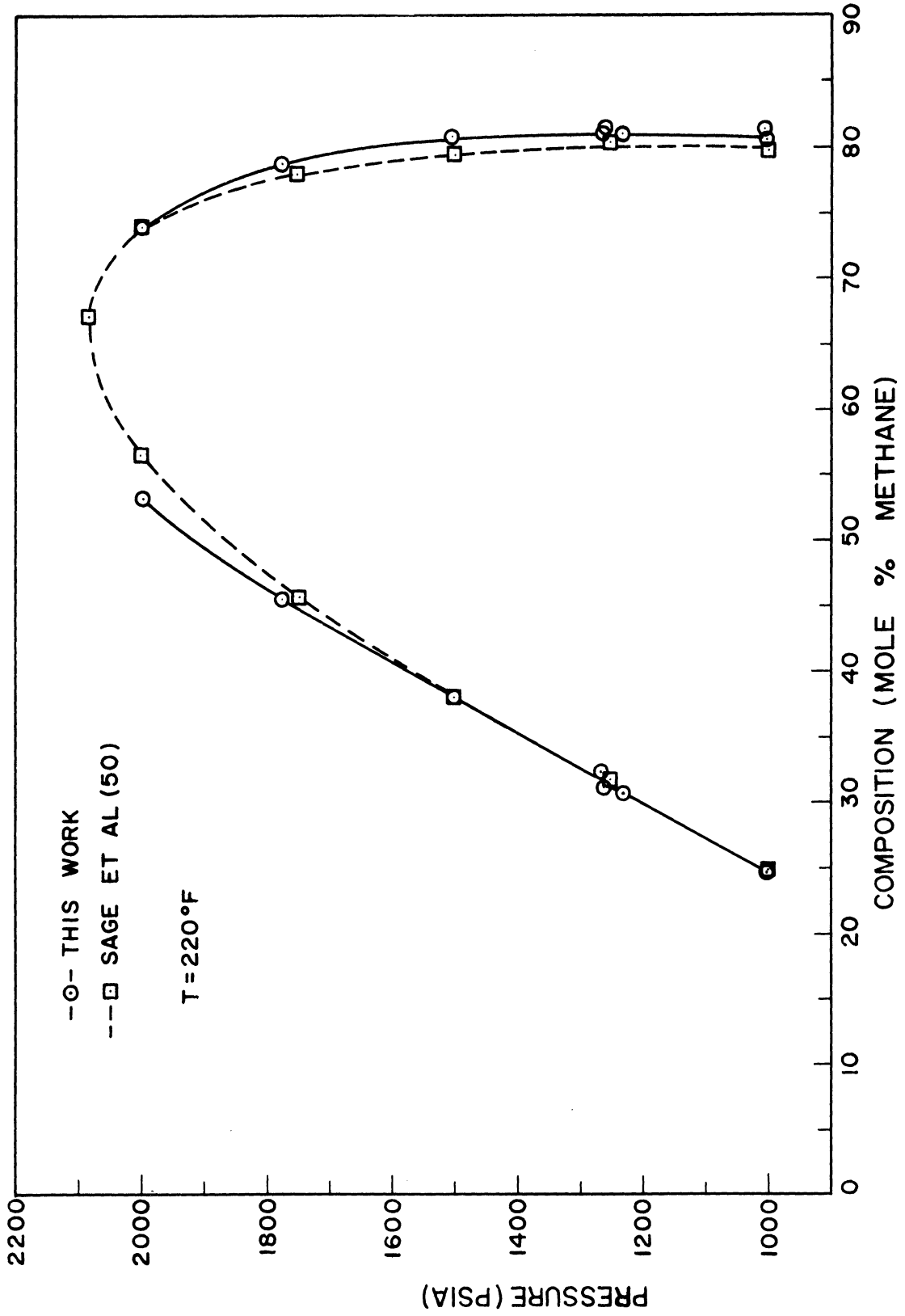

Figure 4. Pressure-Composition Diagram for Methane-Normal Pentane Binary System at 220°F.

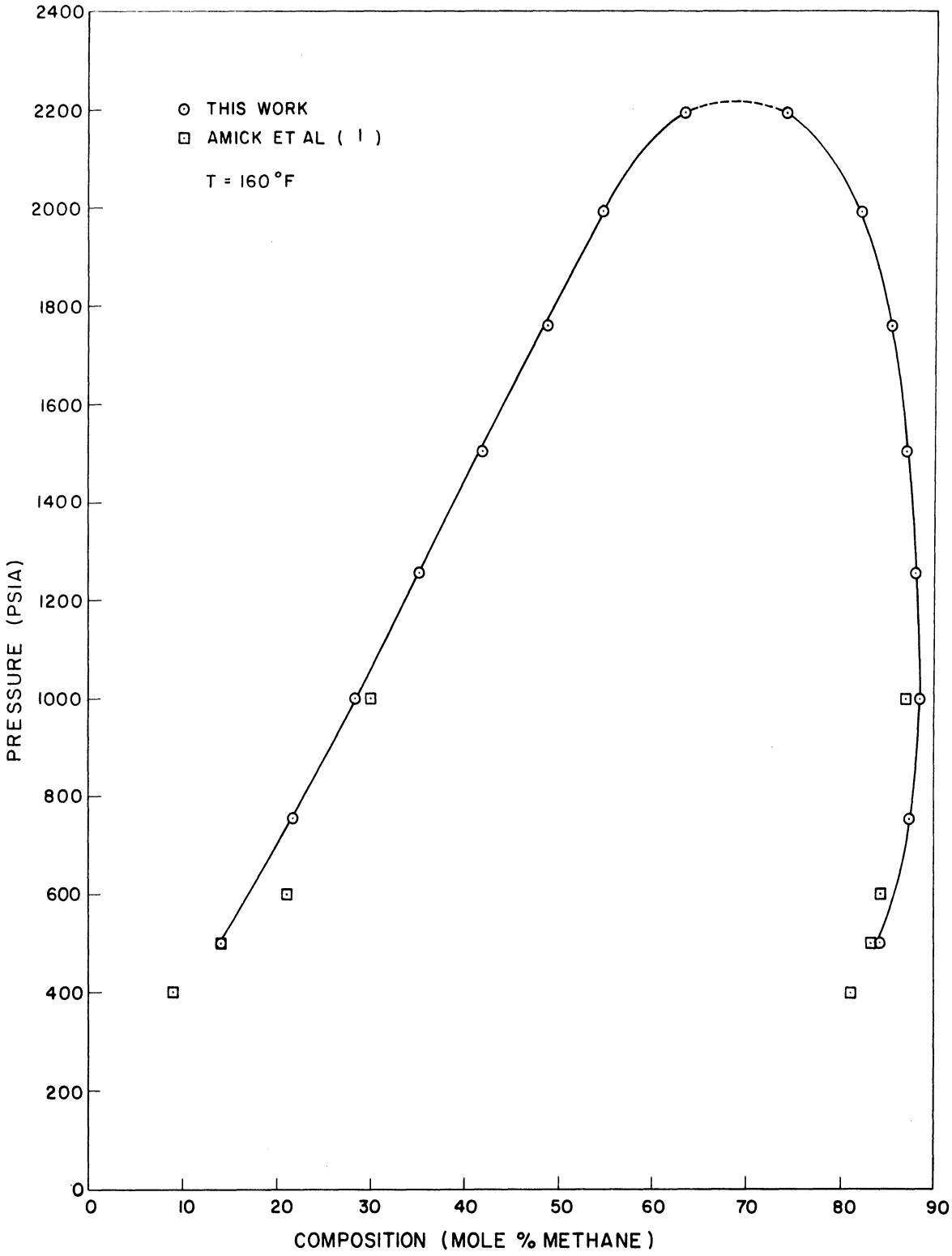

Figure 5. Pressure-Composition Diagram for Methane-Isopentane Binary System at 160°F.

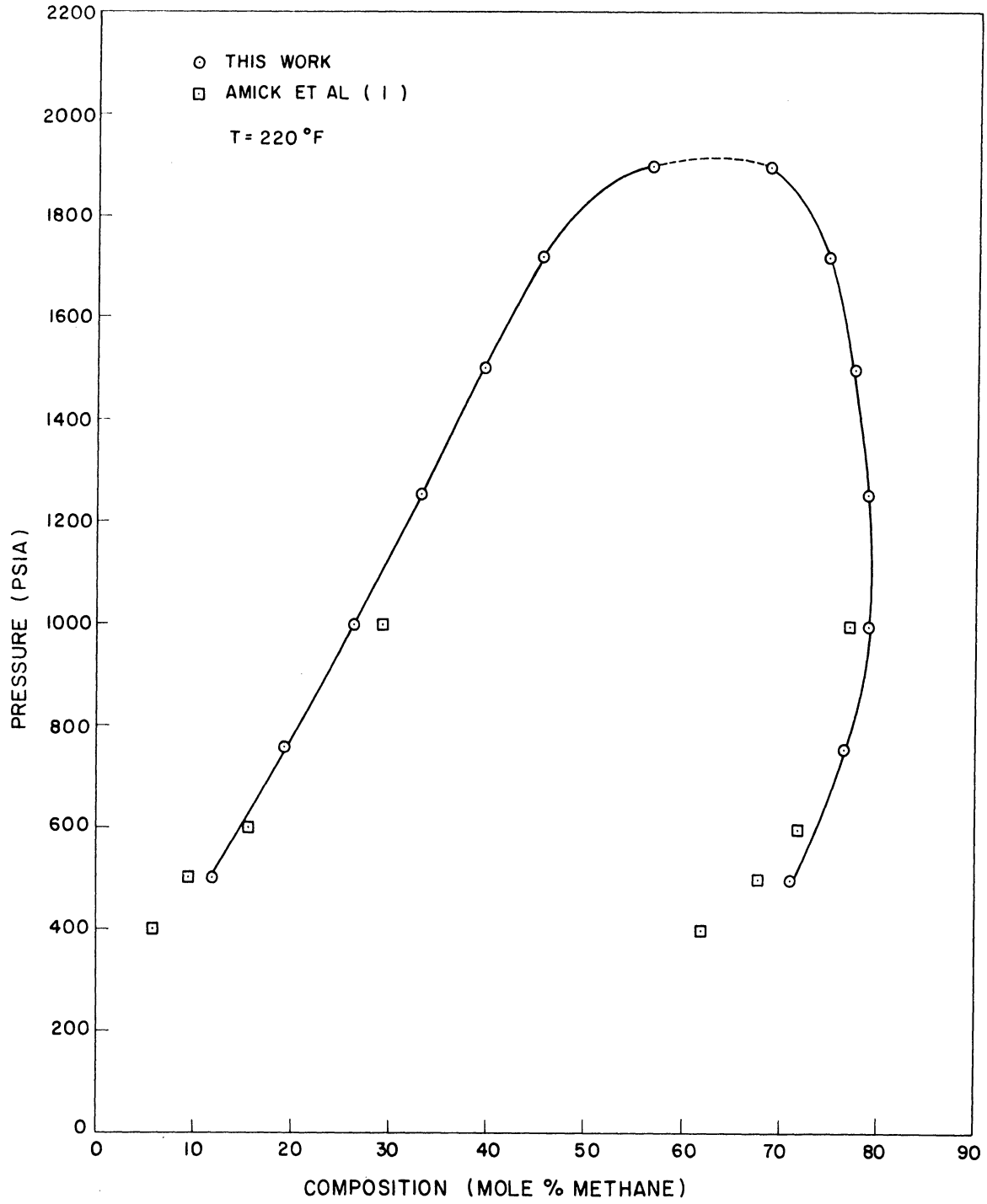

Figure 6. Pressure-Composition Diagram for Methane-Isopentane Binary System at 220°F.

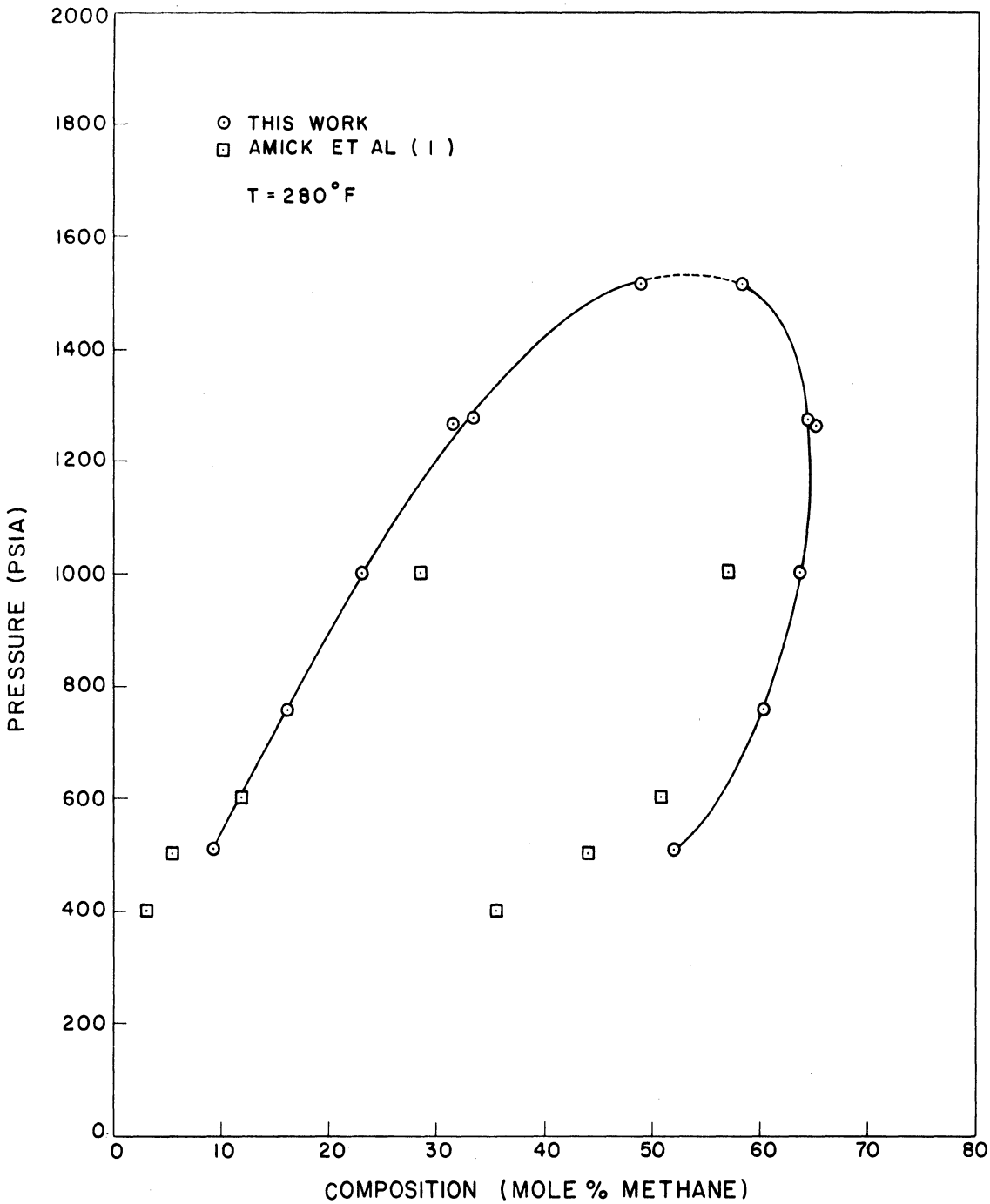

Figure 7. Pressure-Composition Diagram for Methane-Isopentane Binary System at 280°F.

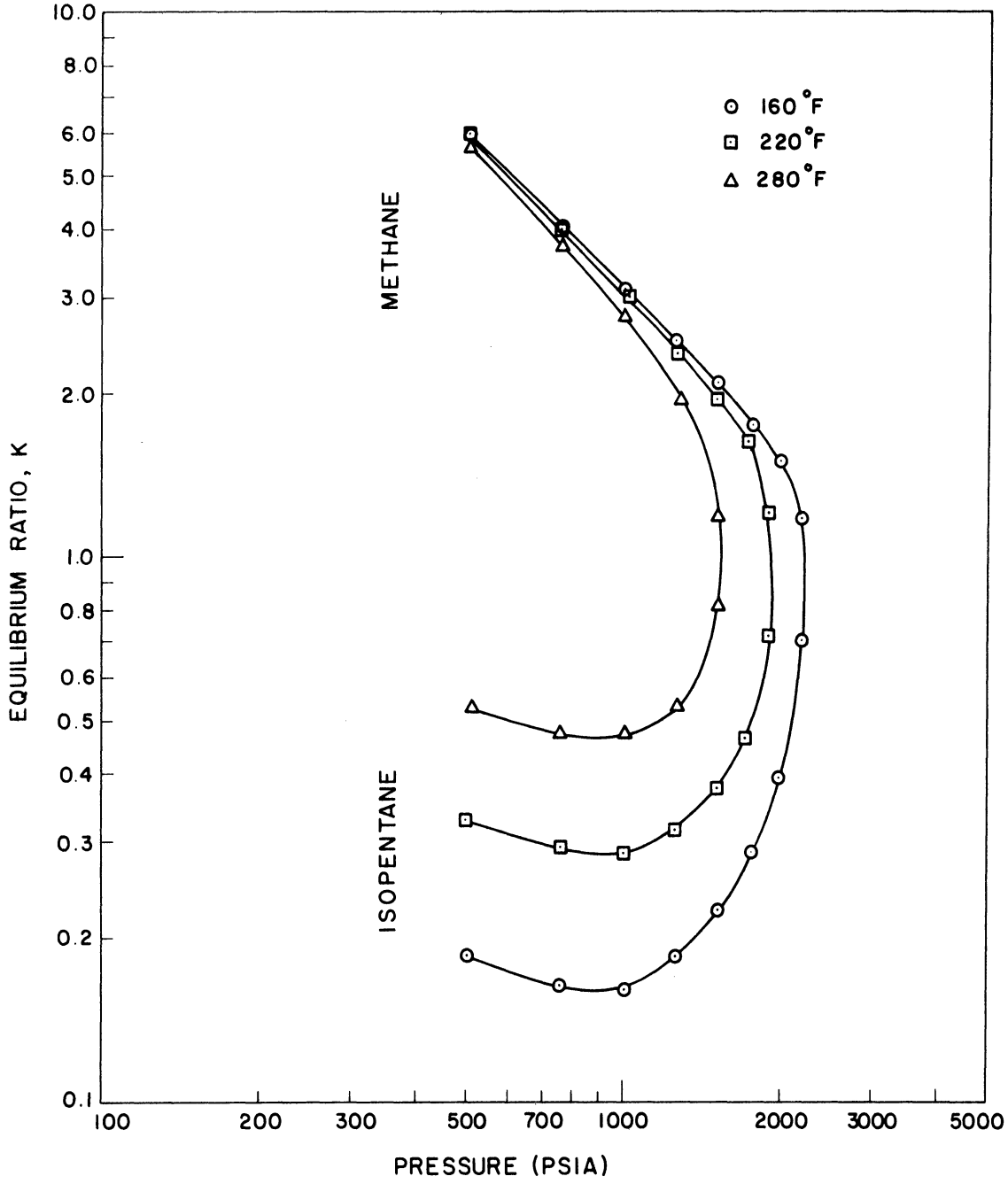

Figure 8. Equilibrium Ratio-Pressure Diagram for Methane-Isopentane Binary System.

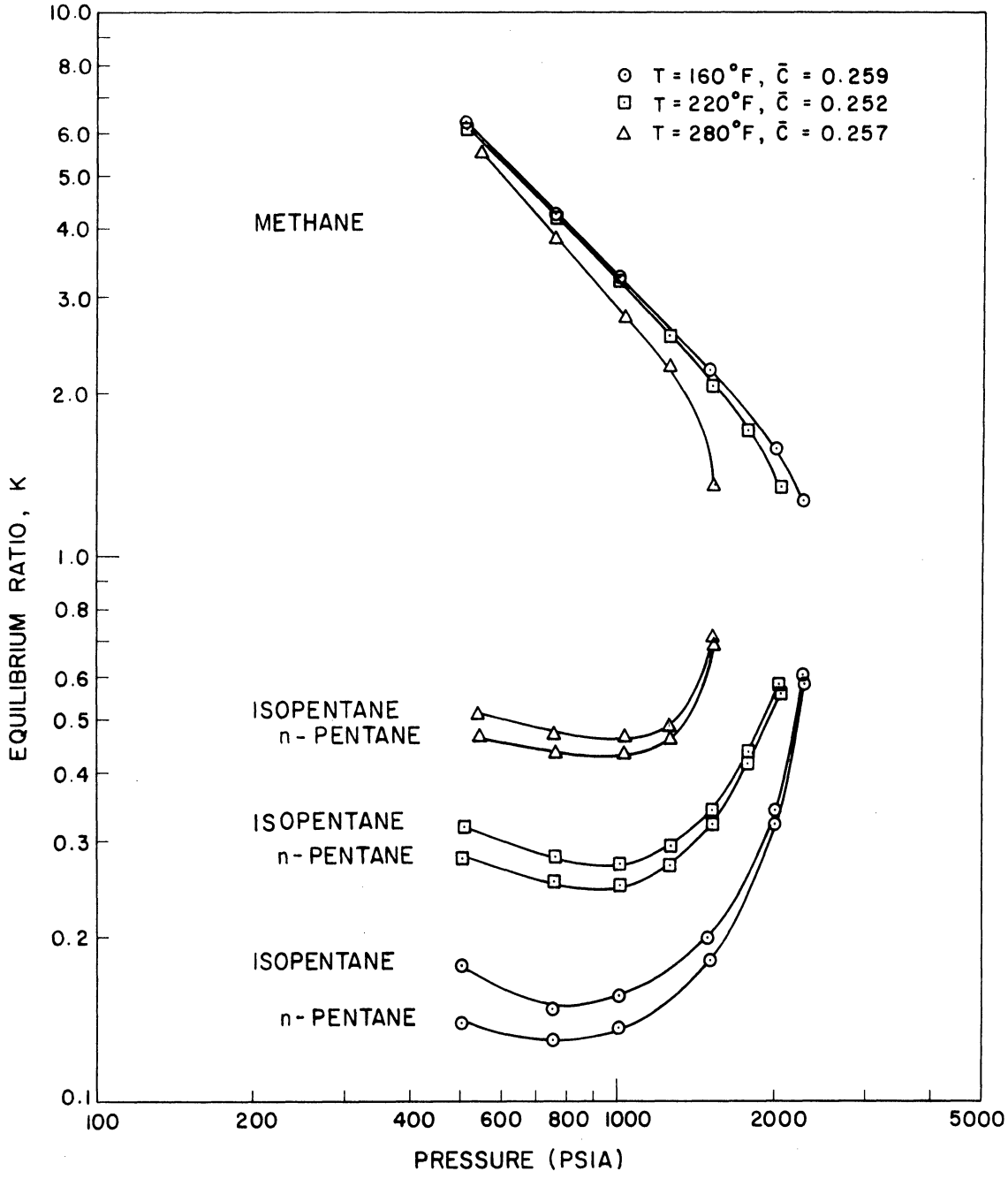

Figure 9. Equilibrium Ratio-Pressure Diagram for Methane-Isopentane-Normal Pentane Ternary System.

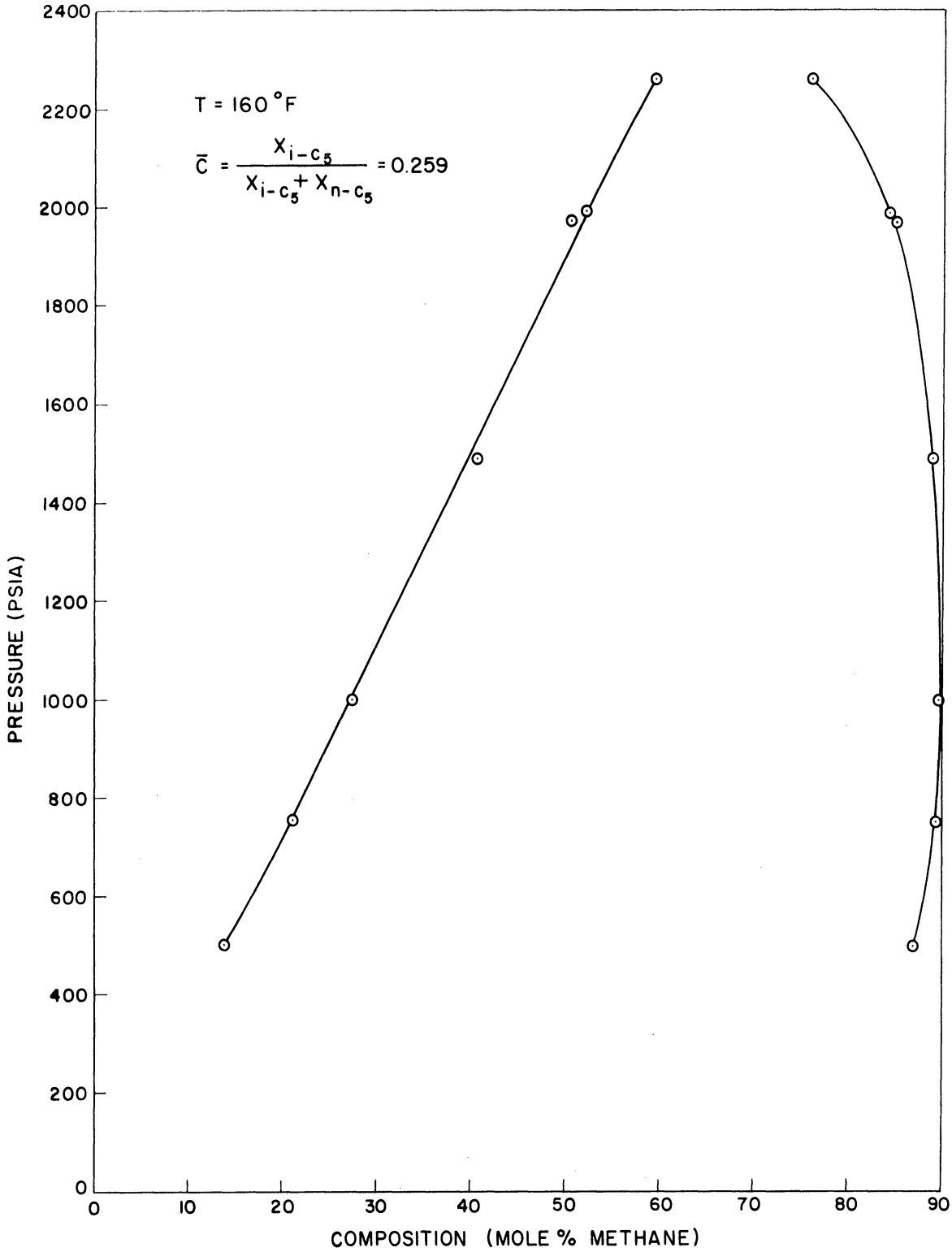

Figure 10. Pressure-Composition Diagram for Methane-Isopentane-Normal Pentane Ternary System at 160°F.

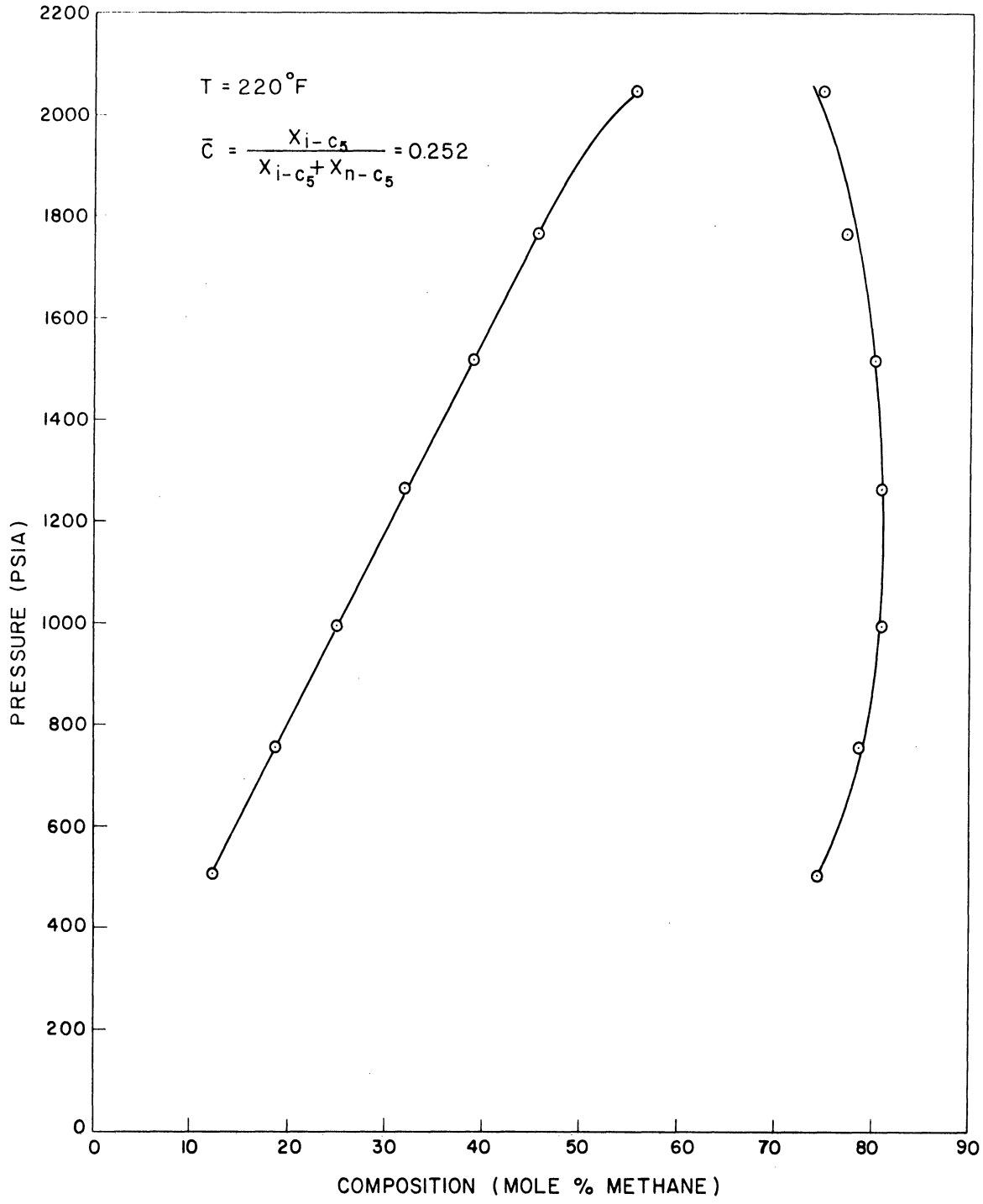

Figure 11. Pressure-Composition Diagram for Methane-Isopentane-Normal Pentane Ternary System at 220°F.

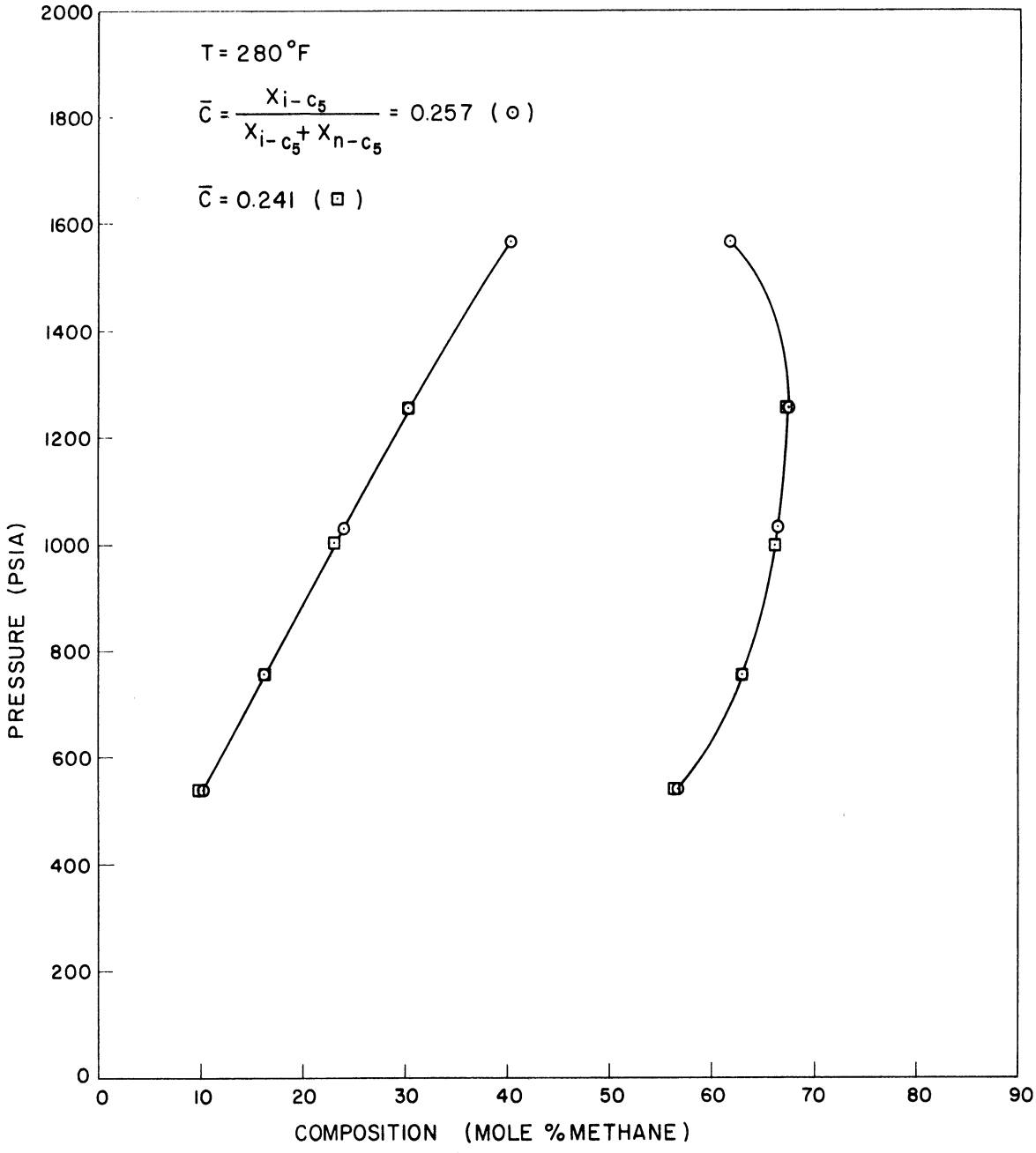

Figure 12. Pressure-Composition Diagram for Methane-Isopentane-Normal Pentane Ternary System at 280°F.

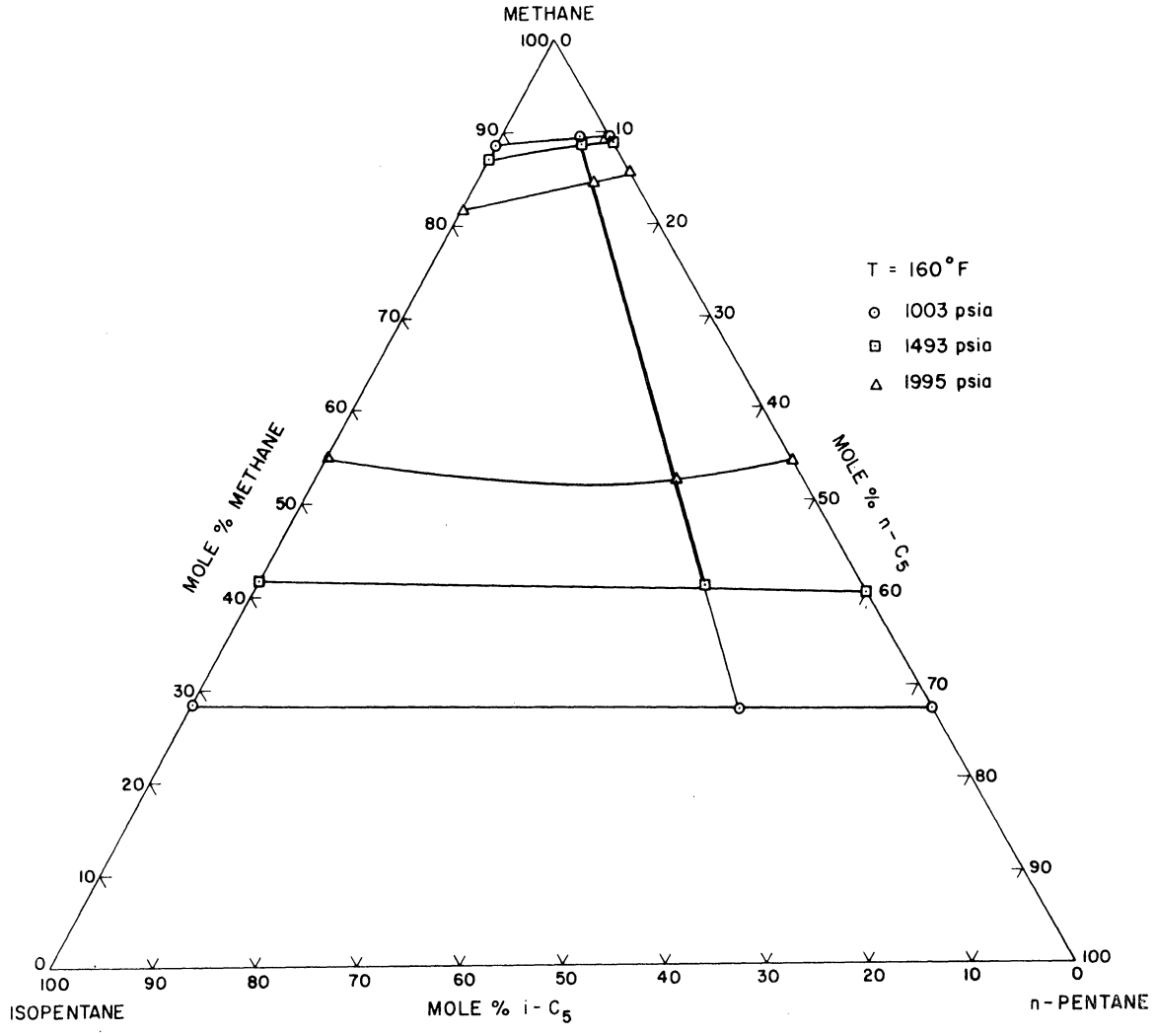

Figure 13. Triangular Composition Diagram for Methane-Isopentane-Normal Pentane System at 160°F.

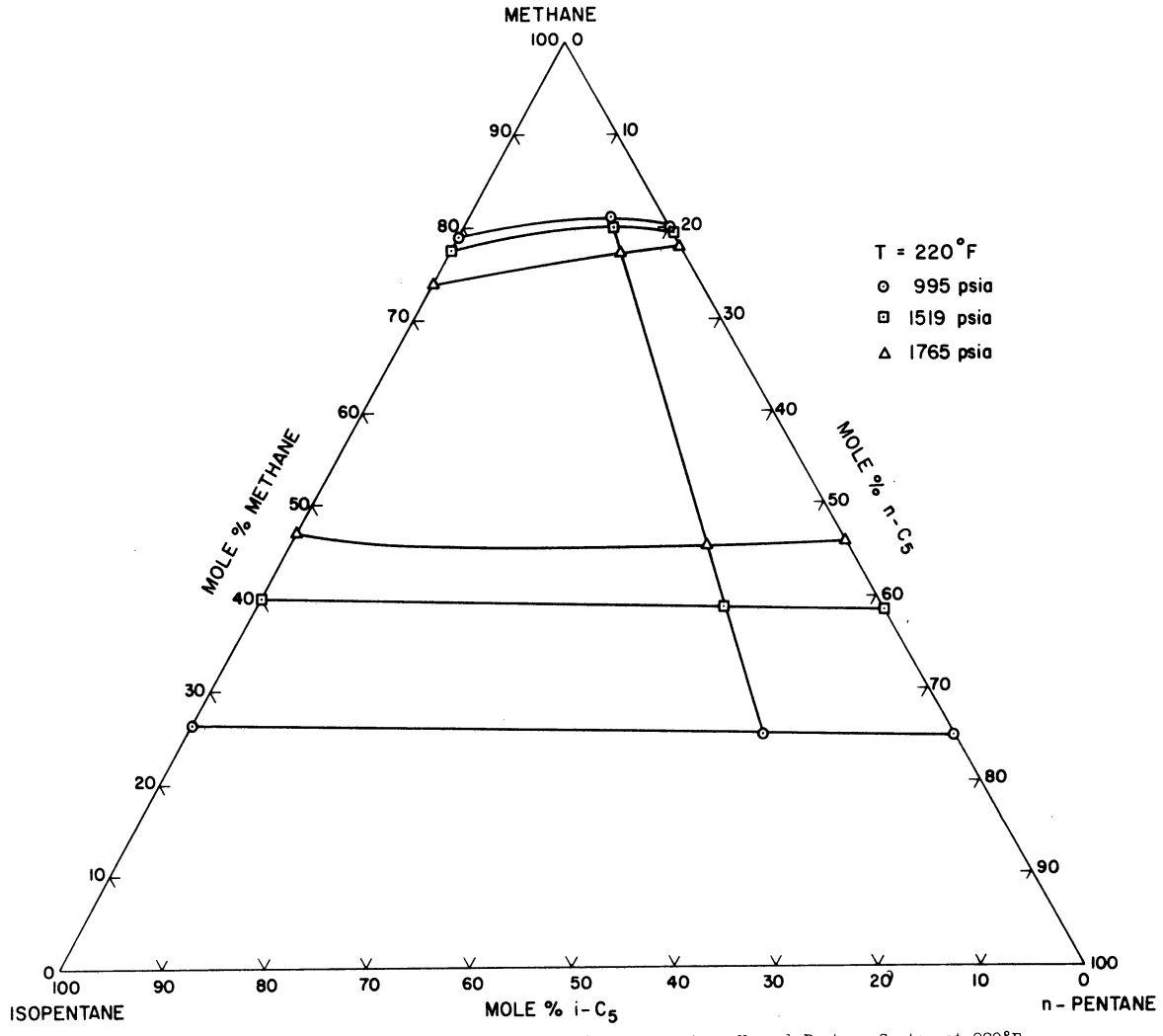

Figure 14. Triangular Composition Diagram for Methane-Isopentane-Normal Pentane System at 220°F.

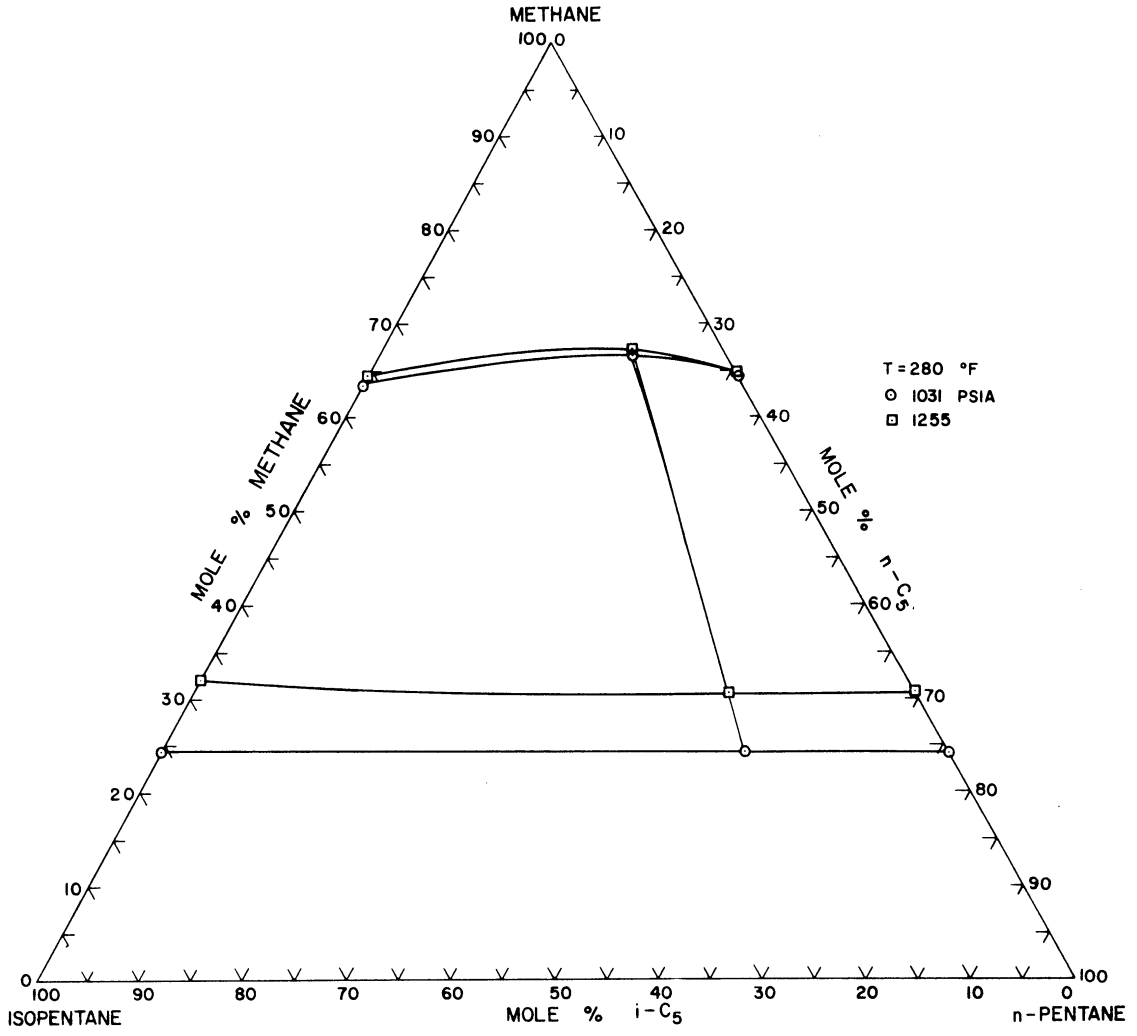

Figure 15. Triangular Composition Diagram for Methane-Isopentane-Normal Pentane System at 280°F.

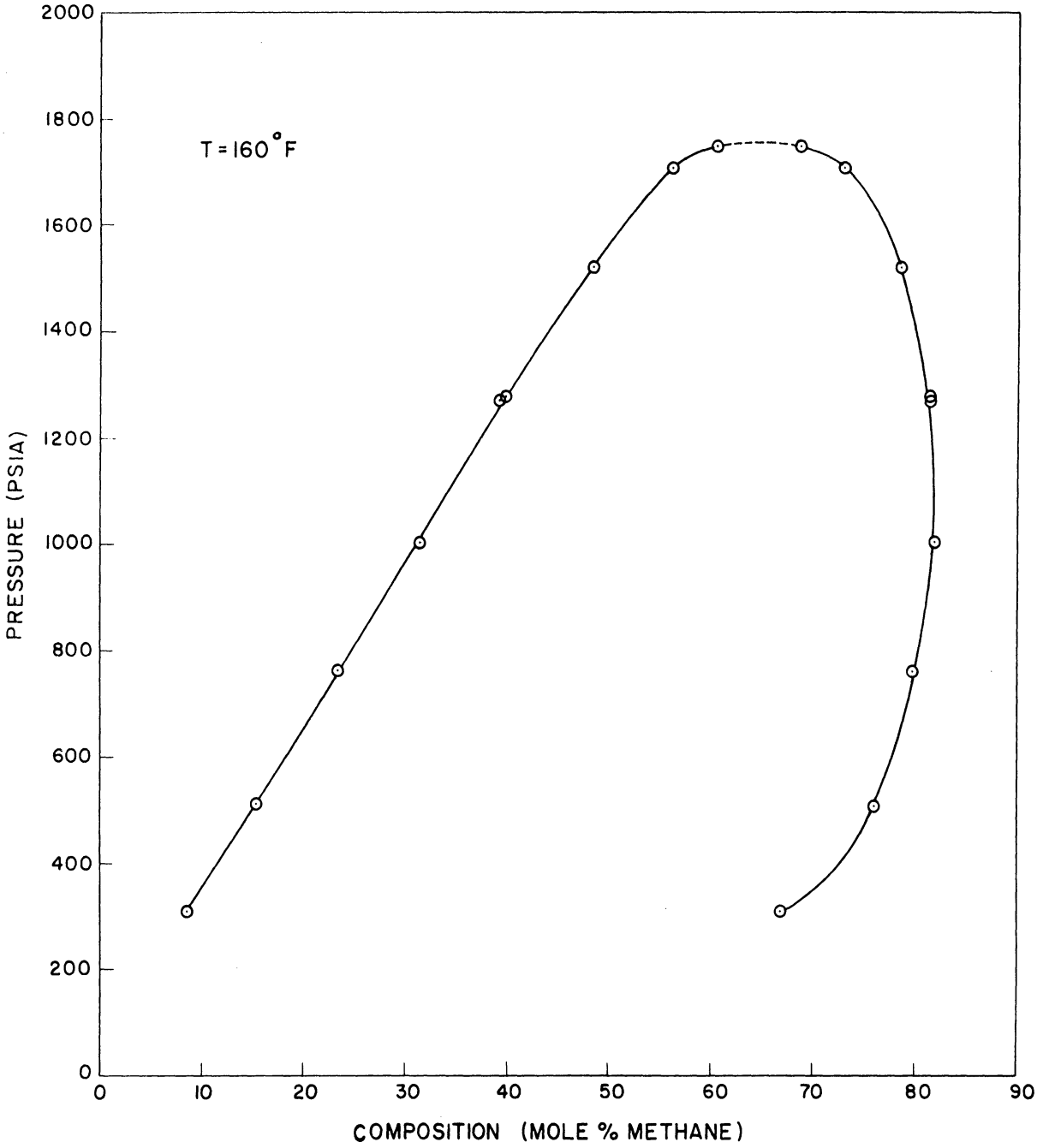

Figure 16. Pressure-Composition Diagram for Methane-Neopentane Binary System at 160°F.

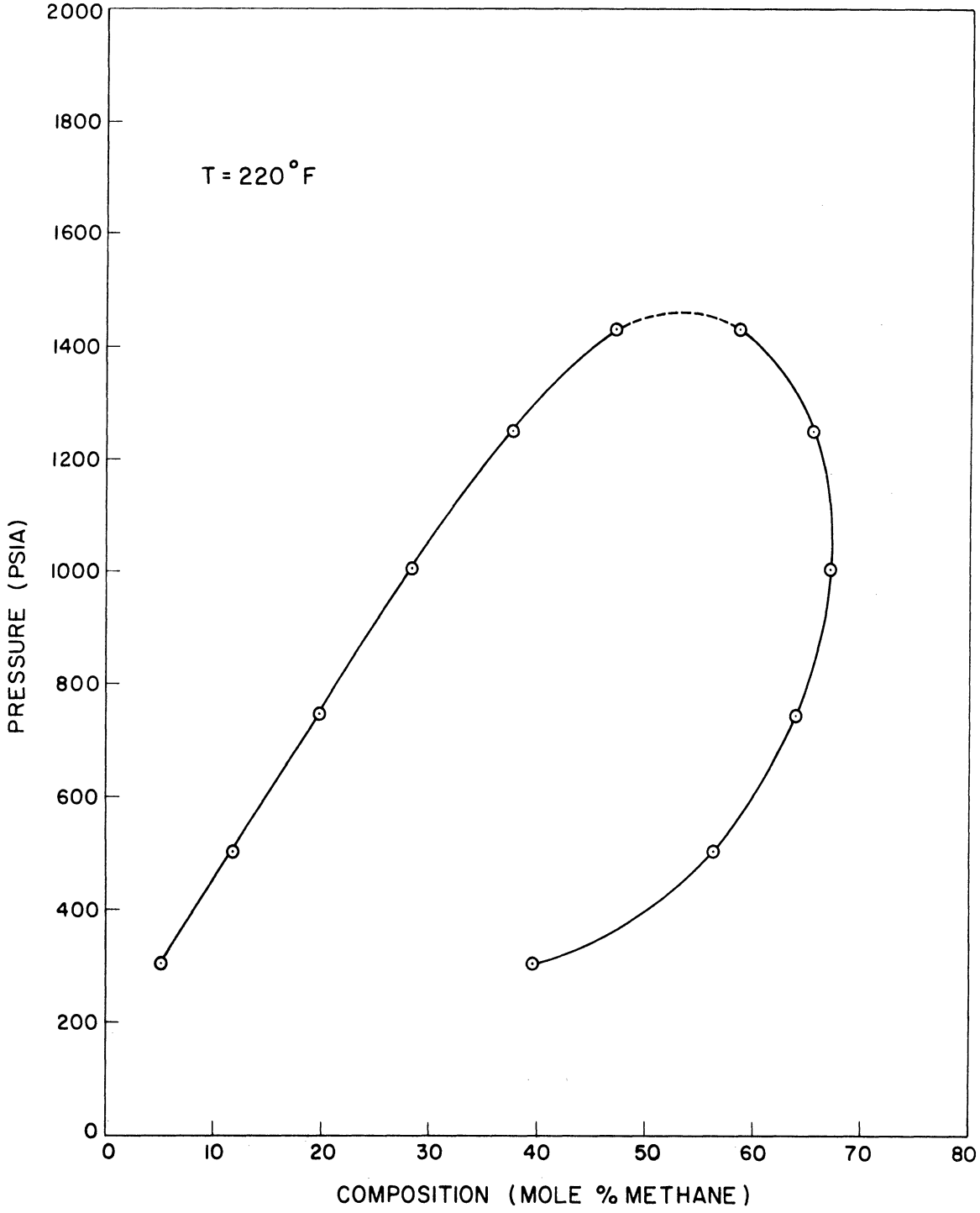

Figure 17. Pressure-Composition Diagram for Methane-Neopentane Binary System at 220°F.

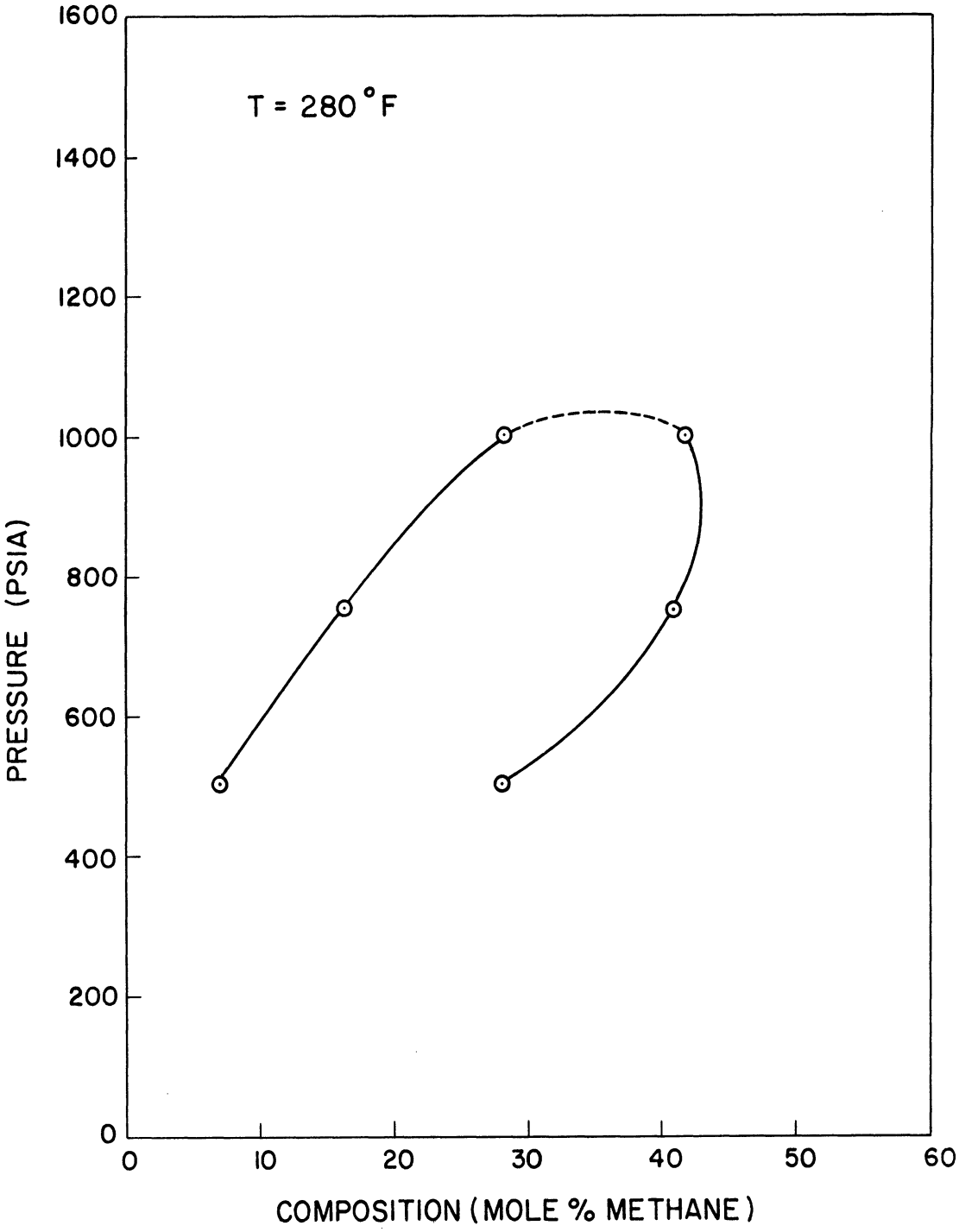

Figure 18. Pressure-Composition Diagram for Methane-Neopentane Binary System at 280°F.

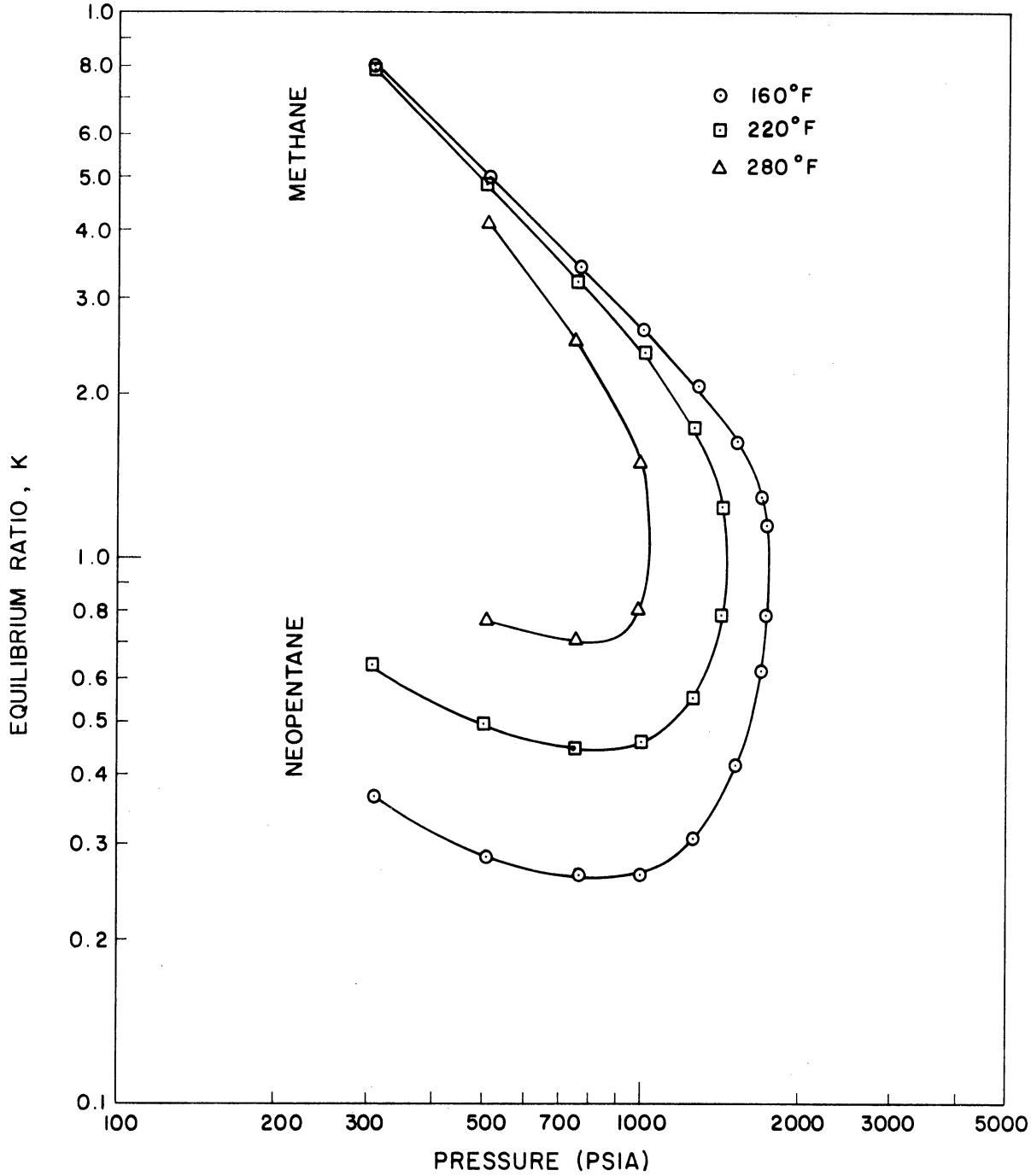

Figure 19. Equilibrium Ratio-Pressure Diagram for Methane-Neopentane Binary System.

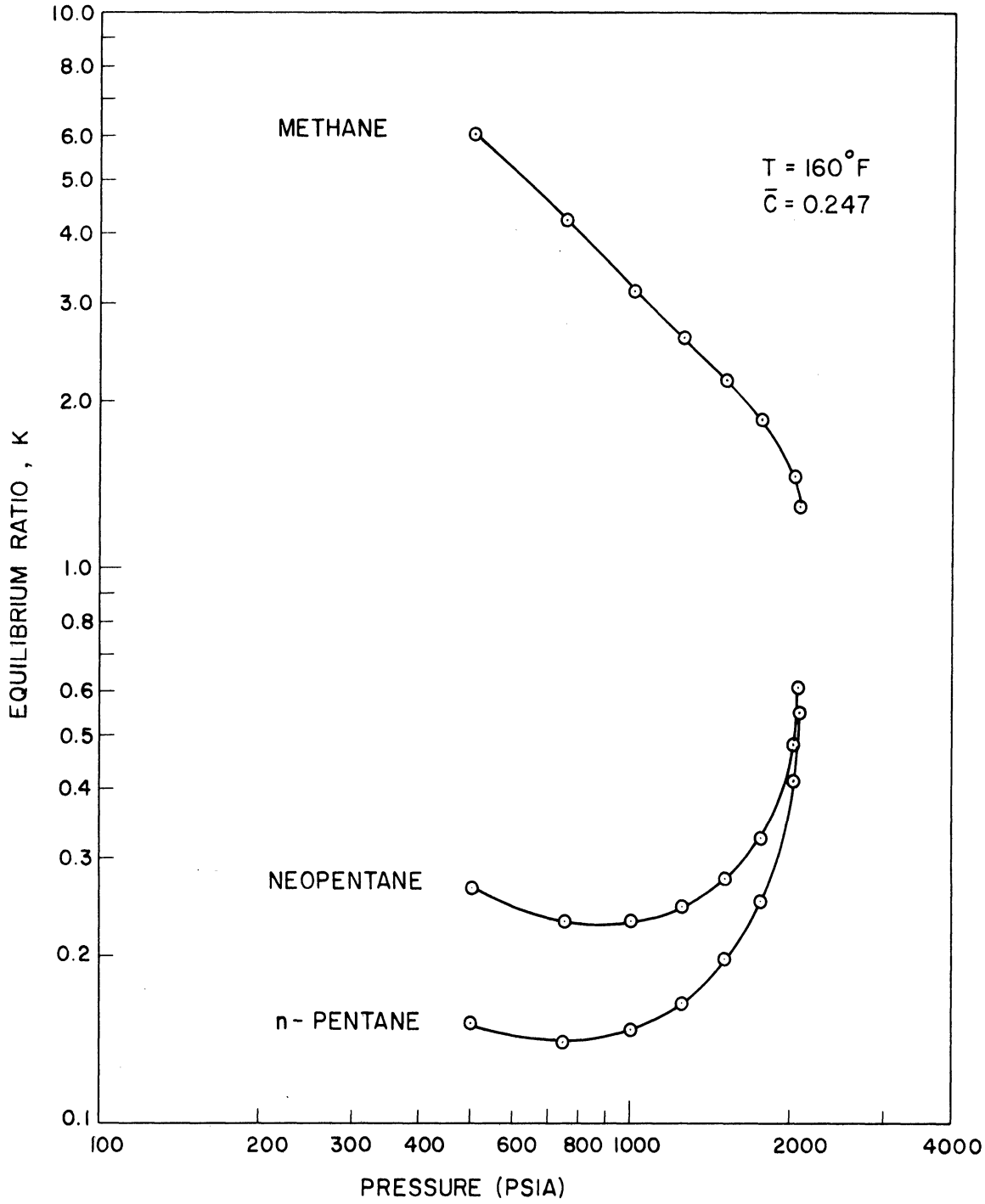

Figure 20. Equilibrium Ratio-Pressure Diagram for Methane-Neopentane-Normal Pentane Ternary System.

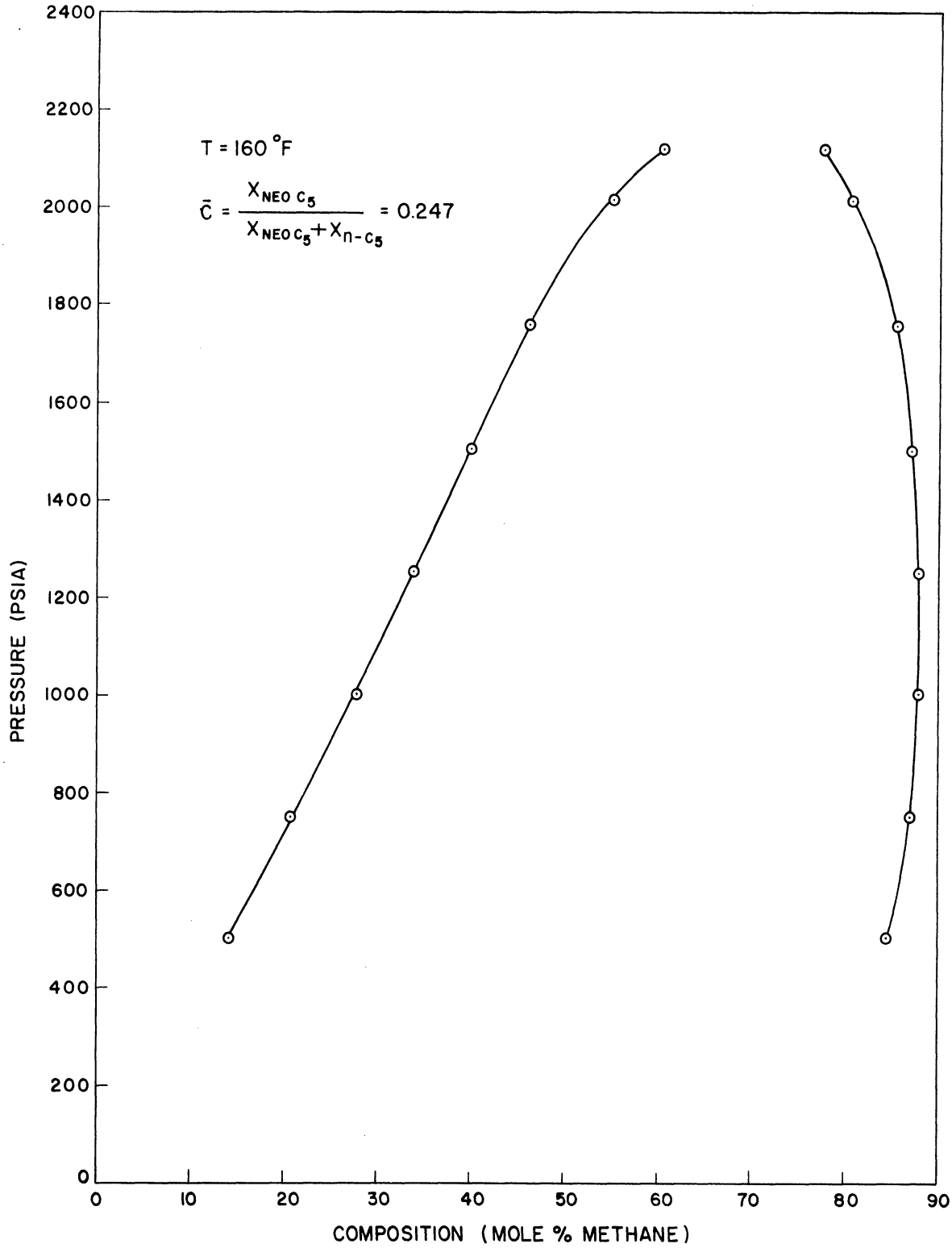

Figure 21. Pressure-Composition Diagram for Methane-Neopentane-Normal Pentane Ternary System at 160°F.

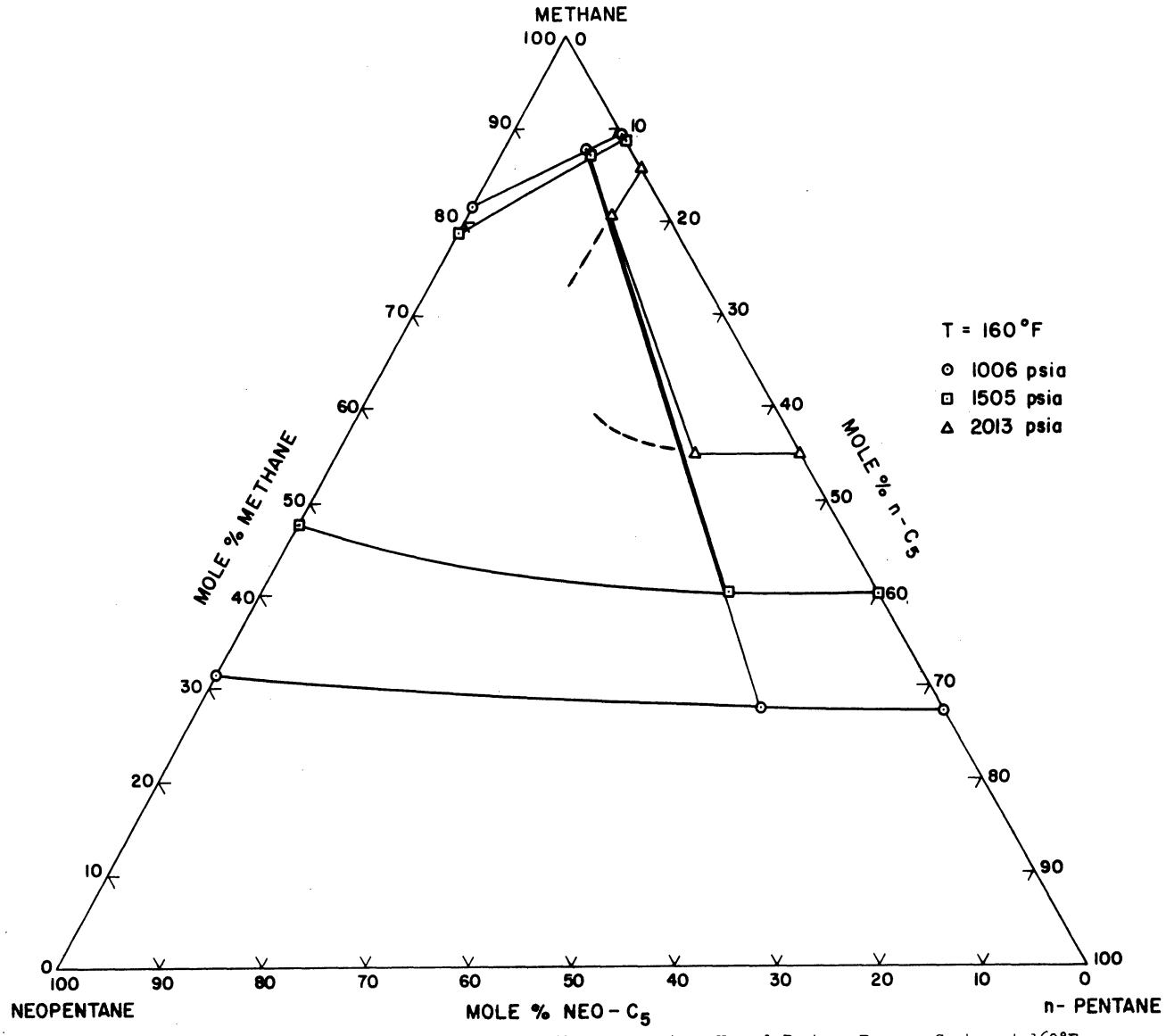

Figure 22. Triangular Composition Diagram for Methane-Neopentane-Normal Pentane Ternary System at 160°F.

VIII. ANALYSIS AND DISCUSSION OF RESULTS

The certainty of the experimental results in this research is dependent upon accuracy of measurements, experimental technique, and purity of the materials used.

The measurements made can be divided into three areas: pressure measurement, temperature measurement, and composition determination. The equilibrium pressures were measured with a Heise pressure gauge. This instrument has a pressure range of 0 to 3,000 psi and its scale is subdivided at 2 pounds per square inch intervals. The model used in this research was accurate to 0.1 percent over its entire range. The gauge was calibrated against a dead-weight tester and found to be accurate over its entire range of full scale. Accordingly, it is believed that the equilibrium pressures were known to within ± 3 pounds per square inch. Calibration of the Heise pressure gauge is given in Appendix C, Table XXVIII.

The temperature of the constant-temperature bath which contained the equilibrium cell was determined with a mercury-in-glass thermometer which was calibrated against standard thermometers. The uncertainty in the measurement of temperature is within $\pm .2°F$. However, temperature variations in the bath were caused by the temperature controller. At temperatures below about 220°F, fluctuations of the bath temperature were below 0.4°F. At a bath temperature of 280°F, the temperature fluctuation was within 0.5°F. Inasmuch as the equilibrium cell has a relatively large heat capacity, the cell contents would incur smaller temperature variations. It is believed that the overall uncertainty in temperature is $\pm .5°F$. Calibration of the mercury-in-glass thermometer is given in Table XXIX of Appendix C.

The compositions of the dew-point gas and the bubble-point liquid were investigated by withdrawal of a small portion of the vapor and liquid phases under isothermal and essentially isobaric conditions. Normally, at pressures below 0.7 of the critical, about a two to three psi pressure drop occurred after the vapor sample was withdrawn from the cell. At pressures near the critical region, a higher (about 8 psi) drop in pressure occurred upon vapor sample withdrawal. The compositions of the vapor and liquid samples were ascertained by gas chromatography. Duplicate analyses of the same sample were run as standard procedure. The data are tabulated in Appendix B, Tables XXVI and XXVII. The duplicate analyses agreed to within about 0.5 percent of methane for the majority of samples. It is believed that the analytical method is accurate to within 1.0 percent of the main constituent in the mixture. The gas chromatograph was calibrated with binary mixtures of known concentration. Details of the calibration procedure are given in Appendix C.

Although the reproducibility of the measurements, in particular the determination of composition, indicates adequate technique in analysis of the vapor phase and liquid phase samples, consideration must also be given to the uncertainty of the experimental technique--that is, certainty of equilibration and the withdrawal of representative samples from the cell. By making several runs at the same temperature and essentially the same pressure for the methane-normal pentane binary system, the reproducibility of the system can be determined. The results presented in Table II and Figure 4 indicate a reproducibility of about 1.0 percent.

Listed in Table I are the purities of the materials used in this research. Only the methane contains a significant impurity, about 0.7 percent nitrogen. Since the column used in the chromatograph cannot separate nitrogen and methane, the methane compositions determined in this work are slightly biased by the nitrogen impurity. To determine the effect of nitrogen on the experimental results, a material balance was made. Specific volume data reported by Sage et al.[50] on the methane-normal pentane binary system and K values of nitrogen reported by Roberts and McKetta[47] were used to make a nitrogen material balance. The results of these calculations showed that the maximum nitrogen concentration in the vapor phase was about 1.0 percent, with no significant accumulation of nitrogen in the system due to the sampling technique. This fact is further substantiated when one compares the result of this work on the methane-normal pentane binary system with that of Sage et al. Figure 4 shows the dew-point gas compositions to be slightly greater than those reported by Sage et al. by about 1.0 percent. The liquid phase compositions determined by them, however, are in very good agreement with those of this work.

Comparison of runs 66 through 69 and runs 66A through 69A further show no significant accumulation of nitrogen due to the sampling technique. Runs 66 through 69 were the last four runs of a series of eighteen runs made with an initial charge of isopentane-normal pentane mixture. Runs 66A through 69A were the first four runs of a new charge of isopentane-normal pentane mixture. Comparison of the methane concentration in the vapor phase of both sets of runs (see Figure 12) indicates no nitrogen accumulation within the accuracy of the analytical

technique. The isopentane to isopentane plus normal pentane concentration in the liquid phase is different, however, for the two sets of runs. This is a result of the relative volatility of isopentane to normal pentane. That is, the concentration on a methane-free basis of isopentane to normal pentane in the liquid phase is somewhat lower for runs 66 through 69 compared to runs 66A through 69A.

Figures 5 through 7 present and compare the phase composition data of this work and that reported by Amick, Johnson, and Dodge[1] for the methane-isopentane binary system. The data reported by Amick et al. are not in good agreement with this work. Their data do show considerable scatter, however, as can be seen in Figures 5 through 7. Amick et al. employed a bubble-and-dew-point device to obtain their data. In contrast to their conclusion, the results of this work show the solubility of methane in isopentane not to be very different from the solubility of methane in normal pentane.

For the methane-isopentane binary system, critical pressures for the three isotherms were determined graphically by extrapolating to zero, plots of system pressure versus the quantity $(y-x)^2$. The corresponding critical compositions of the binary systems investigated were determined by using the law of rectilinear diameters, where plots of equilibrium pressure versus the quantity $(y+x)/2$ were extrapolated to the previously determined critical pressures. It is believed that the graphically determined critical pressures have an uncertainty of $\pm$ 20 pounds per square inch, and the corresponding critical compositions have an uncertainty of less than $\pm$ 1 mole percent methane. Included in Table XIX are the critical pressures and corresponding critical compositions for temperatures 160°F, 220°F, and 280°F.

No data have been found in the literature for the methane-neopentane binary system. Therefore, no comparisons are made with data of this work. Critical pressures and critical compositions are indicated in Figures 16 through 18. They were determined in the same manner as described in the discussion of the methane-isopentane binary system. It is of interest to compare the methane-neopentane system with the methane-isopentane binary system. Figures 16 through 18, in contrast with Figures 5 through 7, reveal a significant difference in solubility of methane in these two pentane binary systems. The solubility difference of methane, expressed in terms of the equilibrium vaporization ratio, K, in the neopentane solution and the isopentane solution is also borne out by comparing Figures 8 and 10, respectively. One would expect this solubility difference in view of the difference of molecular structure of neopentane and isopentane. Because of its symmetrical structure, it is reasonable to assume that liquid neopentane would contain a larger void fraction than liquid isopentane. On this assumption, one can then visualize an increased solubility of a relatively spherical molecule such as methane.

TABLE XIX

GRAPHICALLY DETERMINED CRITICAL PROPERTIES FOR BINARY SYSTEMS

System	Temperature (°F)	Critical Pressure (psia)	Critical Composition (mole fraction methane)
methane-isopentane	160	2213	0.688
methane-isopentane	220	1917	0.638
methane-isopentane	280	1534	0.539
methane-neopentane	160	1755	0.644
methane-neopentane	220	1460	0.528
methane-neopentane	280	1035	0.354

Illustrated in Figures 9 through 15 is the effect of adding the intermediate constituent isopentane to the methane-normal pentane binary system. Figure 9 reveals that the effect of isopentane does not change the equilibrium vaporization ratio for methane significantly for any of the three isotherms. As can be seen in Figure 9, the K curves have similar characteristic shapes as those for binary systems. Figures 9 through 12 are characterized by an additional intensive property. The chosen property (designated as $\overline{C}$) is the average concentration of isopentane to isopentane plus normal pentane in the liquid phase. An average value was used since this mole fraction did change slightly during an isotherm determination. This is a result of the relative volatility of isopentane to normal pentane. For the methane-isopentane-normal pentane ternary system, the change in the mole fraction parameter for the 160°F and 220°F isotherms was less than 2 percent. For the 280°F isotherm, the change in mole fraction of isopentane to isopentane plus normal pentane was less than 2.5 percent. The triangular compostion diagrams, Figures 13 through 15, show reasonable consistency with the binary data of this work and Sage et al.

Figure 20 through 22 present the effect of adding a different intermediate constituent to the methane-normal pentane binary system. For this case, the third constituent is neopentane. Experimental data were obtained at one isotherm, 160°F. The solid lines in Figure 22 are the combining lines connecting the coexisting vapor and liquid phases. Mole fraction of the heavy components on a methane-free basis in the liquid phase is used as the third intensive property in Figures 20 and 21. For the reasons discussed in the preceding paragraph, an average value of

this property is presented in Figures 20 and 21. For this ternary system, the methane- free mole fraction of neopentane to neopentane plus normal pentane incurred about a 3 percent change for the isotherm (160°F) determination.

The general behavior portrayed in Figure 20 is similar to that found for binary systems; however, it does illustrate the influence of neopentane upon the equilibrium behavior of the individual components. Comparison of Figures 9 and 20 indicate a significant influence of the nature of the intermediate component, although a different isomer, upon the phase behavior of the light component, methane. That is, for essentially the same liquid phase parameter, neopentane in contrast with isopentane produces a decrease of the equilibrium ratio of methane for the same temperature and pressure of the system.

IX. ANALYTICAL CORRELATION PROCEDURE

The ultimate goal of phase equilibrium thermodynamics is to develop accurate and reliable methods to predict vapor-liquid phase behavior of complex mixtures. However, such methods can only be deemed reliable when subjected to direct comparison with experimental data. The correlation procedure adopted for the calculation of the equilibrium vaporization ratio K for the components investigated in this research is a modified form of the Chao-Seader correlation.[10]

Chao and Seader express the equilibrium vaporization ratio in terms of rigorously defined thermodynamic quantities (Equation (51))

$$K_i \equiv \frac{y_i}{x_i} \equiv \frac{\nu_i^\circ \gamma_i}{\phi_i}$$

where ν_i° is the liquid phase fugacity coefficient, and is defined as f_i°/P, γ_i is the liquid phase activity coefficient, and ϕ_i is the vapor phase fugacity coefficient. Equation (51) is obtained by substitution of Equations (18) and (22) into Equation (12). That is,

$$y_i \phi_i P = x_i \gamma_i f_i^\circ \tag{66}$$

Rearranging Equation (66) in terms of the definition of the equilibrium ratio, K_i yields Equation (51). In this section a detailed discussion is given on the method employed to calculate the thermodynamic functions in Equation (51).

A. Equation of State

A good equation of state is necessary in deriving thermodynamic functions to represent experimental vapor-liquid equilibrium data. For

this work the equation presented by Benedict, Webb, and Rubin[4] was chosen to evaluate the specific volume of the vapor phase, the compressiblity factor Z, and the vapor phase fugacity coefficient ϕ. The reasons for selecting this equation as opposed to other equations of state were twofold. First, the B-W-R equation can be used to predict thermodynamic properties in the critical region. Second, constants used to describe the behavior of the vapor phase region have been determined for all the pure components studied in this research.

The relationship between the fugacity coefficient and pressure, temperature, and volume is given by Equation (25). Substitution of the B-W-R equation into Equation (21) yields an expression for the fugacity coefficient ϕ_i :

$$RT \ln \phi_i = RT \ln \frac{1}{Z} + \left[(B_o + B_{oi}) RT - 2 (A_o A_{oi})^{1/2} - 2 (C_{oi} C_o)^{1/2} / T^2 \right] \frac{1}{V} + \frac{3}{2} \left[RT (b^2 b_i)^{1/3} - (a^2 a_i)^{1/3} \right] \frac{1}{V^2}$$

$$+ \frac{3}{5} \left[a (\alpha^2 \alpha_i)^{1/3} + \alpha (a^2 a_i)^{1/3} \right] \frac{1}{V^5} + \qquad (67)$$

$$+ \frac{3 \frac{1}{V^2} (c^2 c_i)^{1/3}}{T^2} \left[\frac{1 - \exp(-\gamma \frac{1}{V^2})}{\gamma \frac{1}{V^2}} - \frac{\exp(-\gamma \frac{1}{V^2})}{2} \right]$$

$$- \frac{2 \frac{1}{V^2} c}{T^2} \left(\frac{\gamma_i}{\gamma} \right)^{1/2} \left[\frac{1 - \exp(-\gamma \frac{1}{V^2})}{\gamma \frac{1}{V^2}} - \exp(-\gamma \frac{1}{V^2}) - \frac{\gamma \frac{1}{V^2} \exp(-\gamma \frac{1}{V^2})}{2} \right]$$

In the case of this research, the constants used for the computations were obtained from the literature and are given in Table XX.

TABLE XX

CONSTANTS FOR BWR EQUATION OF STATE FOR INDIVIDUAL MATERIALS USED IN THIS RESEARCH

Substance	Methane[4]	Neopentane[7]	Isopentane[4]	Normal Pentane[4]
Bo	0.0426000	0.170530	0.160053	0.156751
Ao	1.855500	12.9635	12.7959	12.1794
Co x 10^{-6}	0.0225700	1.273	1.74632	2.12121
b	0.00338004	0.0668120	0.0668120	0.0668120
a	0.0494000	3.4905	3.75620	4.07480
c x 10^{-6}	0.00254500	0.546	0.695000	0.824170
α x 10^{3}	0.124359	2.000	1.70000	1.81000
γ x 10^{2}	0.600000	5.000	4.63000	4.75000

Units:

P = Normal atmosphere

d = gm-moles/liter

T = ^{o}K = ^{o}C + 273.16

R = 0.08207 (liter)(atm)/(gm-mole)(^{o}K)

B. Activity Coefficient

The various forms of representing activity coefficients have been previously discussed. Prausnitz, Edmister, and Chao[42] have recommended that the Hildebrand-Scott[20] regular solution theory correlation for activity coefficient be used in non-polar mixtures. Chao and Seader claim good representation of experimental data using this equation.

Equation (45a) is given as

$$RT \ln \gamma_i \equiv \underline{V}_i^{L} \left[\delta_i - \bar{\delta} \right]^2$$

The solubility parameter designated by the symbol δi is defined as Equation (45b)

$$\delta_i \equiv \left[\frac{\Delta E^v}{\underline{V}_i} \right]^{1/2}$$

where ΔE^v at ordinary temperatures can be identified with the energy of vaporation or the energy required to vaporize the liquid to infinite volume, and $\underline{V}_i$ is the molal volume of constituent i. The symbol $\bar{\delta}$ designates the volume average value of the solubility parameter for the solution and is given in mathematical form as:

$$\bar{\delta} \equiv \frac{\sum_i x_i \underline{V}_i \delta_i}{\sum_i x_i \underline{V}_i} \tag{68}$$

Equations (45a), (45b), and (68) are given by Chao and Seader.

At temperatures well below the critical, the energy of vaporization is essentially the enthalpy of vaporization minus the quantity RT, so that Equation (45b) may be rewritten as

$$\delta_i = \left[\frac{\Delta \underline{H}_i - RT}{\underline{V}_i} \right]^{1/2} \tag{69}$$

The approximate variation of the solubility parameter with temperature is given by Hildebrand and Scott[20] as

$$\frac{d \ln \delta}{dT} \simeq -1.25 \alpha \tag{70}$$

where α denotes the coefficient of thermal expansion.

Prausnitz, Edmister, and Chao have prepared a plot of log δ as a function of temperature for several hydrocarbons. Chao and Seader give values of the solubility parameter for one temperature only, since they assume the solubility parameter is independent of temperature. At the outset, values for the solubility parameter used in this correlation were taken from the plot of Praunitz et al. Later constant values for the solubility parameter as given by Chao and Seader were used. Direct comparisons of the predicted equilibrium vaporization ratios, using both sets of values of the solubility parameter, indicated that better agreement between the observed equilibrium vaporization ratios determined from this work and those predicted by the correlation could be obtained when solubility parameter values presented by Chao and Seader were used.

The values of solubility parameter used in this work are presented in Table XXI.

TABLE XXI

SOLUBILITY PARAMETERS

Component	δ $(cal/ml)^{1/2}$	Source
Methane	5.68	(10)
Neopentane	6.25	(20)
Isopentane	6.75	(20)
Normal Pentane	7.02	(10)

Table XXII presents the critical constants used in this correlation. Also included in Table XXII are the values for liquid molal volume and the acentric factor as presented by Chao and Seader.

TABLE XXII

CONSTANTS FOR PURE COMPONENTS

Component	T_c (°F)	P_c (PSIA)	ω	$\bar{V}^L$ (ml/gm-mole)
Methane	-115.8	673.1	0.0	52
Neopentane	321.1	464.0	0.195	123.3
Isopentane	370.1	483.0	0.2104	117.4
Normal Pentane	385.9	489.5	0.2387	116.1

C. Fugacity Coefficient of the Pure Liquid Component

The fugacity coefficient for a pure liquid is defined as the reference fugacity f_i^o divided by the total pressure P. The reference fugacity of a pure liquid is usually, but not always, taken to be the fugacity of the pure component at a system temperature and under its own vapor pressure. In equation form, we write the reference fugacity as

$$f_i^\circ = P^\square \left[\frac{f_i^\circ}{P^\square} \right] \tag{71}$$

where the term in parenthesis is the liquid phase fugacity coefficient based on the vapor pressure. The fugacity coefficient at the vapor pressure can be corrected to the system pressure by the Poynting effect. Then dividing Equation (71) by the total pressure P gives

$$\frac{f_i^\circ}{P} = \frac{P^\square}{P} \left[\frac{f_i^\circ}{P^\square} \right] \exp\left[\frac{\bar{V}_i}{RT} dP \right] \tag{72}$$

If integration is carried out assuming an average value for the specific volume for the liquid, the following results

$$\ln v^{\circ} = \ln \frac{P^{\square}}{P} + \ln \left[\frac{f_i^{\circ}}{P^{\square}} \right] + \frac{V_{i\,ave.}(P - P^{\square})}{RT} \quad (73)$$

Generalized fugacity coefficients as functions of reduced temperature, reduced pressure, and critical compressibility factor, Z_c, have been presented by Lydersen, Greenkorn, and Hougen.[34] Curl and Pitzer[13] present generalized fugacity coefficients as a function of reduced temperature, reduced pressure, and a third parameter which they call the acentric factor. A correlation does exist between the critical compressiblity factor and the acentric factor. Riedel[46] demonstrates this relationship.

The acentric factor which Curl and Pitzer define as (Equation (31))

$$\omega \equiv \left[1.000 + \log P_r^{\square} \right]_{T_r = 0.7}$$

indicates the deviation of the behavior of substances from that of simple fluids. Chao and Seader extend the Curl and Pitzer correlation of the liquid phase fugacity coefficient to conditions where a liquid mixture component does not exist as a pure liquid. The extension is achieved through calculation from experimental vapor-liquid equilibrium data. The analytical expression given by Chao and Seader for the liquid phase fugacity coefficient is

$$\log v^{\circ} = \log v^{(0)} + \omega \log v^{(1)} \quad (74a)$$

The term $\nu^{(o)}$ is the fugacity coefficient of simple fluids which are characterized by a zero acentric factor. The term $\nu^{(1)}$ is a correction term, and accounts for the departure of the properties of real fluids from those of simple fluids. Chao and Seader have expressed the quantities $\nu^{(o)}$ and $\nu^{(1)}$ as functions of reduced temperature and pressure. These terms have been fitted with the following functional forms.

$$\log \nu^{(0)} = A_0 + \frac{A_1}{T_r} + A_2 T_r + A_3 T_r^2 + A_4 T_r^3 \qquad (74b)$$
$$\left[A_5 + A_6 T_r + A_7 T_r^2\right] P_r + \left[A_8 + A_9 T_r\right] P_r^2 - \log P_r$$

and

$$\log \nu^{(1)} = -4.23893 + 8.65808 T_r \qquad (74c)$$
$$-\frac{1.22060}{T_r} - 3.15224 T_r^3 - 0.025\left[P_r - 0.6\right]$$

The coefficients in Equation (74b) as given by Chao and Seader are presented in Table XXIII.

TABLE XXIII

CONSTANTS FOR LIQUID PHASE FUGACITY COEFFICIENT EXPRESSION

	Simple Fluid	Methane
A_0	5.75748	2.43840
A_1	-3.01761	-2.24550
A_2	-4.98500	-0.34084
A_3	2.02299	0.00212
A_4	0	-0.00223
A_5	0.08427	0.10486
A_6	0.26667	-0.03691
A_7	-0.31138	0
A_8	-0.02655	0
A_9	0.02883	0

The acentric factors listed in Table XXII are not derived from the original definition. The values are those presented by Chao and Seader and were determined as a parameter for the best fitting of the vapor pressure data for pure components according to the Chao-Seader correlation given by

$$\omega = \frac{\sum_i \log \nu_i^{(1)} \left[\log \phi_i - \log \nu_i^{(0)}\right]}{\sum_i \left[\log \nu_i^{(1)}\right]^2} \qquad (75)$$

A computer program was written to calculate equilibrium vaporization ratios from Equation (51). At the outset Equations (45), (67), and (74) were used in conjunction with Equation (57) to calculate the equilibrium vaporization ratios of the compounds studied in this work. After several trial runs, it became apparent that the calculated equilibrium ratios for methane were always greater than observed values, and that this discrepancy increased with increasing pressure. In view of the fact that the formulation of activity coefficients (Equation (45a)) is independent of pressure and that the Benedict, Webb, and Rubin equation[4] is believed to be reliable in representing the P-V-T behavior of gaseous mixtures, the expression for liquid phase fugacity coefficient was modified.

Since the acentric factor equals zero for methane, Equation (74a) reduces to

$$\log \nu^{\circ} = \log \nu^{(0)} \qquad (76)$$

The expression for $\log \nu^{(0)}$ (Equation (74b)) was then divided by the quantity $(1+Px10^{-4})$ where P is the total pressure of the system. It should be remembered that this quantity has no theoretical implications and that it is only a first order approximation to better fit the experimental data.

Table XXV in Appendix A presents comparisons of the calculated equilibrium vaporization ratios with the observed equilibrium vaporization ratios. The percent deviation is defined by

$$\text{Percent Deviation} = \frac{K_{OBS} - K_{CALC}}{K_{OBS}} \times 100 \qquad (77)$$

Also included in this table are the numerical values for the vapor and liquid phase fugacity coefficients, liquid activity coefficients, vapor specific volume, and the compressiblity of the vapor.

At the end of each system investigated in this research is the numerical value for the average absolute percent deviation. As can be seen, calculated K values and observed K values are in reasonably good agreement, except near the critical region. The average absolute deviation for the methane-normal pentane binary system is about 4 percent. For the methane-isopentane binary system, the average absolute deviation is within 8 percent. The average absolute percent deviation for the methane-neopentane-normal pentane ternary and methane-isopentane-normal pentane ternary systems are 6.3 percent and 6.0 percent, respectively. Inspection of Table XXV for the methane-neopentane binary system reveals the predicted methane K values to be in greater error than the predicted neopentane K values, especially at higher temperatures. This observation concurs with the temperature restriction for methane imposed on the Chao-Seader correlation. In other words, the Hildebrand equation cannot predict accurately methane behavior at temperatures above 0.93 of the pseudocritical temperature of the equilibrium liquid mixture. It appears unlikely that the complex behavior of liquid

mixtures composed of constituents with such different physical properties as methane and pentanes can be represented in the critical region by such relatively simplified expressions as Equations (45) and (74).

X. SUMMARY AND CONCLUSIONS

The methane-normal pentane binary system was investigated at a temperature of 220°F. Comparison of this work with previous investigations is good.

Phase equilibrium data were obtained for the methane-isopentane binary system at temperatures of 160°F, 220°F, and 280°F and pressures from about 500 pounds per square inch up to the critical region. The data are presented in both graphical and tabular form.

Vapor-liquid equilibrium data have been obtained throughout the coexisting-phase region for the methane-neopentane binary system at pressures from about 300 pounds per square inch to the critical region for temperatures of 160°F, 220°F, and 280°F. Pressure versus composition curves and equilibrium vaporization ratio versus pressure diagrams are included. Experimental equilibrium vaporization ratios of methane are significantly lower in a methane-neopentane binary system than in a methane-isopentane binary system. The critical pressures are lower for the methane-neopentane binary system compared to the methane-isopentane binary system for temperatures of 160°F, 220°F and 280°F.

Equilibrium vaporization ratios have been experimentally determined for the methane-isopentane-normal pentane ternary system at temperatures of 160°F, 220°F, and 280°F and pressures from about 500 pounds per square inch up to the critical region. Data are presented graphically and are also tabulated.

The two-phase equilibrium behavior for the methane-neopentane-normal pentane ternary system has been experimentally determined for a

temperature of 160°F and pressures from about 500 pounds per square inch up to the critical region. The experimental results are tabulated and presented graphically.

A computer program has been written to calculate equilibrium vaporization ratios. The correlation employs the Benedict, Webb, and Rubin[4] equation of state to predict vapor phase fugacity coefficients. Hildebrand's regular solution theory is applied to the liquid phase. And the expression given by Chao and Seader[10] is used to calculate the liquid phase fugacity coefficient. Comparison of the K-value correlation with all the experimental points determined in this work indicate an average absolute percent deviation within 10 percent.

REFERENCES

1. Amick, E.H., Jr., Johnson, W.B., and Dodge, B.F., "P-V-T-X Relationships for the System: Methane-Isopentane," Chemical Engineering Progress Symposium Series, 48, 3, 65 (1952).

2. Beattie, J.A., and Bridgeman, O.C., "A New Equation of State for Fluids," Proc. Am. Acad. Arts & Sci., 63, 229 (1928).

3. Beattie, J.A., Douslin, D.R., and Levine, S.W., "Vapor Pressure and Critical Constants of Neopentane," J. Chem. Phys., 19, 948 (1951).

4. Benedict, M., Webb, G.B., and Rubin, L.C., "An Empirical Equation for Thermodynamic Properties of Light Hydrocarbons and Their Mixtures," Chem. Eng. Progress, 47, 8, 419 and 517 and 609 (1951); J. Chem. Phys., 8, 334 (1940); J. Chem. Phys., 10, 747 (1942).

5. Boomer, E.H., Johnson, C.A., and Piercey, H.G.A., "Equilibria in Two-Phase Gas-Liquid Hydrocarbon Systems II. Methane and Pentane," Can. J. Research, B16, 319 (1938).

6. Brainard, A.J., "A Study of the Vapor-Liquid Equilibrium for the Quaternary System Hydrogen-Benzene-Cyclohexane-Normal Hexane," Doctoral Thesis, The University of Michigan, Ann Arbor, 1964.

7. Canjar, L.N., Smith, R.F., Volianitis, E., Galluzzo, J.F., and Cabarcos, M., "Correlation of Constants in the Benedict-Webb-Rubin Equation of State," Ind. & Eng. Chem., 47, 6, 1028 (1955).

8. Carlson, H.C., and Colburn, A.P., "Vapor-Liquid Equilibria of Non-Ideal Solutions," Ind. & Eng. Chem., 34, 581 (1942).

9. Case, L.O., Elements of the Phase Rule, Edwards Letter Shop, Ann Arbor, Michigan, 1939.

10. Chao, K.C., and Seader,J.D., "A General Correlation of Vapor-Liquid Equilibria in Hydrocarbon Mixtures," A.I.Ch.E. Jour., 7, 4, 598 (1961).

11. Chueh, P.L., Muirbrook, N.K., and Prausnitz, J.M., "Part II. Thermodynamic Analysis," A.I.Ch.E. Jour., 11, 6, 1097 (1965).

12. Chueh, P.L., and Prausnitz, J.M., "Vapor-Liquid Equilibria at High Pressures; Partial Molal Volumes in Multicomponent Liquid Mixtures," to be submitted to A.I.Ch.E. Jour.

13. Curl, R.F., Jr., and Pitzer, K.S., "Volumetric and Thermodynamic Properties of Fluids--Enthalpy, Free Energy and Entropy," Ind. & Eng. Chem., 50, 265 (1958).

14. Flory, P.J.,"Thermodynamics of High Polymer Solutions," J. Chem. Phys., 10, 51 (1942).

15. Gibbs, J.W., The Collected Works of J.W. Gibbs, Volumes I and II Longmans, Green and Company, New York, 1931.

16. Grayson, H.G., and Streed, C.W., "Vapor-Liquid Equilibria for High Temperature, High Pressure Hydrogen-Hydrocarbon Systems," presented at the Sixth World Petroleum Congress in Frankfurt/Main, June, 1963.

17. Hadden, S.T., "Convergence Pressure in Hydrocarbon Vapor-Liquid Equilibria," Chem. Eng. Progress Symposium Series, 49, 7, 53 (1953).

18. Heichelheim, H.R., Kobe, K.A., Silberberg, I.H., and McKetta, J.J., "Compressibility Factors of 2,2-Dimethylpropane (Neopentane)," J. Chem. Eng. Data, 7, 4, 507, (1962).

19. Hildebrand, J.H., and Scott, R.L., Regular Solutions, Prentice-Hall, Inc., Englewood Cliffs, New Jersey, 1962.

20. Hildebrand, J.H., and Scott, R.L., The Solubility of Nonelectrolytes, Dover Publications, Inc., New York, 1964.

21. Hildebrand, J.H., and Wood, S.E., "The Derivation of Equations for Regular Solutions," J. Chem. Phys., 1, 817 (1933).

22. Hirschfelder, J.O., Curtiss, C.F., and Bird, R.B., Molecular Theory of Gases and Liquids, John Wiley and Sons, Inc., New York, 1954.

23. Huggins, M.L., "Thermodynamic Properties of Solutions of Long-Chain Compounds," Annals of New York Academy of Science, 43, 1 (1942).

24. Katz, D.L., Cornell, D., Kobayashi, R., Poettman, F.H., Vary, J.A., Elenbaas, J.R., and Weinaug, C.F., Handbook of Natural Gas Engineering, McGraw-Hill Book Company, Inc., New York, 1959.

25. Katz, D.L., and Hachmuth, K.H., "Vaporization Equilibrium Constants in a Crude Oil-Natural Gas System," Ind. & Eng. Chem, 29, 1072 (1937).

26. Katz, D.L., and Kurata, F., "Retrograde Condensation," Ind. & Eng. Chem., 32, 817 (1940).

27. Kellogg Charts, Liquid-Vapor Equilibrium in Mixtures of Light Hydrocarbons, M. W. Kellogg Company, Inc. New York, 1950.

28. Kihara, T., "Virial Coefficients and Models of Molecules in Gases," Rev. Modern Phys., 25, 4, 831 (1953).

29. Lennard-Jones, J.E., "On the Determination of Molecular Fields-II from the Equation of State of a Gas," Proc. Royal Soc. (London), A106, 463 (1924).

30. Lenoir, J.M., and White, G.A., "Predicting Convergence Pressures," Petroleum Refiner, 37, 3, 173 (1958).

31. Lewis, W.K., and Luke, C.D., "Properties of Hydrocarbon Mixtures at High Pressures," Trans. ASME, 54, 17, (1932).

32. Lewis, G.N., and Randall, M., Thermodynamics, McGraw-Hill Book Company, Inc., New York, 1923.

33. Lyckman, E.W., Eckert, C.A., and Prausnitz, J.M., "Generalized Liquid Volumes and Solubility Parameters for Regular Solution Application," Chem. Eng. Sci., 20, 703, (1965).

34. Lydersen, A.L., Greenkorn, R.A., and Hougen, O.A., Engineering Experiment Station Report Number 4, University of Wisconsin, Madison, 1955.

35. Martin, J.J., and Hou, C.Y., "Development of an Equation of State for Gases," A.I.Ch.E. Jour., 1, 142 (1955).

36. NGAA K-Value Charts, Engineering Data Book, Natural Gasoline Supply Men's Association, Tulsa, Oklahoma, 1957.

37. O'Connell, J.P., and Prausnitz, J.M., "Thermodynamics of Gas Solubility in Mixed Solvents," Ind. & Eng. Chem. Fundamentals, 3, 4, 347 (1964).

37a. Organick, E.I., "Equilibrium Ratio Charts for Hydrocarbon Systems, a new Publication by NGAA," Proceedings Thirty-Fourth Annual Convention, Natural Gasoline Association of America, April, 1955.

38. Orye, R.V., and Prausnitz, J.M., "Multicomponent Equilibrium with the Wilson Equation," Ind. & Eng. Chem., 57, 18 (1965).

39. Pitzer, K.S., Lippman, D.Z., Curl, R.F., Jr., Huggins, C.M., and Petersen, D.E., "The Volumetric and Thermodynamic Properties of Fluids. II," J. Am. Chem. Soc., 77, 3433 (1955).

40. Prausnitz, J.M., "Thermodynamic Representation of High-Pressure Vapor-Liquid Equilibria," Chem. Eng. Sci., 18, 613 (1963).

41. Prausnitz, J.M., Eckert, C.A., Orye, R.V., and O'Connell, J.P., Computer Calculations for Multicomponent Vapor-Liquid Equilibria, Prentice-Hall, Inc., Englewood Cliffs, New Jersey, 1967.

42. Prausnitz, J.M., Edmister, W.C., and Chao, K.C., "Hydrocarbon Vapor-Liquid Equilibria and Solubility Parameter," A.I.Ch.E. Jour., 6, 2, 214, (1960).

43. Redlich, O., Ackerman, F.J., Gunn, R.D., Jacobson, M., and Lau, S., "Thermodynamics of Solutions," Ind. & Eng. Chem. Fundamentals, 4, 4, 369 (1965).

44. Redlich, O., and Dunlop, A.K., "Thermodynamics of Solution: VIII. An Improved Equation of State," Chem. Eng. Progress Symposium Series, 59, 44, 95 (1963).

45. Redlich, O., and Kwong, J.N.S., "On the Thermodynamics of Solutions. V," Chem. Reviews, 44, 1, 233 (1949).

46. Riedel, L., "Kritischer Koeffizient, Dichte des Gesättigten Damfes und Verdampfungswärme," Chem. Ing. Tech., 26, 679 (1954).

47. Roberts, L.R., and McKetta, J.J., "Vapor-Liquid Equilibria in the n-Butane-Methane-Nitrogen System," J. Chem. Eng. Data, 8, 161 (1963).

48. Rzasa, M.J., Glass, E.E., and Opfell, J.B., "Prediction of Critical Properties and Equilibrium Vaporization Constants for Complex Hydrocarbon Systems," Chem. Eng. Progress Symposium Series, 48, 2, 28 (1952).

49. Sage, B.H., and Reamer, H.H., "Some Methods of Experimental Study of Vapor-Liquid Equilibria," Chemical Engineering Progress Symposium Series, 48, 2, 3 (1952).

50. Sage, B.H., Reamer, H.H., Olds, R.H., and Lacey, W.N., "Phase Equilibria in Hydrocarbon Systems," Ind. & Eng. Chem., 34, 9, 1108 (1942).

51. Scatchard, G., "Equilibria in Non-Electrolyte Solutions in Relation to the Vapor Pressures and Densities of the Components," Chem. Rev., 8, 321 (1931).

52. Scatchard, G., "Change of Volume on Mixing and the Equations for Non-Electrolyte Mixtures," Trans. Faraday Soc., 33, 160 (1937).

53. Scatchard, G., and Hamer, W.J., "The Application of Equations for the Chemical Potentials to Partly Miscible Solutions," J. Am. Chem. Soc., 57, 1805 (1935).

54. Souders, M., Jr., Selheimer, W.W., and Brown, G.G., "Equilibria Between Liquid and Vapor Solutions of Paraffin Hydrocarbons," Ind. & Eng. Chem., 24, 517 (1932).

54a. Stalkup, F.I., and Kobayashi, R., A.I.Ch.E. Jour., 9, 121,(1963).

55. Wilson, G.M., "A New Expression for the Excess Free Energy of Mixing," J. Am. Chem. Soc., 86, 127 (1964).

56. Winn, F.W., "Simplified Nomographic Presentation--Hydrocarbon Vapor-Liquid Equilibria," Chem. Eng. Progress Symposium Series, 48, 2, 121 (1952).

57. Wohl, K., "Thermodynamic Evaluation of Binary and Ternary Liquid Systems," Trans. A. I. Ch. E., 42, 215 (1946).

APPENDIX A

CORRELATION OF VAPOR-LIQUID EQUILIBRIUM DATA

Table XXIV presents the computer program written in the MAD (Michigan Algorithm Decoder) language to calculate equilibrium vaporization ratios of the compounds studied in this research. The program is divided into four sections. In the first section, the vapor phase fugacity coefficient is calculated using the BWR equation of state. In the second section use is made of Hildebrand's regular solution theory to calculate the liquid activity coefficient. In the third section of the program, the expression given by Chao and Seader is used to calculate the liquid phase fugacity coefficient. Finally, in the fourth section, comparisons are made between the observed and calculated equilibrium vaporization ratios.

Table XXV presents the results of the analytical model used to predict the phase behavior of the components studied in this research.

TABLE XXIV

MAD COMPUTER PROGRAM FOR EQUILIBRIUM VAPORIZATION RATIO CALCULATION

```
      $ COMPILE MAD,EXECUTE,PRINT OBJECT,DUMP

MAD (06 JAN 1967 VERSION) PROGRAM LISTING ... ... ...


                BOOLEAN BOOL      ,SWITCH
                DIMENSION PC(4), TC(4), OMEG(4), VBAR(4), LNU(4), NU(4), LNUO(4),
               1 LNU1(4), SP(4), Y(4), YCALC(4), X(4), XCALC(4),  AO(4),
               2 BO(4), CO(4), B(4), A(4), C(4), ALF(4), GAM(4), PR(4),
               3 TR(4), RTLNPH(4), LNPH(4), PHI(4), KEXP(4),KCALC(4),TR(4),
               4 PR(4),LNSP(4),AC(4)    ,PCC(4),TCC(4),KDEV(4)
                INTEGER I,J,N,COUNT,NSUB,NSUBT,RUNUM,IND

                CALCULATION OF CONSTANTS FOR THE BWR EQUATION

      START     READ DATA N,PC,TC,OMEG ,VBAR,AO,BO,CO,A,B,GAM,ALF,NSUB
                WHENEVER N .E. 2
                WHENEVER NSUB .E. 1
                PRINT COMMENT$1METHANE NORMAL PENTANE BINARY SYSTEM$
                OR WHENEVER NSUB . E. 2
                PRINT COMMENT $1METHANE ISOPENTANE BINARY SYSTEM$
                OTHERWISE
                PRINT COMMENT$1METHANE NEOPENTANE BINARY SYSTEM$
                END OF CONDITIONAL
                OTHERWISE
                WHENEVER NSUBT .E. 1
                PRINT COMMENT$1METHANE ISOPENTANE NORMAL PENTANE TERNARY SYST
               1 EM$
                OTHERWISE
                PRINT COMMENT $1METHANE NEOPENTANE NORMAL PENTANE TERNARY SYS
               1 TEM$
                END OF CONDITIONAL
                END OF CONDITIONAL
                ADEV = 0.0
                IND = 0
                COUNT = 0
                BOOL = 1B
      BEGIN     READ DATA PRESS,TF,Y,X,SP,BOOL
                READ FORMAT QQQQQ,RUNUM
                VECTOR VALUES QQQQQ = $C6*$
                IND = IND + 1
                THROUGH LP0 , FOR I = 1,1, I .G. N
      LP0       KEXP(I) = Y(I)/X(I)
                AOMIX = 0.0
                THROUGH LP1, FOR  I = 1,1, I.G.N
                SUM = Y(I)*SQRT.(AO(I))
      LP1       AOMIX = AOMIX + SUM
                AOMIX = AOMIX.P.2
                BOMIX = 0.0
                THROUGH LP2, FOR  I = 1,1, I.G.N
                SUM = Y(I)    *BO(I)
      LP2       BOMIX = BOMIX + SUM
                COMIX = 0.0
                THROUGH LP3, FOR  I = 1,1, I.G.N
                SUM = Y(I)* SQRT.(CO(I))
      LP3       COMIX = SUM + COMIX
                COMIX = COMIX.P.2
                BMIX = 0.0
```

```
            K = 1./3.
            THROUGH LP4 , FOR I=1,1, I.G.N
            SUM = Y(I)*B(I).P.K
LP4         BMIX = BMIX + SUM
            BMIX = BMIX .P.3
            AMIX = 0.0
            THROUGH LP5 , FOR I =1,1, I .G.N
            SUM =  Y(I) * A(I).P.K
LP5         AMIX = AMIX + SUM
            AMIX = AMIX .P.3
            CMIX = 0.0
            THROUGH LP6 , FOR I=1,1, I.G.N
            SUM = Y(I) *C(I).P.K
LP6         CMIX = CMIX + SUM
            CMIX = CMIX .P.3
            ALFMIX = 0.0
            THROUGH LP7 , FOR I=1,1, I.G.N
            SUM = Y(I) * ALF(I).P.K
LP7         ALFMIX = ALFMIX + SUM
            ALFMIX = ALFMIX .P.3
            GAMMIX = 0.0
            THROUGH LP8 , FOR I= 1,1, I.G. N
            SUM = Y(I) * SQRT.(GAM(I))
LP8         GAMMIX = GAMMIX + SUM
            GAMMIX = GAMMIX .P.2

            CALCULATION OF SPECIFIC VOLUME BY BWR EQUATION OF STATE

            PRESS = PRESS/ 14.696
            PRESA = PRESS*14.696
            R = 0.0820544
ITER        T = (TF + 459.67)/ 1.8
            RT = R*T
            PGIVEN = PRESS
             V1=R T/PGIVEN
            DELV =  0.1*V1
             K1=BOMIX*R T-AOMIX-COMIX/(T*T)
             K2=BMIX*R T-AMIX+AMIX*ALFMIX/(V1*V1*V1)
             K3=(CMIX/(T*T))*(1.0+GAMMIX/(V1*V1))*(EXP.(GAMMIX/-
          1  (V1*V1)))
             P1=R T/V1+K1/(V1*V1)+(K2+K3)/(V1*V1*V1)
            QSIN = P1 - PRESS
S1          V1 = V1 - DELV
             K1=BOMIX*R T-AOMIX-COMIX/(T*T)
             K2=BMIX*R T-AMIX+AMIX*ALFMIX/(V1*V1*V1)
             K3=(CMIX/(T*T))*(1.0+GAMMIX/(V1*V1))*(EXP.(GAMMIX/-
          1  (V1*V1)))
             P1=R T/V1+K1/(V1*V1)+(K2+K3)/(V1*V1*V1)
            PSIN = P1 - PRESS
            WHENEVER  PSIN*QSIN .G. 0.0
            TRANSFER TO S1
            OR WHENEVER  PSIN*QSIN  .L. 0.0
            V1 = V1 + DELV
            DELV = DELV/2.
            WHENEVER  .ABS. PSIN  .L. .10 , TRANSFER TO ROOT
            TRANSFER TO S1
            OTHERWISE
            TRANSFER TO ROOT
            END OF CONDITIONAL
ROOT        CONTINUE
```

```
          CALCULATION OF THE VAPOR FUGACITY COEFFICIENT

            D3 = 1./V1
            Z = PRESS*V1/RT
            THROUGH LP9 , FOR I = 1,1, I.G. N
            RTLNPH(I)= RT*ELOG.(1./Z) + ((BOMIX + BO(I))*RT - 2.*SQRT.
           1 (AOMIX*AO(I)) - 2.*SQRT.(COMIX*CO(I))/T/T)*D3 + 3./2.*(RT*(
           2 BMIX.P.2*B(I)).P.K - (AMIX.P.2*A( I)).P.K)*D3.P.2 + 3./5.*
           3 (AMIX*(ALFMIX.P.2 *ALF(I)).P.K + ALFMIX*(AMIX.P.2 *A(I)).P.K)
           4 *D3.P.5 + 3.*D3.P.2*(CMIX .P.2*C(I)) .P.K/ T/T *((1. - EXP.(
           5  -GAMMIX*D3.P.2))/(GAMMIX*D3.P.2)-EXP.(-GAMMIX*D3.P.2)/2.)
           7  -2.*D3.P.2 *CMIX/T/T*SQRT.(GAM(I)/GAMMIX)*((1.-EXP.(-GAMMIX
           8 *D3.P.2))/(GAMMIX*D3.P.2) -EXP.(-GAMMIX * D3.P.2) -GAMMIX*
           8  D3 .P.2 * EXP.(-GAMMIX*D3 .P.2)/2.)
            LNPH(I) = RT LNPH(I)/RT
LP9         PHI(I) = EXP.(LNPH(I))

          CALCULATION OF LIQUID PHASE FUGACITY COEFFICIENT

            THROUGH LP10, FOR I=1,1, I.G.N
            TC(I)=(TCC(I)+459.69)/1.8
            PC(I) =PCC(I)/14.696
            TR(I) = T/TC(I)
            PR(I) = PRESS/PC(I)
            LNU1(I)= -4.23893 + 8.65808*TR(I) -1.2206/TR(I) -3.15224*
           1 TR(I).P.3 -0.025*(PR(I) - 0.6)
            WHENEVER   I.E.1
            LNU0(I) =(2.4384 -2.2455/TR(I) -0.34084*TR(I) +0.00212*
           1  TR(I).P.2 -0.00223*TR(I).P.3 +(0.10486-0.03691*TR(I)
           2  )*PR(I) - ELOG.(PR(I))/2.303)/(1.+PRESA*1.E-4)
            OTHERWISE
            LNU0(I) = 5.75748 -3.01761/TR(I) -4.985*TR(I) +2.02299*TR(I)
           1  .P.2 +(0.08427 + 0.26667*TR(I) -0.31138*TR(I).P.2)*PR(I) +
           2  (-0.02655 + 0.02883* TR(I) )*PR(I).P.2 - ELOG.(PR(I))/2.303
            END OF CONDITIONAL
            LNU(I)=LNU0(I) +OMEG(I)* LNU1(I)
            LNU(I) = 2.303*LNU(I)
LP10        NU(I) = EXP.(LNU(I))

          CALCULATION OF ACTIVITY COEFFICIENT

              RAC=1.987
              RTAC=RAC*T
            NUM = 0.0
            DEN = 0.0
            THROUGH LP11, FOR I=1,1, I.G.N
            SNUM = X(I) * VBAR(I) * SP(I)
            NUM=NUM + SNUM
            SDEN = X(I) * VBAR(I)
LP11        DEN = DEN + SDEN
            SPB = NUM/DEN
            THROUGH LP12 , FOR I= 1,1,  I.G.N
            LNSP(I) = VBAR(I) * (SP(I)-SPB).P.2/RTAC
LP12        AC(I) = EXP.(LNSP(I))
            THROUGH LP13 , FOR I = 1,1, I .G. N
            KCALC (I) = AC(I) * NU (I) / PHI(I)
            KDEV(I)= (KEXP(I)-KCALC(I))*100./KEXP(I)
            COUNT = COUNT + 1
LP13        ADEV = ADEV + .ABS.(KDEV(I))
```

```
   WHENEVER IND .E. 4
   PRINT FORMAT QQ1,RUNUM
   VECTOR VALUESQQ1=$1H1,H*RUN NUMBER *,C6*$
   IND = 1
   OTHERWISE
   PRINT FORMAT QQ1A, RUNUM
   VECTOR VALUES QQ1A=$1H-,H*RUN NUMBER *,C6*$
   END OF CONDITIONAL
   PRINT FORMAT QQ2,PRESA,TF
   VECTOR VALUESQQ2=$1HO,H*PRESSURE = *,F5.0,H* PSIA*,S5,H*TEMPERATURE = *
  1 ,F4.0,H* DEG F**$
   PRINT FORMATQQ2A,V1,Z
   VECTOR VALUESQQ2A=$1H ,H*VAP. SPEC. VOL. = *,F6.4,H* LIT/GMOLE*,S5,
  1 H*COMPRESSIBILITY = *,F4.3*$
   WHENEVER N .E.2
   WHENEVER NSUB .F.1
   PRINT FORMAT QQ3
   VECTOR VALUES QQ3=$1HO,S25,H*METHANE          NOR-PENTANE**$
   OR WHENEVER NSUB .E. 2
   PRINT FORMAT QQ4
   VECTOR VALUESQQ4=$1HO,S25,H*METHANE          ISOPENTANE**$
   OTHERWISE
   PRINT FORMAT QQ5
   VECTOR VALUESQQ5=$1HO,S25,H*METHANE          NEOPENTANE**$
   END OF CONDITIONAL
   PRINT FORMAT QQ8,Y(1),Y(2)
   VECTOR VALUES QQ8=$1H ,H*VAPOR PHASE COMP*,S10,F5.4,S12,F5.4*$
   PRINT FORMAT QQ9 ,PHI(1),PHI(2)
   VECTOR VALUESQQ9 =$1H ,H*VAPOR PHASE FUG COEF*,S5,F6.4,S11,F6.4*$
   PRINT FORMATQQ10,X(1),X(2)
   VECTOR VALUESQQ10=$1H ,H*LIQUID PHASE COMP*,S9,F5.4,S12,F5.4*$
   PRINT FORMATQQ11,NU(1),NU(2)
   VECTOR VALUESQQ11=$1H ,H*LIQUID PHASE FUG COEF*,S3,F6.3,S11,F6.3*$
   PRINT FORMATQQ12,AC(1),AC(2)
   VECTOR VALUESQQ12=$1H ,H*LIQUID ACT COEF*,S10,F5.3,S12,F5.3*$
   PRINT FORMATQQ13,KEXP(1),KEXP(2)
   VECTOR VALUESQQ13=$1H ,H*K OBS*,S19,F6.3,S11,F6.3*$
   PRINT FORMATQQ14,KCALC(1),KCALC(2)
   VECTOR VALUESQQ14=$1H ,H*K CALC*,S18,F6.3,S11,F6.3*$
   PRINT FORMATQQ15,KDEV(1),KDEV(2)
   VECTOR VALUESQQ15=$1H ,H*PERCENT DEV*,S11,F7.2,S10,F7.2*$
   OTHERWISE
   WHENEVER NSUBT . E.1
   PRINT FORMAT QQ6
   VECTOR VALUES QQ6=$1HO,S25,H*METHANE          ISOPENTANE          NOR-PENTA
  1 NE**$
   OTHERWISE
   PRINT FORMAT QQ7
   VECTOR VALUESQQ7=$1HO,S25,H*METHANE          NEOPENTANE          NOR-PENTAN
  1 E**$
   END OF CONDITIONAL
   PRINT FORMATQQ16,Y(1),Y(2),Y(3)
   VECTOR VALUESQQ16=$1H ,H*VAPOR PHASE COMP*,S10,F5.4,S12,F5.4,S13,F5.4*$
   PRINT FORMAT QQ17,PHI(1),PHI(2),PHI(3)
   VECTOR VALUESQQ17=$1H ,H*VAPOR PHASE FUG COEF*,S5,F6.4,S11,F6.4,S12,
  1 F6.4*$
   PRINT FORMATQQ18,X(1),X(2),X(3)
   VECTOR VALUESQQ18=$1H ,H*LIQUID PHASE COMP*,S9,F5.4,S12,F5.4,S13,F5.4*$
   PRINT FORMATQQ19,NU(1),NU(2),NU(3)
   VECTOR VALUESQQ19=$1H ,H*LIQUID PHASE FUG COEF*,S3,F6.3,S11,F6.3,S12,
```

```
1 F6.3*$
  PRINT FORMATQQ20,AC(1),AC(2) ,AC(3)
  VECTOR VALUESQQ20=$1H ,H*LIQUID ACT COEF*,S10,F5.3,S12,F5.3,S13,F5.3*$
  PRINT FORMATQQ21,KEXP(1),KEXP(2) ,KEXP(3)
  VECTOR VALUESQQ21=$1H ,H*K OBS*,S19,F6.3,S11,F6.3,S13,F5.3*$
  PRINT FORMATQQ22,KCALC(1),KCALC(2)  ,KCALC(3)
  VECTOR VALUESQQ22=$1H ,H*K CALC*,S18,F6.3,S11,F6.3,S12,F6.3*$
  PRINT FORMATQQ23,KDEV(1),KDEV(2)   ,KDEV(3)
  VECTOR VALUESQQ23=$1H ,H*PERCENT DEV*,S11,F7.2,S10,F7.2,S11,F7.2*$
  END OF CONDITIONAL
  WHENEVER BOOL .E. 1B
  TRANSFER TO BEGIN
  OTHERWISE
  TADEV = ADEV/COUNT
  PRINT FORMAT QQ50,TADEV
  VECTOR VALUESQQ50=$1H0,H*AVE. ABS. PERCENT DEV. FOR SYSTEM = *,F6.3*$
  TRANSFER TO START
  END OF CONDITIONAL
  END OF PROGRAM

THE FOLLOWING NAMES HAVE OCCURRED ONLY ONCE IN THIS PROGRAM.
COMPILATION WILL CONTINUE.

     ITER          *073
```

TABLE XXV

COMPARISON OF OBSERVED AND CALCULATED VAPOR-LIQUID EQUILIBRIUM DATA

METHANE NORMAL PENTANE BINARY SYSTEM

RUN NUMBER 21

PRESSURE = 1502 PSIA TEMPERATURE = 220 DEG F
VAP. SPEC. VOL. = .2454 LIT/GMOLE COMPRESSIBILITY = .809

	METHANE	NOR-PENTANE
VAPOR PHASE COMP	.8080	.1920
VAPOR PHASE FUG COEF	1.0092	.2985
LIQUID PHASE COMP	.3800	.6200
LIQUID PHASE FUG COEF	1.985	.092
LIQUID ACT COEF	1.080	1.013
K OBS	2.126	.310
K CALC	2.123	.313
PERCENT DEV	.15	-1.12

RUN NUMBER 22

PRESSURE = 1265 PSIA TEMPERATURE = 220 DEG F
VAP. SPEC. VOL. = .2992 LIT/GMOLE COMPRESSIBILITY = .831

	METHANE	NOR-PENTANE
VAPOR PHASE COMP	.8110	.1885
VAPOR PHASE FUG COEF	1.0042	.3587
LIQUID PHASE COMP	.3240	.6760
LIQUID PHASE FUG COEF	2.292	.101
LIQUID ACT COEF	1.088	1.009
K OBS	2.503	.279
K CALC	2.483	.284
PERCENT DEV	.81	-1.95

RUN NUMBER 23

PRESSURE = 1231 PSIA TEMPERATURE = 220 DEG F
VAP. SPEC. VOL. = .3098 LIT/GMOLE COMPRESSIBILITY = .837

	METHANE	NOR-PENTANE
VAPOR PHASE COMP	.8100	.1898
VAPOR PHASE FUG COEF	1.0001	.3664
LIQUID PHASE COMP	.3060	.6940
LIQUID PHASE FUG COEF	2.346	.103
LIQUID ACT COEF	1.091	1.008
K OBS	2.647	.273
K CALC	2.559	.282
PERCENT DEV	3.34	-3.22

RUN NUMBER 24

PRESSURE = 1023 PSIA TEMPERATURE = 220 DEG F
VAP. SPEC. VOL. = .3783 LIT/GMOLE COMPRESSIBILITY = .850

	METHANE	NOR-PENTANE
VAPOR PHASE COMP	.8060	.1941
VAPOR PHASE FUG COEF	1.0061	.4268
LIQUID PHASE COMP	.2530	.7470
LIQUID PHASE FUG COEF	2.762	.115
LIQUID ACT COEF	1.098	1.005
K OBS	3.186	.260
K CALC	3.016	.270
PERCENT DEV	5.34	-3.90

RUN NUMBER 25

PRESSURE = 1001 PSIA TEMPERATURE = 220 DEG F
VAP. SPEC. VOL. = .4094 LIT/GMOLE COMPRESSIBILITY = .900

	METHANE	NOR-PENTANE
VAPOR PHASE COMP	.8050	.1953
VAPOR PHASE FUG COEF	.9582	.4291
LIQUID PHASE COMP	.2470	.7530
LIQUID PHASE FUG COEF	2.817	.116
LIQUID ACT COEF	1.099	1.005
K OBS	3.259	.259
K CALC	3.232	.272
PERCENT DEV	.84	-4.94

RUN NUMBER 26

PRESSURE = 1999 PSIA TEMPERATURE = 220 DEG F
VAP. SPEC. VOL. = .1644 LIT/GMOLE COMPRESSIBILITY = .722

	METHANE	NOR-PENTANE
VAPOR PHASE COMP	.7400	.2600
VAPOR PHASE FUG COEF	1.0885	.1700
LIQUID PHASE COMP	.5320	.4680
LIQUID PHASE FUG COEF	1.590	.081
LIQUID ACT COEF	1.056	1.032
K OBS	1.391	.556
K CALC	1.543	.493
PERCENT DEV	-10.94	11.32

RUN NUMBER 27

PRESSURE = 1777 PSIA TEMPERATURE = 220 DEG F
VAP. SPEC. VOL. = .1984 LIT/GMOLE COMPRESSIBILITY = .774

	METHANE	NOR-PENTANE
VAPOR PHASE COMP	.7880	.2120
VAPOR PHASE FUG COEF	1.0310	.2314
LIQUID PHASE COMP	.4560	.5440
LIQUID PHASE FUG COEF	1.737	.085
LIQUID ACT COEF	1.068	1.021
K OBS	1.728	.390
K CALC	1.799	.376
PERCENT DEV	-4.12	3.47

RUN NUMBER 28

PRESSURE = 1501 PSIA TEMPERATURE = 220 DEG F
VAP. SPEC. VOL. = .2455 LIT/GMOLE COMPRESSIBILITY = .809

	METHANE	NOR-PENTANE
VAPOR PHASE COMP	.8080	.1916
VAPOR PHASE FUG COEF	1.0094	.2993
LIQUID PHASE COMP	.3820	.6180
LIQUID PHASE FUG COEF	1.986	.092
LIQUID ACT COEF	1.079	1.013
K OBS	2.115	.310
K CALC	2.123	.313
PERCENT DEV	-.37	-.81

RUN NUMBER 29

PRESSURE = 1260 PSIA TEMPERATURE = 220 DEG F
VAP. SPEC. VOL. = .3015 LIT/GMOLE COMPRESSIBILITY = .834

	METHANE	NOR-PENTANE
VAPOR PHASE COMP	.8160	.1845
VAPOR PHASE FUG COEF	1.0025	.3640
LIQUID PHASE COMP	.3100	.6900
LIQUID PHASE FUG COEF	2.299	.101
LIQUID ACT COEF	1.090	1.008
K OBS	2.632	.267
K CALC	2.500	.280
PERCENT DEV	5.01	-4.90

RUN NUMBER 30

PRESSURE = 1005 PSIA TEMPERATURE = 220 DEG F
VAP. SPEC. VOL. = .3894 LIT/GMOLE COMPRESSIBILITY = .859

	METHANE	NOR-PENTANE
VAPOR PHASE COMP	.8140	.1863
VAPOR PHASE FUG COEF	1.0006	.4411
LIQUID PHASE COMP	.2480	.7520
LIQUID PHASE FUG COEF	2.807	.116
LIQUID ACT COEF	1.099	1.005
K OBS	3.282	.248
K CALC	3.083	.264
PERCENT DEV	6.06	-6.63

AVE. ABS. PERCENT DEV. FOR SYSTEM = 3.963

METHANE ISOPENTANE BINARY SYSTEM

RUN NUMBER 31

PRESSURE = 1256 PSIA TEMPERATURE = 220 DEG F
VAP. SPEC. VOL. = .2968 LIT/GMOLE COMPRESSIBILITY = .819

	METHANE	ISOPENTANE
VAPOR PHASE COMP	.7880	.2120
VAPOR PHASE FUG COEF	1.0129	.3673
LIQUID PHASE COMP	.3310	.6690
LIQUID PHASE FUG COEF	2.306	.117
LIQUID ACT COEF	1.055	1.006
K OBS	2.381	.317
K CALC	2.401	.320
PERCENT DEV	-.86	-1.07

RUN NUMBER 32

PRESSURE = 1503 PSIA TEMPERATURE = 220 DEG F
VAP. SPEC. VOL. = .2376 LIT/GMOLE COMPRESSIBILITY = .784

	METHANE	ISOPENTANE
VAPOR PHASE COMP	.7740	.2260
VAPOR PHASE FUG COEF	1.0287	.2954
LIQUID PHASE COMP	.3960	.6040
LIQUID PHASE FUG COEF	1.983	.106
LIQUID ACT COEF	1.049	1.009
K OBS	1.955	.374
K CALC	2.022	.363
PERCENT DEV	-3.47	2.90

RUN NUMBER 33

PRESSURE = 1721 PSIA TEMPERATURE = 220 DEG F
VAP. SPEC. VOL. = .1966 LIT/GMOLE COMPRESSIBILITY = .743

	METHANE	ISOPENTANE
VAPOR PHASE COMP	.7460	.2540
VAPOR PHASE FUG COEF	1.0624	.2338
LIQUID PHASE COMP	.4540	.5460
LIQUID PHASE FUG COEF	1.780	.100
LIQUID ACT COEF	1.043	1.013
K OBS	1.643	.465
K CALC	1.748	.432
PERCENT DEV	-6.40	7.06

RUN NUMBER 34

PRESSURE = 1899 PSIA TEMPERATURE = 220 DEG F
VAP. SPEC. VOL. = .1628 LIT/GMOLE COMPRESSIBILITY = .679

	METHANE	ISOPENTANE
VAPOR PHASE COMP	.6860	.3140
VAPOR PHASE FUG COEF	1.1471	.1741
LIQUID PHASE COMP	.5660	.4340
LIQUID PHASE FUG COEF	1.652	.096
LIQUID ACT COEF	1.032	1.024
K OBS	1.212	.724
K CALC	1.487	.563
PERCENT DEV	-22.66	22.20

RUN NUMBER 35

PRESSURE = 1001 PSIA TEMPERATURE = 220 DEG F
VAP. SPEC. VOL. = .3866 LIT/GMOLE COMPRESSIBILITY = .850

	METHANE	ISOPENTANE
VAPOR PHASE COMP	.7910	.2090
VAPOR PHASE FUG COEF	1.0061	.4495
LIQUID PHASE COMP	.2620	.7380
LIQUID PHASE FUG COEF	2.817	.134
LIQUID ACT COEF	1.061	1.003
K OBS	3.019	.283
K CALC	2.971	.299
PERCENT DEV	1.59	-5.62

RUN NUMBER 36

PRESSURE = 759 PSIA TEMPERATURE = 220 DEG F
VAP. SPEC. VOL. = .5249 LIT/GMOLE COMPRESSIBILITY = .875

	METHANE	ISOPENTANE
VAPOR PHASE COMP	.7650	.2350
VAPOR PHASE FUG COEF	1.0037	.5218
LIQUID PHASE COMP	.1917	.8080
LIQUID PHASE FUG COEF	3.639	.162
LIQUID ACT COEF	1.067	1.002
K OBS	3.991	.291
K CALC	3.869	.310
PERCENT DEV	3.04	-6.63

RUN NUMBER 37

PRESSURE = 499 PSIA TEMPERATURE = 220 DEG F
VAP. SPEC. VOL. = .8098 LIT/GMOLE COMPRESSIBILITY = .887

	METHANE	ISOPENTANE
VAPOR PHASE COMP	.7100	.2900
VAPOR PHASE FUG COEF	1.0205	.6214
LIQUID PHASE COMP	.1181	.8820
LIQUID PHASE FUG COEF	5.453	.222
LIQUID ACT COEF	1.073	1.001
K OBS	6.012	.329
K CALC	5.735	.358
PERCENT DEV	4.61	-8.85

RUN NUMBER 38

PRESSURE = 502 PSIA TEMPERATURE = 160 DEG F
VAP. SPEC. VOL. = .7546 LIT/GMOLE COMPRESSIBILITY = .912

	METHANE	ISOPENTANE
VAPOR PHASE COMP	.8410	.1593
VAPOR PHASE FUG COEF	.9811	.6045
LIQUID PHASE COMP	.1418	.8580
LIQUID PHASE FUG COEF	4.933	.115
LIQUID ACT COEF	1.078	1.001
K OBS	5.931	.186
K CALC	5.423	.190
PERCENT DEV	8.56	-2.39

RUN NUMBER 39

PRESSURE = 755 PSIA TEMPERATURE = 160 DEG F
VAP. SPEC. VOL. = .4880 LIT/GMOLE COMPRESSIBILITY = .887

	METHANE	ISOPENTANE
VAPOR PHASE COMP	.8720	.1283
VAPOR PHASE FUG COEF	.9682	.5001
LIQUID PHASE COMP	.2180	.7820
LIQUID PHASE FUG COEF	3.353	.085
LIQUID ACT COEF	1.071	1.002
K OBS	4.000	.164
K CALC	3.710	.171
PERCENT DEV	7.24	-4.13

RUN NUMBER 40

PRESSURE = 1001 PSIA TEMPERATURE = 160 DEG F
VAP. SPEC. VOL. = .3603 LIT/GMOLE COMPRESSIBILITY = .869

	METHANE	ISOPENTANE
VAPOR PHASE COMP	.8850	.1146
VAPOR PHASE FUG COEF	.9536	.4161
LIQUID PHASE COMP	.2830	.7170
LIQUID PHASE FUG COEF	2.601	.071
LIQUID ACT COEF	1.065	1.004
K OBS	3.127	.160
K CALC	2.905	.172
PERCENT DEV	7.11	-7.42

RUN NUMBER 41

PRESSURE = 1253 PSIA TEMPERATURE = 160 DEG F
VAP. SPEC. VOL. = .2770 LIT/GMOLE COMPRESSIBILITY = .836

	METHANE	ISOPENTANE
VAPOR PHASE COMP	.8790	.1206
VAPOR PHASE FUG COEF	.9490	.3291
LIQUID PHASE COMP	.3510	.6490
LIQUID PHASE FUG COEF	2.147	.063
LIQUID ACT COEF	1.058	1.007
K OBS	2.504	.186
K CALC	2.395	.192
PERCENT DEV	4.38	-3.18

RUN NUMBER 42

PRESSURE = 1505 PSIA TEMPERATURE = 160 DEG F
VAP. SPEC. VOL. = .2220 LIT/GMOLE COMPRESSIBILITY = .805

	METHANE	ISOPENTANE
VAPOR PHASE COMP	.8690	.1308
VAPOR PHASE FUG COEF	.9467	.2566
LIQUID PHASE COMP	.4180	.5820
LIQUID PHASE FUG COEF	1.853	.057
LIQUID ACT COEF	1.051	1.012
K OBS	2.079	.225
K CALC	2.058	.225
PERCENT DEV	1.00	-.20

RUN NUMBER 43A

PRESSURE = 1759 PSIA TEMPERATURE = 160 DEG F
VAP. SPEC. VOL. = .1822 LIT/GMOLE COMPRESSIBILITY = .772

	METHANE	ISOPENTANE
VAPOR PHASE COMP	.8530	.1474
VAPOR PHASE FUG COEF	.9508	.1953
LIQUID PHASE COMP	.4890	.5110
LIQUID PHASE FUG COEF	1.648	.053
LIQUID ACT COEF	1.044	1.018
K OBS	1.744	.288
K CALC	1.809	.277
PERCENT DEV	-3.70	3.85

RUN NUMBER 44

PRESSURE = 1992 PSIA TEMPERATURE = 160 DEG F
VAP. SPEC. VOL. = .1517 LIT/GMOLE COMPRESSIBILITY = .728

	METHANE	ISOPENTANE
VAPOR PHASE COMP	.8210	.1791
VAPOR PHASE FUG COEF	.9756	.1426
LIQUID PHASE COMP	.5450	.4550
LIQUID PHASE FUG COEF	1.509	.051
LIQUID ACT COEF	1.038	1.024
K OBS	1.506	.394
K CALC	1.605	.363
PERCENT DEV	-6.56	7.75

RUN NUMBER 45

PRESSURE = 2191 PSIA TEMPERATURE = 160 DEG F
VAP. SPEC. VOL. = .1237 LIT/GMOLE COMPRESSIBILITY = .653

	METHANE	ISOPENTANE
VAPOR PHASE COMP	.7410	.2590
VAPOR PHASE FUG COEF	1.0655	.0898
LIQUID PHASE COMP	.6330	.3670
LIQUID PHASE FUG COEF	1.416	.049
LIQUID ACT COEF	1.028	1.038
K OBS	1.171	.706
K CALC	1.367	.563
PERCENT DEV	-16.77	20.22

RUN NUMBER 46

PRESSURE = 511 PSIA TEMPERATURE = 280 DEG F
VAP. SPEC. VOL. = .8000 LIT/GMOLE COMPRESSIBILITY = .825

	METHANE	ISOPENTANE
VAPOR PHASE COMP	.5200	.4800
VAPOR PHASE FUG COEF	1.0993	.6221
LIQUID PHASE COMP	.0916	.9080
LIQUID PHASE FUG COEF	5.619	.364
LIQUID ACT COEF	1.069	1.000
K OBS	5.677	.529
K CALC	5.462	.585
PERCENT DEV	3.78	-10.72

RUN NUMBER 47

PRESSURE = 759 PSIA TEMPERATURE = 280 DEG F
VAP. SPEC. VOL. = .5305 LIT/GMOLE COMPRESSIBILITY = .812

	METHANE	ISOPENTANE
VAPOR PHASE COMP	.6030	.3970
VAPOR PHASE FUG COEF	1.0916	.5290
LIQUID PHASE COMP	.1613	.3390
LIQUID PHASE FUG COEF	3.814	.265
LIQUID ACT COEF	1.064	1.001
K OBS	3.738	.473
K CALC	3.718	.502
PERCENT DEV	.56	-6.09

RUN NUMBER 48

PRESSURE = 1001 PSIA TEMPERATURE = 280 DEG F
VAP. SPEC. VOL. = .3898 LIT/GMOLE COMPRESSIBILITY = .787

	METHANE	ISOPENTANE
VAPOR PHASE COMP	.6360	.3640
VAPOR PHASE FUG COEF	1.1036	.4519
LIQUID PHASE COMP	.2310	.7590
LIQUID PHASE FUG COEF	2.936	.217
LIQUID ACT COEF	1.058	1.002
K OBS	2.753	.473
K CALC	2.815	.482
PERCENT DEV	-2.26	-1.74

RUN NUMBER 49

PRESSURE = 1267 PSIA TEMPERATURE = 280 DEG F
VAP. SPEC. VOL. = .3031 LIT/GMOLE COMPRESSIBILITY = .775

	METHANE	ISOPENTANE
VAPOR PHASE COMP	.6510	.3490
VAPOR PHASE FUG COEF	1.1044	.3797
LIQUID PHASE COMP	.3150	.6850
LIQUID PHASE FUG COEF	2.370	.186
LIQUID ACT COEF	1.052	1.005
K OBS	2.067	.509
K CALC	2.257	.493
PERCENT DEV	-9.19	3.21

RUN NUMBER 49A

PRESSURE = 1277 PSIA TEMPERATURE = 280 DEG F
VAP. SPEC. VOL. = .2928 LIT/GMOLE COMPRESSIBILITY = .755

	METHANE	ISOPENTANE
VAPOR PHASE COMP	.6430	.3570
VAPOR PHASE FUG COEF	1.1301	.3718
LIQUID PHASE COMP	.3300	.6700
LIQUID PHASE FUG COEF	2.354	.185
LIQUID ACT COEF	1.050	1.005
K OBS	1.948	.533
K CALC	2.187	.501
PERCENT DEV	-12.27	5.89

RUN NUMBER 50

PRESSURE = 1517 PSIA TEMPERATURE = 280 DEG F
VAP. SPEC. VOL. = .2205 LIT/GMOLE COMPRESSIBILITY = .675

	METHANE	ISOPENTANE
VAPOR PHASE COMP	.5810	.4190
VAPOR PHASE FUG COEF	1.2430	.2779
LIQUID PHASE COMP	.4880	.5120
LIQUID PHASE FUG COEF	2.027	.168
LIQUID ACT COEF	1.037	1.015
K OBS	1.191	.818
K CALC	1.691	.614
PERCENT DEV	-42.03	25.03

AVE. ABS. PERCENT DEV. FOR SYSTEM = 7.719

METHANE NEOPENTANE BINARY SYSTEM

RUN NUMBER 71

PRESSURE = 511 PSIA TEMPERATURE = 160 DEG F
VAP. SPEC. VOL. = .7159 LIT/GMOLE COMPRESSIBILITY = .881

	METHANE	NEOPENTANE
VAPOR PHASE COMP	.7610	.2390
VAPOR PHASE FUG COEF	.9991	.5958
LIQUID PHASE COMP	.1532	.8470
LIQUID PHASE FUG COEF	4.849	.174
LIQUID ACT COEF	1.022	1.000
K OBS	4.967	.282
K CALC	4.958	.292
PERCENT DEV	.18	-3.47

RUN NUMBER 72

PRESSURE = 763 PSIA TEMPERATURE = 160 DEG F
VAP. SPEC. VOL. = .4625 LIT/GMOLE COMPRESSIBILITY = .850

	METHANE	NEOPENTANE
VAPOR PHASE COMP	.7970	.2030
VAPOR PHASE FUG COEF	.9883	.4866
LIQUID PHASE COMP	.2320	.7680
LIQUID PHASE FUG COEF	3.321	.129
LIQUID ACT COEF	1.020	1.001
K OBS	3.435	.264
K CALC	3.426	.266
PERCENT DEV	.28	-.76

RUN NUMBER 73

PRESSURE = 1005 PSIA TEMPERATURE = 160 DEG F
VAP. SPEC. VOL. = .3421 LIT/GMOLE COMPRESSIBILITY = .828

	METHANE	NEOPENTANE
VAPOR PHASE COMP	.8190	.1809
VAPOR PHASE FUG COEF	.9762	.4076
LIQUID PHASE COMP	.3120	.6880
LIQUID PHASE FUG COEF	2.592	.108
LIQUID ACT COEF	1.018	1.002
K OBS	2.625	.263
K CALC	2.701	.266
PERCENT DEV	-2.91	-1.26

RUN NUMBER 74

PRESSURE = 1273 PSIA TEMPERATURE = 160 DEG F
VAP. SPEC. VOL. = .2573 LIT/GMOLE COMPRESSIBILITY = .789

	METHANE	NEOPENTANE
VAPOR PHASE COMP	.8130	.1867
VAPOR PHASE FUG COEF	.9764	.3189
LIQUID PHASE COMP	.3910	.6090
LIQUID PHASE FUG COEF	2.119	.095
LIQUID ACT COEF	1.015	1.003
K OBS	2.079	.307
K CALC	2.204	.298
PERCENT DEV	-6.00	2.83

RUN NUMBER 74A

PRESSURE = 1281 PSIA TEMPERATURE = 160 DEG F
VAP. SPEC. VOL. = .2552 LIT/GMOLE COMPRESSIBILITY = .787

	METHANE	NEOPENTANE
VAPOR PHASE COMP	.8130	.1874
VAPOR PHASE FUG COEF	.9766	.3159
LIQUID PHASE COMP	.3970	.6020
LIQUID PHASE FUG COEF	2.109	.094
LIQUID ACT COEF	1.015	1.003
K OBS	2.048	.311
K CALC	2.192	.300
PERCENT DEV	-7.04	3.69

RUN NUMBER 75A

PRESSURE = 1521 PSIA TEMPERATURE = 160 DEG F
VAP. SPEC. VOL. = .2009 LIT/GMOLE COMPRESSIBILITY = .736

	METHANE	NEOPENTANE
VAPOR PHASE COMP	.7840	.2160
VAPOR PHASE FUG COEF	.9968	.2374
LIQUID PHASE COMP	.4820	.5180
LIQUID PHASE FUG COEF	1.838	.087
LIQUID ACT COEF	1.013	1.005
K OBS	1.627	.417
K CALC	1.868	.367
PERCENT DEV	-14.83	11.98

RUN NUMBER 76B

PRESSURE = 1709 PSIA TEMPERATURE = 160 DEG F
VAP. SPEC. VOL. = .1617 LIT/GMOLE COMPRESSIBILITY = .666

	METHANE	NEOPENTANE
VAPOR PHASE COMP	.7270	.2730
VAPOR PHASE FUG COEF	1.0595	.1707
LIQUID PHASE COMP	.5600	.4400
LIQUID PHASE FUG COEF	1.683	.082
LIQUID ACT COEF	1.011	1.007
K OBS	1.298	.620
K CALC	1.605	.486
PERCENT DEV	-23.64	21.69

RUN NUMBER 77

PRESSURE = 1748 PSIA TEMPERATURE = 160 DEG F
VAP. SPEC. VOL. = .1484 LIT/GMOLE COMPRESSIBILITY = .625

	METHANE	NEOPENTANE
VAPOR PHASE COMP	.6850	.3150
VAPOR PHASE FUG COEF	1.1165	.1458
LIQUID PHASE COMP	.6030	.3970
LIQUID PHASE FUG COEF	1.655	.082
LIQUID ACT COEF	1.009	1.009
K OBS	1.136	.793
K CALC	1.496	.564
PERCENT DEV	-31.70	28.86

RUN NUMBER 82

PRESSURE = 310 PSIA TEMPERATURE = 160 DEG F
VAP. SPEC. VOL. = 1.2052 LIT/GMOLE COMPRESSIBILITY = .900

	METHANE	NEOPENTANE
VAPOR PHASE COMP	.6670	.3330
VAPOR PHASE FUG COEF	1.0140	.6914
LIQUID PHASE COMP	.0952	.9150
LIQUID PHASE FUG COEF	7.916	.262
LIQUID ACT COEF	1.023	1.000
K OBS	7.829	.364
K CALC	7.987	.380
PERCENT DEV	-2.02	-4.31

RUN NUMBER 83

PRESSURE = 308 PSIA TEMPERATURE = 220 DEG F
VAP. SPEC. VOL. = 1.2104 LIT/GMOLE COMPRESSIBILITY = .819

	METHANE	NEOPENTANE
VAPOR PHASE COMP	.3950	.6050
VAPOR PHASE FUG COEF	1.1112	.7007
LIQUID PHASE COMP	.0505	.9490
LIQUID PHASE FUG COEF	8.806	.478
LIQUID ACT COEF	1.022	1.000
K OBS	7.822	.638
K CALC	8.097	.682
PERCENT DEV	-3.52	-6.90

RUN NUMBER 84

PRESSURE = 503 PSIA TEMPERATURE = 220 DEG F
VAP. SPEC. VOL. = .7468 LIT/GMOLE COMPRESSIBILITY = .825

	METHANE	NEOPENTANE
VAPOR PHASE COMP	.5630	.4370
VAPOR PHASE FUG COEF	1.0752	.6055
LIQUID PHASE COMP	.1168	.8830
LIQUID PHASE FUG COEF	5.410	.314
LIQUID ACT COEF	1.020	1.000
K OBS	4.820	.495
K CALC	5.135	.518
PERCENT DEV	-6.52	-4.73

RUN NUMBER 85

PRESSURE = 748 PSIA TEMPERATURE = 220 DEG F
VAP. SPEC. VOL. = .5479 LIT/GMOLE COMPRESSIBILITY = .900

	METHANE	NEOPENTANE
VAPOR PHASE COMP	.6390	.3610
VAPOR PHASE FUG COEF	.9655	.4934
LIQUID PHASE COMP	.1970	.8030
LIQUID PHASE FUG COEF	3.685	.230
LIQUID ACT COEF	1.019	1.000
K OBS	3.244	.450
K CALC	3.892	.467
PERCENT DEV	-20.00	-3.84

RUN NUMBER 86

PRESSURE = 1008 PSIA TEMPERATURE = 220 DEG F
VAP. SPEC. VOL. = .3501 LIT/GMOLE COMPRESSIBILITY = .775

	METHANE	NEOPENTANE
VAPOR PHASE COMP	.6700	.3300
VAPOR PHASE FUG COEF	1.0718	.4210
LIQUID PHASE COMP	.2820	.7180
LIQUID PHASE FUG COEF	2.799	.187
LIQUID ACT COEF	1.017	1.001
K OBS	2.376	.460
K CALC	2.656	.445
PERCENT DEV	-11.78	3.25

RUN NUMBER 87A

PRESSURE = 1251 PSIA TEMPERATURE = 220 DEG F
VAP. SPEC. VOL. = .2627 LIT/GMOLE COMPRESSIBILITY = .722

	METHANE	NEOPENTANE
VAPOR PHASE COMP	.6540	.3460
VAPOR PHASE FUG COEF	1.1122	.3341
LIQUID PHASE COMP	.3770	.6230
LIQUID PHASE FUG COEF	2.314	.164
LIQUID ACT COEF	1.014	1.002
K OBS	1.735	.555
K CALC	2.110	.491
PERCENT DEV	-21.64	11.59

RUN NUMBER 88A

PRESSURE = 1434 PSIA TEMPERATURE = 220 DEG F
VAP. SPEC. VOL. = .2004 LIT/GMOLE COMPRESSIBILITY = .631

	METHANE	NEOPENTANE
VAPOR PHASE COMP	.5850	.4150
VAPOR PHASE FUG COEF	1.2384	.2498
LIQUID PHASE COMP	.4710	.5290
LIQUID PHASE FUG COEF	2.062	.152
LIQUID ACT COEF	1.012	1.004
K OBS	1.242	.784
K CALC	1.685	.610
PERCENT DEV	-35.64	22.24

RUN NUMBER 91

PRESSURE = 506 PSIA TEMPERATURE = 280 DEG F
VAP. SPEC. VOL. = .6733 LIT/GMOLE COMPRESSIBILITY = .687

	METHANE	NEOPENTANE
VAPOR PHASE COMP	.2800	.7200
VAPOR PHASE FUG COEF	1.2835	.6102
LIQUID PHASE COMP	.0683	.9320
LIQUID PHASE FUG COEF	5.674	.487
LIQUID ACT COEF	1.020	1.000
K OBS	4.100	.773
K CALC	4.508	.798
PERCENT DEV	-9.96	-3.33

RUN NUMBER 92

PRESSURE = 755 PSIA TEMPERATURE = 280 DEG F
VAP. SPEC. VOL. = .4471 LIT/GMOLE COMPRESSIBILITY = .681

	METHANE	NEOPENTANE
VAPOR PHASE COMP	.4070	.5930
VAPOR PHASE FUG COEF	1.2681	.5063
LIQUID PHASE COMP	.1632	.8370
LIQUID PHASE FUG COEF	3.834	.349
LIQUID ACT COEF	1.018	1.000
K OBS	2.494	.708
K CALC	3.077	.690
PERCENT DEV	-23.39	2.60

RUN NUMBER 93B

PRESSURE = 1004 PSIA TEMPERATURE = 280 DEG F
VAP. SPEC. VOL. = .3023 LIT/GMOLE COMPRESSIBILITY = .612

	METHANE	NEOPENTANE
VAPOR PHASE COMP	.4160	.5840
VAPOR PHASE FUG COEF	1.3795	.4005
LIQUID PHASE COMP	.2810	.7190
LIQUID PHASE FUG COEF	2.927	.281
LIQUID ACT COEF	1.015	1.001
K OBS	1.480	.812
K CALC	2.155	.703
PERCENT DEV	-45.55	13.45

AVE. ABS. PERCENT DEV. FOR SYSTEM = 11.594

METHANE NEOPENTANE NORMAL PENTANE TERNARY SYSTEM

RUN NUMBER 95

PRESSURE = 503 PSIA TEMPERATURE = 160 DEG F
VAP. SPEC. VOL. = .7634 LIT/GMOLE COMPRESSIBILITY = .925

	METHANE	NEOPENTANE	NOR-PENTANE
VAPOR PHASE COMP	.8450	.0577	.0972
VAPOR PHASE FUG COEF	.9792	.6428	.5902
LIQUID PHASE COMP	.1407	.2160	.6430
LIQUID PHASE FUG COEF	4.924	.176	.095
LIQUID ACT COEF	1.089	1.044	1.013
K OBS	6.006	.267	.151
K CALC	5.478	.286	.163
PERCENT DEV	8.79	-7.09	-7.87

RUN NUMBER 96

PRESSURE = 751 PSIA TEMPERATURE = 160 DEG F
VAP. SPEC. VOL. = .4975 LIT/GMOLE COMPRESSIBILITY = .900

	METHANE	NEOPENTANE	NOR-PENTANE
VAPOR PHASE COMP	.8710	.0459	.0827
VAPOR PHASE FUG COEF	.9708	.5443	.4830
LIQUID PHASE COMP	.2060	.1997	.5940
LIQUID PHASE FUG COEF	3.370	.131	.071
LIQUID ACT COEF	1.082	1.037	1.017
K OBS	4.228	.230	.139
K CALC	3.757	.250	.149
PERCENT DEV	11.15	-8.55	-7.22

RUN NUMBER 97

PRESSURE = 1251 PSIA TEMPERATURE = 160 DEG F
VAP. SPEC. VOL. = .2810 LIT/GMOLE COMPRESSIBILITY = .847

	METHANE	NEOPENTANE	NOR-PENTANE
VAPOR PHASE COMP	.8780	.0404	.0818
VAPOR PHASE FUG COEF	.9611	.3756	.3059
LIQUID PHASE COMP	.3370	.1640	.4980
LIQUID PHASE FUG COEF	2.150	.096	.052
LIQUID ACT COEF	1.068	1.024	1.029
K OBS	2.605	.246	.164
K CALC	2.390	.261	.174
PERCENT DEV	8.23	-5.83	-6.20

RUN NUMBER 98

PRESSURE = 1505 PSIA TEMPERATURE = 160 DEG F
VAP. SPEC. VOL. = .2254 LIT/GMOLE COMPRESSIBILITY = .817

	METHANE	NEOPENTANE	NOR-PENTANE
VAPOR PHASE COMP	.8700	.0410	.0891
VAPOR PHASE FUG COEF	.9626	.3039	.2340
LIQUID PHASE COMP	.4000	.1482	.4520
LIQUID PHASE FUG COEF	1.853	.087	.047
LIQUID ACT COEF	1.061	1.018	1.036
K OBS	2.175	.277	.197
K CALC	2.043	.292	.209
PERCENT DEV	6.09	-5.50	-6.07

RUN NUMBER 99

PRESSURE = 1759 PSIA TEMPERATURE = 160 DEG F
VAP. SPEC. VOL. = .1851 LIT/GMOLE COMPRESSIBILITY = .784

	METHANE	NEOPENTANE	NOR-PENTANE
VAPOR PHASE COMP	.8550	.0429	.1025
VAPOR PHASE FUG COEF	.9711	.2396	.1717
LIQUID PHASE COMP	.4610	.1314	.4080
LIQUID PHASE FUG COEF	1.648	.081	.044
LIQUID ACT COEF	1.054	1.012	1.045
K OBS	1.855	.326	.251
K CALC	1.788	.344	.267
PERCENT DEV	3.60	-5.29	-6.41

RUN NUMBER 100

PRESSURE = 2013 PSIA TEMPERATURE = 160 DEG F
VAP. SPEC. VOL. = .1463 LIT/GMOLE COMPRESSIBILITY = .709

	METHANE	NEOPENTANE	NOR-PENTANE
VAPOR PHASE COMP	.8050	.0536	.1413
VAPOR PHASE FUG COEF	1.0317	.1629	.1008
LIQUID PHASE COMP	.5500	.1112	.3390
LIQUID PHASE FUG COEF	1.498	.077	.041
LIQUID ACT COEF	1.043	1.005	1.063
K OBS	1.464	.482	.417
K CALC	1.514	.476	.437
PERCENT DEV	-3.45	1.19	-4.90

RUN NUMBER 101

PRESSURE = 2120 PSIA TEMPERATURE = 160 DEG F
VAP. SPEC. VOL. = .1316 LIT/GMOLE COMPRESSIBILITY = .672

	METHANE	NEOPENTANE	NOR-PENTANE
VAPOR PHASE COMP	.7750	.0591	.1655
VAPOR PHASE FUG COEF	1.0804	.1346	.0760
LIQUID PHASE COMP	.6020	.0976	.3000
LIQUID PHASE FUG COEF	1.447	.076	.041
LIQUID ACT COEF	1.036	1.002	1.076
K OBS	1.287	.606	.552
K CALC	1.388	.564	.575
PERCENT DEV	-7.82	6.82	-4.16

RUN NUMBER 102

PRESSURE = 1006 PSIA TEMPERATURE = 160 DEG F
VAP. SPEC. VOL. = .3611 LIT/GMOLE COMPRESSIBILITY = .875

	METHANE	NEOPENTANE	NOR-PENTANE
VAPOR PHASE COMP	.8790	.0406	.0807
VAPOR PHASE FUG COEF	.9626	.4522	.3854
LIQUID PHASE COMP	.2780	.1760	.5460
LIQUID PHASE FUG COEF	2.589	.108	.059
LIQUID ACT COEF	1.075	1.030	1.023
K OBS	3.162	.231	.148
K CALC	2.893	.247	.156
PERCENT DEV	8.51	-6.95	-5.42

AVE. ABS. PERCENT DEV. FOR SYSTEM = 6.382

METHANE ISOPENTANE NORMAL PENTANE TERNARY SYSTEM

RUN NUMBER 51

PRESSURE = 504 PSIA TEMPERATURE = 160 DEG F
VAP. SPEC. VOL. = .7619 LIT/GMOLE COMPRESSIBILITY = .925

	METHANE	ISOPENTANE	NOR-PENTANE
VAPOR PHASE COMP	.8710	.0395	.0892
VAPOR PHASE FUG COEF	.9750	.6244	.6102
LIQUID PHASE COMP	.1386	.2230	.6390
LIQUID PHASE FUG COEF	4.914	.115	.095
LIQUID ACT COEF	1.113	1.002	1.004
K OBS	6.284	.177	.140
K CALC	5.608	.184	.156
PERCENT DEV	10.76	-3.81	-11.78

RUN NUMBER 52

PRESSURE = 755 PSIA TEMPERATURE = 160 DEG F
VAP. SPEC. VOL. = .4949 LIT/GMOLE COMPRESSIBILITY = .900

	METHANE	ISOPENTANE	NOR-PENTANE
VAPOR PHASE COMP	.8940	.0305	.0755
VAPOR PHASE FUG COEF	.9628	.5195	.5037
LIQUID PHASE COMP	.2110	.2060	.5830
LIQUID PHASE FUG COEF	3.353	.085	.071
LIQUID ACT COEF	1.103	1.001	1.007
K OBS	4.237	.148	.130
K CALC	3.840	.164	.141
PERCENT DEV	9.37	-10.98	-9.02

RUN NUMBER 53

PRESSURE = 1003 PSIA TEMPERATURE = 160 DEG F
VAP. SPEC. VOL. = .3622 LIT/GMOLE COMPRESSIBILITY = .875

	METHANE	ISOPENTANE	NOR-PENTANE
VAPOR PHASE COMP	.8970	.0296	.0733
VAPOR PHASE FUG COEF	.9511	.4240	.4072
LIQUID PHASE COMP	.2740	.1888	.5370
LIQUID PHASE FUG COEF	2.596	.071	.059
LIQUID ACT COEF	1.094	1.000	1.011
K OBS	3.274	.157	.136
K CALC	2.986	.165	.146
PERCENT DEV	8.80	-5.09	-7.01

RUN NUMBER 54

PRESSURE = 1493 PSIA TEMPERATURE = 160 DEG F
VAP. SPEC. VOL. = .2294 LIT/GMOLE COMPRESSIBILITY = .825

	METHANE	ISOPENTANE	NOR-PENTANE
VAPOR PHASE COMP	.8890	.0307	.0803
VAPOR PHASE FUG COEF	.9365	.2765	.2598
LIQUID PHASE COMP	.4060	.1536	.4410
LIQUID PHASE FUG COEF	1.865	.057	.047
LIQUID ACT COEF	1.075	1.002	1.023
K OBS	2.190	.200	.182
K CALC	2.140	.208	.187
PERCENT DEV	2.27	-4.02	-2.50

RUN NUMBER 55

PRESSURE = 1975 PSIA TEMPERATURE = 160 DEG F
VAP. SPEC. VOL. = .1590 LIT/GMOLE COMPRESSIBILITY = .756

	METHANE	ISOPENTANE	NOR-PENTANE
VAPOR PHASE COMP	.8490	.0405	.1107
VAPOR PHASE FUG COEF	.9529	.1600	.1452
LIQUID PHASE COMP	.5040	.1290	.3670
LIQUID PHASE FUG COEF	1.518	.051	.042
LIQUID ACT COEF	1.060	1.007	1.038
K OBS	1.685	.314	.302
K CALC	1.688	.320	.299
PERCENT DEV	-.20	-1.80	.97

RUN NUMBER 55A

PRESSURE = 1995 PSIA TEMPERATURE = 160 DEG F
VAP. SPEC. VOL. = .1551 LIT/GMOLE COMPRESSIBILITY = .745

	METHANE	ISOPENTANE	NOR-PENTANE
VAPOR PHASE COMP	.8420	.0422	.1159
VAPOR PHASE FUG COEF	.9618	.1523	.1377
LIQUID PHASE COMP	.5210	.1229	.3560
LIQUID PHASE FUG COEF	1.507	.051	.042
LIQUID ACT COEF	1.057	1.008	1.041
K OBS	1.616	.343	.326
K CALC	1.657	.335	.315
PERCENT DEV	-2.51	2.48	3.35

RUN NUMBER 58

PRESSURE = 2268 PSIA TEMPERATURE = 160 DEG F
VAP. SPEC. VOL. = .1214 LIT/GMOLE COMPRESSIBILITY = .663

	METHANE	ISOPENTANE	NOR-PENTANE
VAPOR PHASE COMP	.7580	.0632	.1783
VAPOR PHASE FUG COEF	1.0547	.0890	.0772
LIQUID PHASE COMP	.5930	.1039	.3030
LIQUID PHASE FUG COEF	1.385	.048	.040
LIQUID ACT COEF	1.046	1.016	1.057
K OBS	1.278	.608	.588
K CALC	1.374	.549	.541
PERCENT DEV	-7.48	9.77	8.08

RUN NUMBER 59

PRESSURE = 1765 PSIA TEMPERATURE = 220 DEG F
VAP. SPEC. VOL. = .1957 LIT/GMOLE COMPRESSIBILITY = .759

	METHANE	ISOPENTANE	NOR-PENTANE
VAPOR PHASE COMP	.7710	.0613	.1681
VAPOR PHASE FUG COEF	1.0462	.2391	.2212
LIQUID PHASE COMP	.4540	.1391	.4070
LIQUID PHASE FUG COEF	1.746	.099	.086
LIQUID ACT COEF	1.061	1.003	1.027
K OBS	1.698	.441	.413
K CALC	1.771	.414	.397
PERCENT DEV	-4.30	5.99	3.88

RUN NUMBER 60

PRESSURE = 2047 PSIA TEMPERATURE = 220 DEG F
VAP. SPEC. VOL. = .1630 LIT/GMOLE COMPRESSIBILITY = .733

	METHANE	ISOPENTANE	NOR-PENTANE
VAPOR PHASE COMP	.7470	.0652	.1878
VAPOR PHASE FUG COEF	1.0753	.1894	.1725
LIQUID PHASE COMP	.5550	.1117	.3330
LIQUID PHASE FUG COEF	1.563	.093	.080
LIQUID ACT COEF	1.047	1.010	1.043
K OBS	1.346	.584	.564
K CALC	1.523	.496	.486
PERCENT DEV	-13.12	15.04	13.79

RUN NUMBER 61

PRESSURE = 1519 PSIA TEMPERATURE = 220 DEG F
VAP. SPEC. VOL. = .2407 LIT/GMOLE COMPRESSIBILITY = .803

	METHANE	ISOPENTANE	NOR-PENTANE
VAPOR PHASE COMP	.8010	.0527	.1466
VAPOR PHASE FUG COEF	1.0132	.3091	.2907
LIQUID PHASE COMP	.3890	.1540	.4570
LIQUID PHASE FUG COEF	1.966	.106	.092
LIQUID ACT COEF	1.070	1.001	1.019
K OBS	2.059	.342	.321
K CALC	2.077	.343	.322
PERCENT DEV	-.88	-.21	-.30

RUN NUMBER 62

PRESSURE = 1263 PSIA TEMPERATURE = 220 DEG F
VAP. SPEC. VOL. = .2997 LIT/GMOLE COMPRESSIBILITY = .831

	METHANE	ISOPENTANE	NOR-PENTANE
VAPOR PHASE COMP	.8100	.0509	.1391
VAPOR PHASE FUG COEF	1.0044	.3791	.3607
LIQUID PHASE COMP	.3190	.1716	.5090
LIQUID PHASE FUG COEF	2.295	.117	.101
LIQUID ACT COEF	1.080	1.000	1.013
K OBS	2.539	.297	.273
K CALC	2.467	.308	.284
PERCENT DEV	2.86	-3.77	-3.97

RUN NUMBER 63

PRESSURE = 995 PSIA TEMPERATURE = 220 DEG F
VAP. SPEC. VOL. = .3933 LIT/GMOLE COMPRESSIBILITY = .859

	METHANE	ISOPENTANE	NOR-PENTANE
VAPOR PHASE COMP	.8100	.0510	.1394
VAPOR PHASE FUG COEF	1.0009	.4613	.4435
LIQUID PHASE COMP	.2510	.1876	.5610
LIQUID PHASE FUG COEF	2.833	.135	.117
LIQUID ACT COEF	1.088	1.000	1.008
K OBS	3.227	.272	.248
K CALC	3.080	.292	.265
PERCENT DEV	4.55	-7.37	-6.81

RUN NUMBER 64

PRESSURE = 753 PSIA TEMPERATURE = 220 DEG F
VAP. SPEC. VOL. = .5291 LIT/GMOLE COMPRESSIBILITY = .875

	METHANE	ISOPENTANE	NOR-PENTANE
VAPOR PHASE COMP	.7980	.0577	.1545
VAPOR PHASE FUG COEF	1.0086	.5375	.5203
LIQUID PHASE COMP	.1867	.2050	.6090
LIQUID PHASE FUG COEF	3.666	.163	.141
LIQUID ACT COEF	1.097	1.001	1.005
K OBS	4.221	.281	.254
K CALC	3.986	.303	.272
PERCENT DEV	5.56	-7.60	-7.32

RUN NUMBER 65

PRESSURE = 507 PSIA TEMPERATURE = 220 DEG F
VAP. SPEC. VOL. = .8027 LIT/GMOLE COMPRESSIBILITY = .894

	METHANE	ISOPENTANE	NOR-PENTANE
VAPOR PHASE COMP	.7440	.0701	.1854
VAPOR PHASE FUG COEF	1.0174	.6321	.6164
LIQUID PHASE COMP	.1202	.2200	.6600
LIQUID PHASE FUG COEF	5.368	.220	.190
LIQUID ACT COEF	1.105	1.003	1.003
K OBS	6.190	.319	.281
K CALC	5.829	.348	.309
PERCENT DEV	5.83	-9.33	-10.17

RUN NUMBER 66

PRESSURE = 538 PSIA TEMPERATURE = 280 DEG F
VAP. SPEC. VOL. = .7642 LIT/GMOLE COMPRESSIBILITY = .831

	METHANE	ISOPENTANE	NOR-PENTANE
VAPOR PHASE COMP	.5630	.1162	.3200
VAPOR PHASE FUG COEF	1.0923	.6171	.5990
LIQUID PHASE COMP	.0998	.2200	.6810
LIQUID PHASE FUG COEF	5.330	.348	.313
LIQUID ACT COEF	1.098	1.003	1.002
K OBS	5.641	.528	.470
K CALC	5.359	.566	.524
PERCENT DEV	5.00	-7.22	-11.44

RUN NUMBER 67

PRESSURE = 780 PSIA TEMPERATURE = 280 DEG F
VAP. SPEC. VOL. = .5338 LIT/GMOLE COMPRESSIBILITY = .819

	METHANE	ISOPENTANE	NOR-PENTANE
VAPOR PHASE COMP	.6300	.0967	.2730
VAPOR PHASE FUG COEF	1.0872	.5371	.5180
LIQUID PHASE COMP	.1622	.2020	.6360
LIQUID PHASE FUG COEF	3.809	.265	.239
LIQUID ACT COEF	1.092	1.002	1.004
K OBS	3.884	.479	.429
K CALC	3.825	.495	.463
PERCENT DEV	1.53	-3.31	-7.75

RUN NUMBER 68

PRESSURE = 1001 PSIA TEMPERATURE = 280 DEG F
VAP. SPEC. VOL. = .3940 LIT/GMOLE COMPRESSIBILITY = .800

	METHANE	ISOPENTANE	NOR-PENTANE
VAPOR PHASE COMP	.6620	.0866	.2510
VAPOR PHASE FUG COEF	1.0917	.4613	.4416
LIQUID PHASE COMP	.2310	.1866	.5820
LIQUID PHASE FUG COEF	2.936	.217	.196
LIQUID ACT COEF	1.004	1.000	1.007
K OBS	2.866	.464	.431
K CALC	2.914	.471	.446
PERCENT DEV	-1.68	-1.51	-3.51

RUN NUMBER 69

PRESSURE = 1253 PSIA TEMPERATURE = 280 DEG F
VAP. SPEC. VOL. = .3164 LIT/GMOLE COMPRESSIBILITY = .800

	METHANE	ISOPENTANE	NOR-PENTANE
VAPOR PHASE COMP	.6740	.0809	.2450
VAPOR PHASE FUG COEF	1.0761	.3904	.3709
LIQUID PHASE COMP	.3064	.1644	.5291
LIQUID PHASE FUG COEF	2.394	.188	.169
LIQUID ACT COEF	1.075	1.000	1.011
K OBS	2.200	.492	.463
K CALC	2.391	.481	.462
PERCENT DEV	-8.70	2.28	.29

RUN NUMBER 66A

PRESSURE = 541 PSIA TEMPERATURE = 280 DEG F
VAP. SPEC. VOL. = .7614 LIT/GMOLE COMPRESSIBILITY = .831

	METHANE	ISOPENTANE	NOR-PENTANE
VAPOR PHASE COMP	.5680	.1197	.3120
VAPOR PHASE FUG COEF	1.0925	.6187	.6007
LIQUID PHASE COMP	.1030	.2320	.6650
LIQUID PHASE FUG COEF	5.310	.347	.312
LIQUID ACT COEF	1.097	1.003	1.002
K OBS	5.515	.516	.469
K CALC	5.333	.563	.521
PERCENT DEV	3.28	-9.13	-11.00

RUN NUMBER 67A

PRESSURE = 757 PSIA TEMPERATURE = 280 DEG F
VAP. SPEC. VOL. = .5359 LIT/GMOLE COMPRESSIBILITY = .819

	METHANE	ISOPENTANE	NOR-PENTANE
VAPOR PHASE COMP	.6290	.1020	.2690
VAPOR PHASE FUG COEF	1.0874	.5377	.5187
LIQUID PHASE COMP	.1642	.2140	.6210
LIQUID PHASE FUG COEF	3.824	.266	.239
LIQUID ACT COEF	1.091	1.001	1.004
K OBS	3.831	.477	.433
K CALC	3.836	.495	.463
PERCENT DEV	-.13	-3.93	-6.99

RUN NUMBER 68A

PRESSURE = 1031 PSIA TEMPERATURE = 280 DEG F
VAP. SPEC. VOL. = .3830 LIT/GMOLE COMPRESSIBILITY = .797

	METHANE	ISOPENTANE	NOR-PENTANE
VAPOR PHASE COMP	.6650	.0910	.2440
VAPOR PHASE FUG COEF	1.0936	.4530	.4332
LIQUID PHASE COMP	.2420	.1956	.5630
LIQUID PHASE FUG COEF	2.856	.213	.192
LIQUID ACT COEF	1.082	1.000	1.007
K OBS	2.748	.465	.433
K CALC	2.826	.470	.446
PERCENT DEV	-2.84	-1.07	-3.00

RUN NUMBER 69A

PRESSURE = 1255 PSIA TEMPERATURE = 280 DEG F
VAP. SPEC. VOL. = .3072 LIT/GMOLE COMPRESSIBILITY = .778

	METHANE	ISOPENTANE	NOR-PENTANE
VAPOR PHASE COMP	.6740	.0870	.2380
VAPOR PHASE FUG COEF	1.1046	.3924	.3724
LIQUID PHASE COMP	.3040	.1797	.5160
LIQUID PHASE FUG COEF	2.390	.188	.169
LIQUID ACT COEF	1.075	1.000	1.011
K OBS	2.217	.484	.461
K CALC	2.325	.478	.459
PERCENT DEV	-4.87	1.28	.39

RUN NUMBER 70B

PRESSURE = 1565 PSIA TEMPERATURE = 280 DEG F
VAP. SPEC. VOL. = .2187 LIT/GMOLE COMPRESSIBILITY = .691

	METHANE	ISOPENTANE	NOR-PENTANE
VAPOR PHASE COMP	.6160	.0994	.2850
VAPOR PHASE FUG COEF	1.2191	.2822	.2618
LIQUID PHASE COMP	.4530	.1384	.4080
LIQUID PHASE FUG COEF	1.975	.165	.149
LIQUID ACT COEF	1.056	1.003	1.024
K OBS	1.360	.718	.699
K CALC	1.711	.588	.584
PERCENT DEV	-25.84	18.15	16.35

AVE. ABS. PERCENT DEV. FOR SYSTEM = 6.073

APPENDIX B

EXPERIMENTAL DATA

Table XXVI presents the experimental data for all three binary systems considered in this research. Data are arranged such that the values presented with an "A" suffix are the averaged values of duplicate or triplicate analyses. Beneath the averaged values are listed the individual analyses of each run. Also included in this table are the equilibrium pressure and temperature for each run.

Table XXVII presents the experimental data for the two ternary systems investigated. As described in the previous paragraph, averaged compositions values are denoted with an "A" suffix. Pressures and temperatures are included for each run.

TABLE XXVI

EXPERIMENTAL DATA FOR BINARY SYSTEMS

METHANE NORMAL PENTANE BINARY SYSTEM

RUN NUMBER	PRESS PSIA	TEMP (F)	VAPOR COMPOSITION C1	VAPOR COMPOSITION N-C5	LIQUID COMPOSITION C1	LIQUID COMPOSITION N-C5
21	1502	220	.8080 A	.1920 A	.3804 A	.6196 A
			.8011	.1989	.3804	.6196
			.8096	.1904		
			.8135	.1865		
22	1265	220	.8115 A	.1885 A	.3242 A	.6758 A
			.8061	.1939	.3221	.6779
			.8169	.1831	.3264	.6736
23	1231	220	.8102 A	.1898 A	.3059 A	.6941 A
			.8066	.1934	.3073	.6927
			.8211	.1789	.3053	.6947
			.8028	.1972	.3050	.6950
24	1023	220	.8059 A	.1941 A	.2527 A	.7473 A
			.7994	.2006	.2521	.7479
			.8124	.1876	.2532	.7468
25	1001	220	.8047 A	.1953 A	.2472 A	.7528 A
			.8008	.1992	.2470	.7530
			.8079	.1921	.2474	.7526
			.8053	.1947		

METHANE NORMAL PENTANE BINARY SYSTEM

RUN NUMBER	PRESS PSIA	TEMP (F)	VAPOR COMPOSITION C1	VAPOR COMPOSITION N-C5	LIQUID COMPOSITION C1	LIQUID COMPOSITION N-C5
26	1999	220	.7400 A	.2600 A	.5316 A	.4684 A
			.7440	.2560	.5323	.4677
			.7360	.2640	.5309	.4691
27	1777	220	.7883 A	.2117 A	.4559 A	.5441 A
			.7835	.2165	.4573	.5427
			.7909	.2091	.4545	.5455
			.7906	.2094		
28	1501	220	.8084 A	.1916 A	.3825 A	.6175 A
			.8083	.1917	.3829	.6171
			.8086	.1914	.3928	.6072
					.3717	.6283
29	1260	220	.8155 A	.1845 A	.3103 A	.6897 A
			.8203	.1797	.3129	.6871
			.8108	.1892	.3078	.6922
30	1005	220	.8137 A	.1863 A	.2481 A	.7519 A
			.8123	.1877	.2493	.7507
			.8151	.1849	.2469	.7531

METHANE ISO-PENTANE BINARY SYSTEM

RUN NUMBER	PRESS PSIA	TEMP (F)	VAPOR COMPOSITION C1	VAPOR COMPOSITION ISOC5	LIQUID COMPOSITION C1	LIQUID COMPOSITION ISOC5
31	1256	220	.7876 A	.2124 A	.3310 A	.6690 A
			.7862	.2138	.3251	.6749
			.7891	.2109	.3328	.6672
					.3368	.6632
					.3293	.6707
32	1503	220	.7742 A	.2258 A	.3960 A	.6040 A
			.7746	.2254	.3946	.6054
			.7738	.2262	.3974	.6026
33	1721	220	.7462 A	.2538 A	.4536 A	.5464 A
			.7440	.2560	.4500	.5500
			.7484	.2516	.4568	.5432
					.4539	.5461
34	1899	220	.6861 A	.3139 A	.5662 A	.4338 A
			.6811	.3189	.5662	.4338
			.6911	.3089	.5663	.4337
			.6861	.3139		
35	1001	220	.7907 A	.2093 A	.2617 A	.7383 A
			.7898	.2102	.2648	.7352
			.7916	.2084	.2608	.7392
					.2594	.7406
					.2619	.7381

METHANE ISO-PENTANE BINARY SYSTEM

RUN NUMBER	PRESS PSIA	TEMP (F)	VAPOR COMPOSITION C1	VAPOR COMPOSITION ISOC5	LIQUID COMPOSITION C1	LIQUID COMPOSITION ISOC5
36	759	220	.7653 A	.2347 A	.1917 A	.8083 A
			.7646	.2354	.1901	.8099
			.7660	.2340	.1897	.8103
					.1955	.8045
37	499	220	.7104 A	.2896 A	.1181 A	.8819 A
			.7120	.2880	.1185	.8815
			.7082	.2918	.1185	.8815
			.7110	.2890	.1173	.8827
38	502	160	.8407 A	.1593 A	.1418 A	.8582 A
			.8396	.1604	.1411	.8589
			.8418	.1582	.1416	.8584
					.1429	.8571
39	755	160	.8717 A	.1283 A	.2182 A	.7818 A
			.8727	.1273	.2198	.7802
			.8708	.1292	.2169	.7831
					.2190	.7810
					.2172	.7828
40	1001	160	.8854 A	.1146 A	.2829 A	.7171 A
			.8867	.1133	.2836	.7164
			.8877	.1123	.2826	.7174
			.8817	.1183	.2825	.7175
41	1253	160	.8794 A	.1206 A	.3513 A	.6487 A
			.8792	.1208	.3508	.6492
			.8796	.1204	.3534	.6466
					.3497	.6503

METHANE ISO-PENTANE BINARY SYSTEM

RUN NUMBER	PRESS PSIA	TEMP (F)	VAPOR COMPOSITION C1	VAPOR COMPOSITION ISOC5	LIQUID COMPOSITION C1	LIQUID COMPOSITION ISOC5
42	1505	160	.8692 A	.1308 A	.4178 A	.5822 A
			.8687	.1313	.4178	.5822
			.8698	.1302	.4179	.5821
43A	1759	160	.8526 A	.1474 A	.4889 A	.5111 A
			.8477	.1523	.4899	.5101
			.8554	.1446	.4879	.5121
			.8546	.1454		
44	1992	160	.6209 A	.1791 A	.5451 A	.4549 A
			.8136	.1864	.5454	.4546
			.8253	.1747	.5448	.4552
			.8237	.1763		
45	2191	160	.7413 A	.2587 A	.6333 A	.3667 A
			.7409	.2591	.6328	.3672
			.7417	.2583	.6361	.3639
					.6311	.3689
46	511	280	.5204 A	.4796 A	.0916 A	.9084 A
			.5202	.4798	.0928	.9072
			.5188	.4812	.0909	.9091
			.5222	.4778	.0912	.9088
47	759	280	.6030 A	.3970 A	.1613 A	.8387 A
			.6018	.3982	.1616	.8384
			.6041	.3959	.1611	.8389

METHANE ISO-PENTANE BINARY SYSTEM

RUN NUMBER	PRESS PSIA	TEMP (F)	VAPOR COMPOSITION C1	VAPOR COMPOSITION ISOC5	LIQUID COMPOSITION C1	LIQUID COMPOSITION ISOC5
48	1001	280	.6360 A	.3640 A	.2313 A	.7687 A
			.6356	.3644	.2302	.7698
			.6405	.3595	.2325	.7675
			.6319	.3681		
49	1267	280	.6510 A	.3490 A	.3152 A	.6848 A
			.6463	.3537	.3151	.6849
			.6556	.3444	.3152	.6848
49A	1277	280	.6432 A	.3568 A	.3301 A	.6699 A
			.6432	.3568	.3300	.6700
					.3302	.6698
50	1517	280	.5814 A	.4186 A	.4881 A	.5119 A
			.5800	.4200	.4867	.5133
			.5828	.4172	.4857	.5143
					.4918	.5082

METHANE NEO-PENTANE BINARY SYSTEM

RUN NUMBER	PRESS PSIA	TEMP (F)	VAPOR COMPOSITION C1	NEOC5	LIQUID COMPOSITION C1	NEOC5
71	511	160	.7608 A	.2392 A	.1532 A	.8468 A
			.7635	.2365	.1535	.8465
			.7580	.2420	.1529	.8471
72	763	160	.7973 A	.2027 A	.2322 A	.7678 A
			.7957	.2043	.2312	.7688
			.7990	.2010	.2331	.7669
					.2324	.7676
73	1005	160	.8191 A	.1809 A	.3118 A	.6882 A
			.8176	.1824	.3114	.6886
			.8214	.1786	.3122	.6878
			.8181	.1819		
74	1273	160	.8133 A	.1867 A	.3909 A	.6091 A
			.8124	.1876	.3914	.6086
			.8142	.1858	.3904	.6096
74A	1281	160	.8126 A	.1874 A	.3975 A	.6025 A
			.8126	.1874	.3991	.6009
					.3959	.6041

METHANE NEO-PENTANE BINARY SYSTEM

RUN NUMBER	PRESS PSIA	TEMP (F)	VAPOR COMPOSITION C1	NEOC5	LIQUID COMPOSITION C1	NEOC5
75A	1521	160	.7842 A	.2158 A	.4815 A	.5185 A
			.7817	.2183	.4822	.5178
			.7866	.2134	.4808	.5192
76B	1709	160	.7274 A	.2726 A	.5601 A	.4399 A
			.7261	.2739	.5595	.4405
			.7286	.2714	.5608	.4392
77	1748	160	.6853 A	.3147 A	.6028 A	.3972 A
			.6835	.3165	.6004	.3996
			.6871	.3129	.6056	.3944
					.6025	.3975
82	310	160	.6670 A	.3330 A	.0852 A	.9148 A
			.6667	.3333	.0849	.9151
			.6672	.3328	.0855	.9145
					.0851	.9149
83	308	220	.3949 A	.6051 A	.0505 A	.9495 A
			.3912	.6088	.0507	.9493
			.3986	.6014	.0503	.9497
			.3949	.6051		
84	503	220	.5631 A	.4369 A	.1168 A	.8832 A
			.5628	.4372	.1163	.8837
			.5616	.4384	.1168	.8832
			.5650	.4350	.1172	.8828

METHANE NEO-PENTANE BINARY SYSTEM

RUN NUMBER	PRESS PSIA	TEMP (F)	VAPOR COMPOSITION C1	VAPOR COMPOSITION NEOC5	LIQUID COMPOSITION C1	LIQUID COMPOSITION NEOC5
85	748	220	.6389 A	.3611 A	.1970 A	.8030 A
			.6374	.3626	.1967	.8033
			.6403	.3597	.1976	.8024
					.1966	.8034
86	1008	220	.6703 A	.3297 A	.2819 A	.7181 A
			.6711	.3289	.2822	.7178
			.6696	.3304	.2816	.7184
87A	1251	220	.6535 A	.3465 A	.3766 A	.6234 A
			.6535	.3465	.3767	.6233
			.6535	.3465	.3765	.6235
88A	1434	220	.5852 A	.4148 A	.4712 A	.5288 A
			.5847	.4153	.4700	.5300
			.5857	.4143	.4724	.5276
91	506	280	.2803 A	.7197 A	.0683 A	.9317 A
			.2801	.7199	.0688	.9312
			.2605	.7195	.0678	.9322
					.0684	.9316
92	755	280	.4068 A	.5932 A	.1632 A	.8368 A
			.4082	.5918	.1635	.8365
			.4054	.5946	.1659	.8341
					.1604	.8396
93B	1004	280	.4159 A	.5841 A	.2813 A	.7187 A
			.4155	.5845	.2817	.7183
			.4158	.5842	.2814	.7186
			.4164	.5836	.2807	.7193

TABLE XXVII

EXPERIMENTAL DATA FOR TERNARY SYSTEMS

METHANE NEOPENTANE NORMAL PENTANE TERNARY SYSTEM

RUN NUMBER	PRESS PSIA	TEMP (F)	VAPOR COMPOSITION C1	NEOC5	N-C5	LIQUID COMPOSITION C1	NEOC5	N-C5
95	503	160	.8451 A	.0577 A	.0972 A	.1407 A	.2165 A	.6429 A
			.8438	.0582	.0980	.1409	.2165	.6426
			.8464	.0571	.0964	.1405	.2164	.6431
96	751	160	.8714 A	.0459 A	.0827 A	.2058 A	.1997 A	.5945 A
			.8708	.0460	.0832	.2054	.2000	.5946
			.8721	.0458	.0822	.2063	.1995	.5943
97	1251	160	.8778 A	.0404 A	.0818 A	.3375 A	.1641 A	.4985 A
			.8771	.0404	.0826	.3367	.1640	.4993
			.8786	.0404	.0810	.3383	.1641	.4976
98	1505	160	.8699 A	.0410 A	.0891 A	.3998 A	.1482 A	.4520 A
			.8699	.0407	.0893	.3976	.1489	.4535
			.8699	.0412	.0889	.4021	.1475	.4505

METHANE NEOPENTANE NORMAL PENTANE TERNARY SYSTEM

RUN NUMBER	PRESS PSIA	TEMP (F)	VAPOR COMPOSITION C1	NEOC5	N-C5	LIQUID COMPOSITION C1	NEOC5	N-C5
99	1759	160	.8546 A	.0429 A	.1025 A	.4607 A	.1314 A	.4079 A
			.8566	.0422	.1012	.4595	.1318	.4086
			.8512	.0438	.1050	.4619	.1310	.4071
			.8559	.0427	.1014			
100	2013	160	.8052 A	.0536 A	.1413 A	.5500 A	.1112 A	.3388 A
			.8037	.0540	.1423	.5494	.1109	.3397
			.8066	.0531	.1402	.5518	.1109	.3374
						.5488	.1118	.3393
101	2120	160	.7753 A	.0591 A	.1655 A	.6019 A	.0976 A	.3005 A
			.7742	.0589	.1669	.6001	.0981	.3019
			.7764	.0594	.1642	.6023	.0979	.2998
						.6033	.0968	.2999
102	1006	160	.8787 A	.0406 A	.0807 A	.2781 A	.1760 A	.5459 A
			.8791	.0404	.0805	.2783	.1759	.5458
			.8782	.0408	.0810	.2779	.1761	.5460

METHANE ISOPENTANE NORMAL PENTANE TERNARY SYSTEM

RUN NUMBER	PRESS PSIA	TEMP (F)	VAPOR COMPOSITION C1	ISOC5	N-C5	LIQUID COMPOSITION C1	ISOC5	N-C5
51	504	160	.8712 A	.0395 A	.0892 A	.1386 A	.2227 A	.6387 A
			.8713	.0402	.0885	.1386	.2227	.6387
			.8712	.0389	.0899			
52	755	160	.8939 A	.0305 A	.0755 A	.2114 A	.2058 A	.5828 A
			.8938	.0305	.0757	.2101	.2057	.5842
			.8940	.0306	.0754	.2127	.2059	.5814
53	1003	160	.8971 A	.0296 A	.0733 A	.2738 A	.1888 A	.5374 A
			.8967	.0300	.0733	.2723	.1888	.5389
			.8976	.0292	.0732	.2753	.1888	.5358
54	1493	160	.8890 A	.0307 A	.0803 A	.4057 A	.1536 A	.4408 A
			.8884	.0309	.0807	.4039	.1539	.4421
			.8896	.0306	.0798	.4074	.1532	.4394

METHANE ISOPENTANE NORMAL PENTANE TERNARY SYSTEM

RUN NUMBER	PRESS PSIA	TEMP (F)	VAPOR COMPOSITION C1	ISOC5	N-C5	LIQUID COMPOSITION C1	ISOC5	N-C5
55	1975	160	.8488 A	.0405 A	.1107 A	.5038 A	.1290 A	.3672 A
			.8491	.0398	.1112	.5029	.1293	.3678
			.8485	.0412	.1103	.5048	.1287	.3665
55A	1995	160	.8419 A	.0422 A	.1159 A	.5210 A	.1229 A	.3561 A
			.8372	.0430	.1198	.5240	.1219	.3541
			.8467	.0414	.1120	.5180	.1239	.3580
58	2268	160	.7585 A	.0632 A	.1783 A	.5934 A	.1039 A	.3027 A
			.7566	.0639	.1795	.5894	.1050	.3056
			.7605	.0625	.1770	.5973	.1029	.2998
59	1765	220	.7706 A	.0613 A	.1681 A	.4537 A	.1391 A	.4072 A
			.7681	.0619	.1700	.4536	.1398	.4066
			.7731	.0607	.1662	.4539	.1384	.4078
60	2047	220	.7470 A	.0652 A	.1878 A	.5552 A	.1117 A	.3331 A
			.7436	.0659	.1906	.5543	.1119	.3338
			.7505	.0645	.1849	.5561	.1115	.3324

METHANE ISOPENTANE NORMAL PENTANE TERNARY SYSTEM

RUN NUMBER	PRESS PSIA	TEMP (F)	VAPOR COMPOSITION C1	ISOC5	N-C5	LIQUID COMPOSITION C1	ISOC5	N-C5
61	1519	220	.8006 A	.0527 A	.1466 A	.3887 A	.1540 A	.4573 A
			.7976	.0539	.1485	.3870	.1548	.4582
			.8037	.0515	.1448	.3905	.1532	.4563
62	1263	220	.8100 A	.0509 A	.1391 A	.3191 A	.1716 A	.5093 A
			.8111	.0507	.1382	.3179	.1716	.5104
			.8089	.0510	.1401	.3203	.1716	.5082
63	995	220	.8096 A	.0510 A	.1394 A	.2513 A	.1876 A	.5611 A
			.8073	.0516	.1410	.2478	.1880	.5642
			.8119	.0504	.1377	.2548	.1872	.5580
64	753	220	.7878 A	.0577 A	.1545 A	.1867 A	.2047 A	.6086 A
			.7845	.0592	.1564	.1857	.2047	.6097
			.7911	.0563	.1526	.1878	.2047	.6075
65	507	220	.7445 A	.0701 A	.1854 A	.1202 A	.2198 A	.6599 A
			.7400	.0725	.1875	.1201	.2193	.6605
			.7490	.0677	.1833	.1203	.2203	.6593

METHANE ISOPENTANE NORMAL PENTANE TERNARY SYSTEM

RUN NUMBER	PRESS PSIA	TEMP (F)	VAPOR COMPOSITION C1	ISOC5	N-C5	LIQUID COMPOSITION C1	ISOC5	N-C5
66	539	280	.5633 A	.1162 A	.3205 A	.0998 A	.2196 A	.6806 A
			.5624	.1165	.3211	.1001	.2195	.6804
			.5642	.1159	.3198	.0994	.2197	.6809
67	760	280	.6303 A	.0967 A	.2730 A	.1622 A	.2017 A	.6361 A
			.6306	.0973	.2721	.1630	.2007	.6363
			.6300	.0962	.2739	.1614	.2028	.6358
68	1001	280	.6623 A	.0866 A	.2510 A	.2311 A	.1866 A	.5822 A
			.6625	.0862	.2512	.2295	.1861	.5844
			.6621	.0870	.2509	.2327	.1872	.5800
69	1253	280	.6738 A	.0809 A	.2452 A	.3064 A	.1644 A	.5291 A
			.6736	.0803	.2461	.3060	.1654	.5287
			.6740	.0816	.2444	.3068	.1635	.5296
66A	541	280	.5682 A	.1197 A	.3120 A	.1030 A	.2321 A	.6649 A
			.5660	.1207	.3133	.1036	.2337	.6627
			.5705	.1188	.3107	.1025	.2305	.6670

METHANE ISOPENTANE NORMAL PENTANE TERNARY SYSTEM

RUN NUMBER	PRESS PSIA	TEMP (F)	VAPOR COMPOSITION C1	ISOC5	N-C5		LIQUID COMPOSITION C1	ISOC5	N-C5	
67A	757	280	.6292	.1020	.2687	A	.1642	.2143	.6215	A
			.6262	.1028	.2710		.1647	.2145	.6207	
			.6323	.1012	.2665		.1637	.2141	.6222	
68A	1031	280	.6646	.0910	.2444	A	.2417	.1956	.5628	A
			.6625	.0918	.2457		.2385	.1967	.5649	
			.6668	.0902	.2430		.2449	.1944	.5607	
69A	1255	280	.6745	.0870	.2385	A	.3042	.1797	.5161	A
			.6679	.0884	.2436		.3070	.1768	.5162	
			.6811	.0856	.2333		.3014	.1827	.5160	
70B	1565	280	.6156	.0994	.2850	A	.4533	.1384	.4083	A
			.6156	.0994	.2850		.4533	.1384	.4083	

APPENDIX C

CALIBRATIONS

A. Calibration of Pressure Gauge

The Heise pressure gauge (Model No. H24564) was calibrated using a dead weight tester. The tester (No. 1315) was supplied by the American Gauge Company. The calibration results are given in Table XXVIII.

TABLE XXVIII

CALIBRATION OF PRESSURE GAUGE

Actual Pressure (psi)	Heise Pressure Gauge Reading	
	UP	DOWN
300	299	300
500	500	500
750	748	750
999	998	999
1249	1248	1249
1499	1499	1499
1749	1748	1749
1999	1997	1998
2249	2246	2247
2498	2496	2496

B. Calibration of Thermometer

The gas-filled mercury in glass thermometer (Model No. 1704431), supplied by the Taylor Thermometer Company and used to measure equilibrium temperatures, was calibrated by comparison with previously calibrated Princo thermometers. The calibrations are given in Table XXIX.

TABLE XXIX

CALIBRATION OF THERMOMETER

Princo Thermometer No. 253197	Taylor Thermometer Reading
71.2°C	160°F ≡ 71.1°C

Princo Thermometer No. 503944	Taylor Thermometer Reading
104.6°C	220°F ≡ 104.4°C
138.1°C	280°F ≡ 137.8°C

C. Calibration of Gas Chromatograph

Several synthetic mixtures of methane-normal pentane, methane-isopentane, and methane-neopentane were prepared for calibration of the Perkin-Elmer gas chromatograph. These mixtures were made up in a mixture-blending system which is described in the "Installation and Training Recommendations" of the Mass Spectrometer Model No. 21-103B, Consolidated Engineering Corporation, Pasadena, California. The mixtures of the three binary systems covered the range of interest for

this work. A computer program was written to calculate the number of moles of gas from the P-V-T measurements. The equation used was of the form:

$$P = RT\left[\frac{n}{V} + \frac{n^2 B}{V^2}\right]$$

The second virial coefficient, B, was determined from the equation presented by Pitzer and Curl.*

Calibrations were performed by introducing a sample of the mixture into the chromatograph in the same manner as described in Chapter VI. Areas under the resulting chromatographic curves were measured, and the area of ratio of methane to the pentane isomer was computed. This resultant area ratio was then plotted as a function of the corresponding known mole ratio.

Figure 23 is a plot of the area ratio as a function of mole ratio of methane to n-pentane. Figure 24 presents the inverse ratios as coordinates to better illustrate some of the data. Figures 25 and 26 are exactly analogous to Figures 23 and 24, except that the former are for the methane-isopentane binary mixtures. Figures 27 and 28 are the calibration curves for the methane-neopentane binary system.

A best "least squares" fit line was drawn through the points in Figures 23, 25, and 27. These calibration curves showed peak area to be linear with molar concentration of the sample. Mole fractions were then obtained from a normalized equation of the following form for

---

* Pitzer, K.S., and R.F. Curl, Jr., "Empirical Equation for the Second Virial Coefficient", J. Am. Chem. Soc., 79, 2369 (1957).

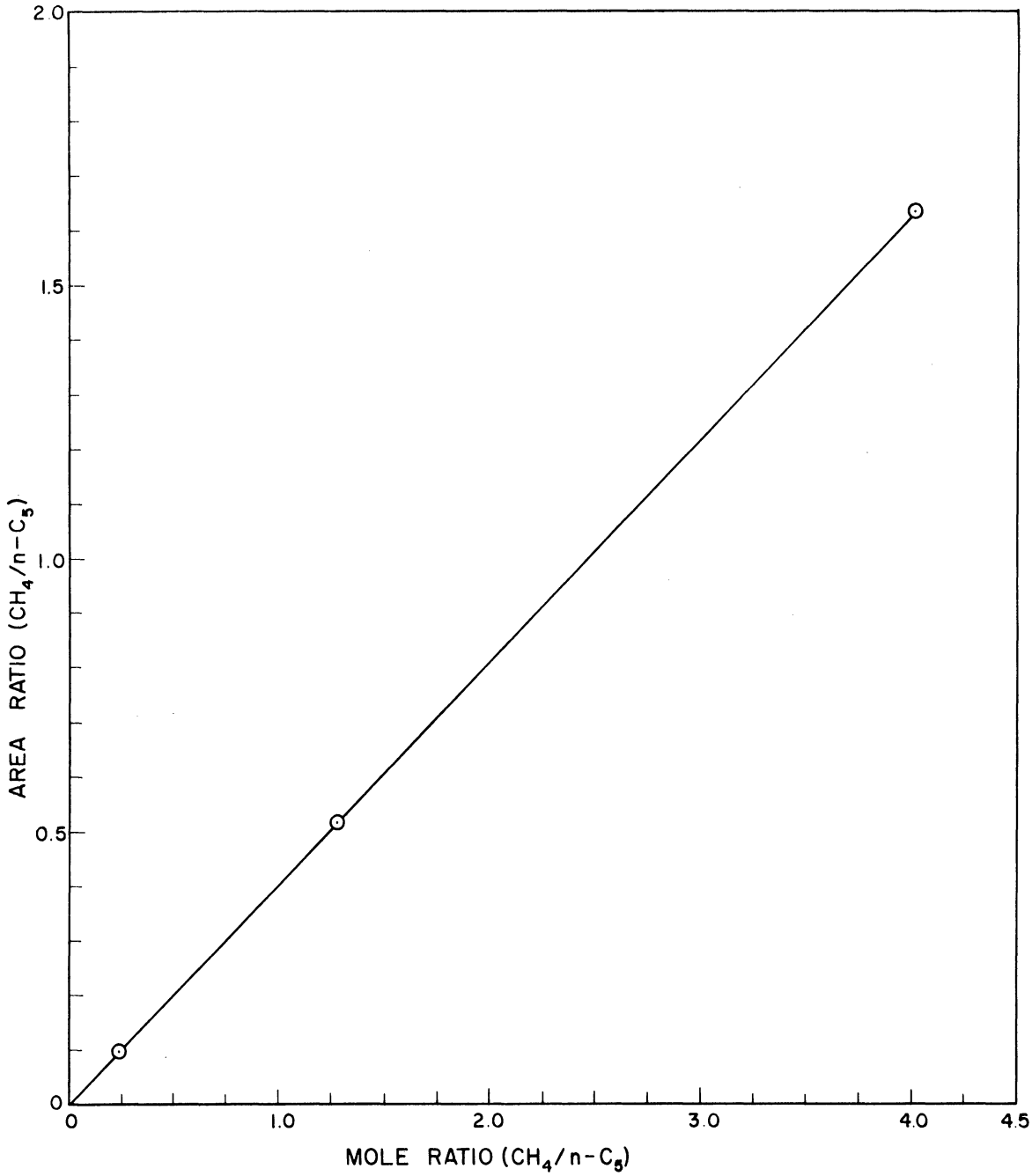

Figure 23. Gas Chromatograph Calibration for Methane-Normal Pentane System on a Normal Pentane Basis.

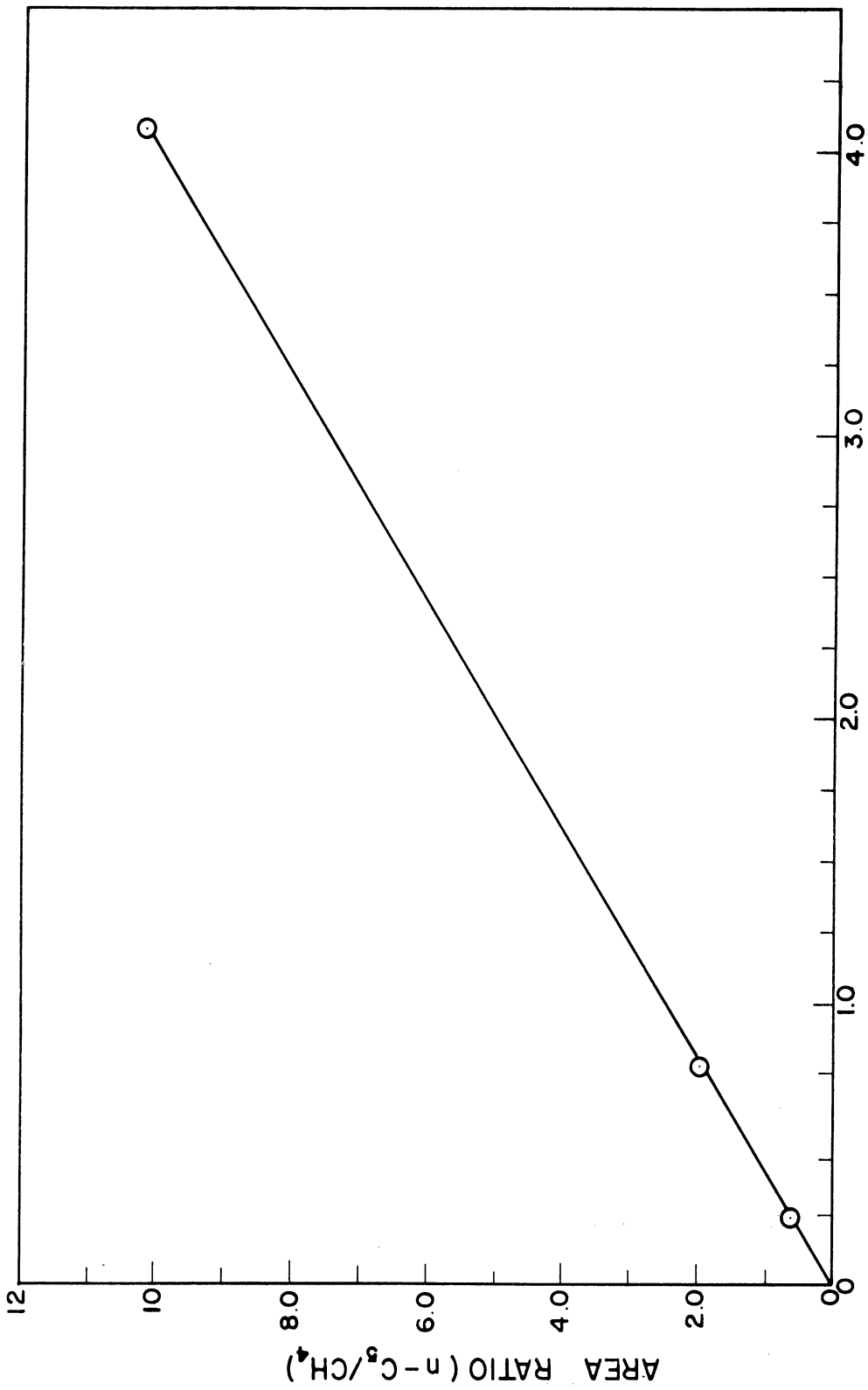

Figure 24. Gas Chromatograph Calibration for Methane-Normal Pentane System on a Methane Basis.

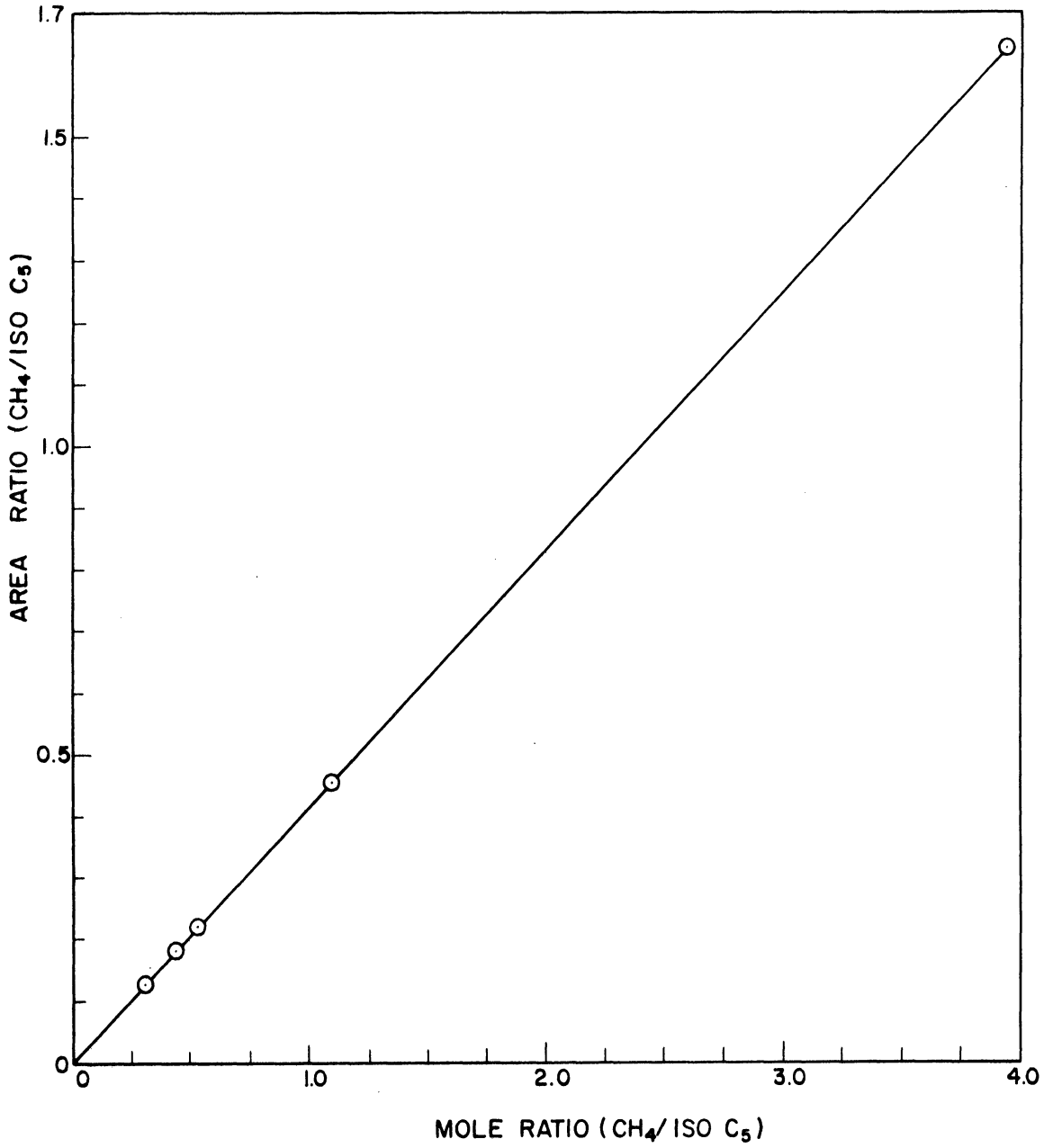

Figure 25. Gas Chromatograph Calibration for Methane-Isopentane System on an Isopentane Basis.

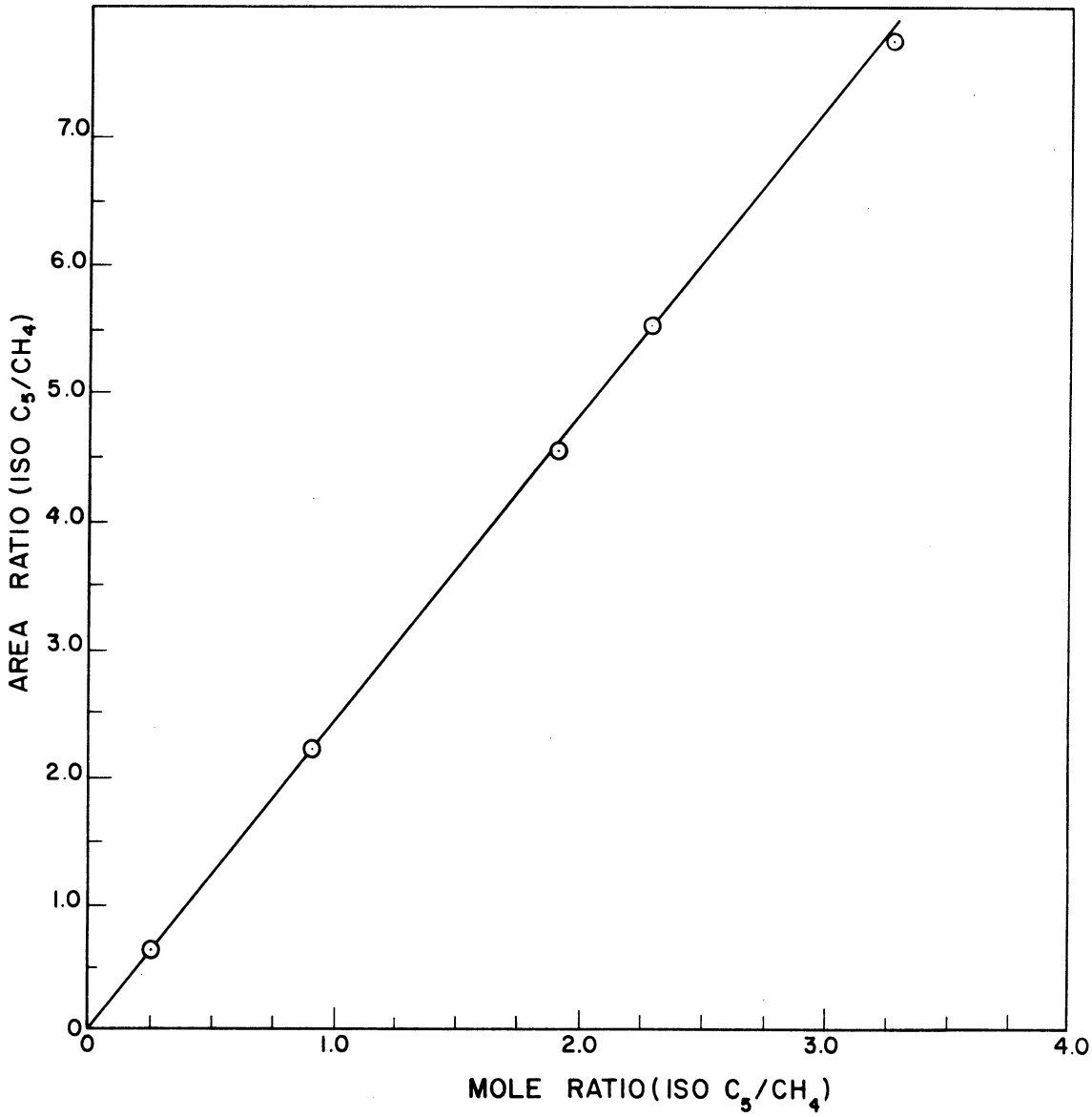

Figure 26. Gas Chromatograph Calibration for Methane-Isopentane System on a Methane Basis.

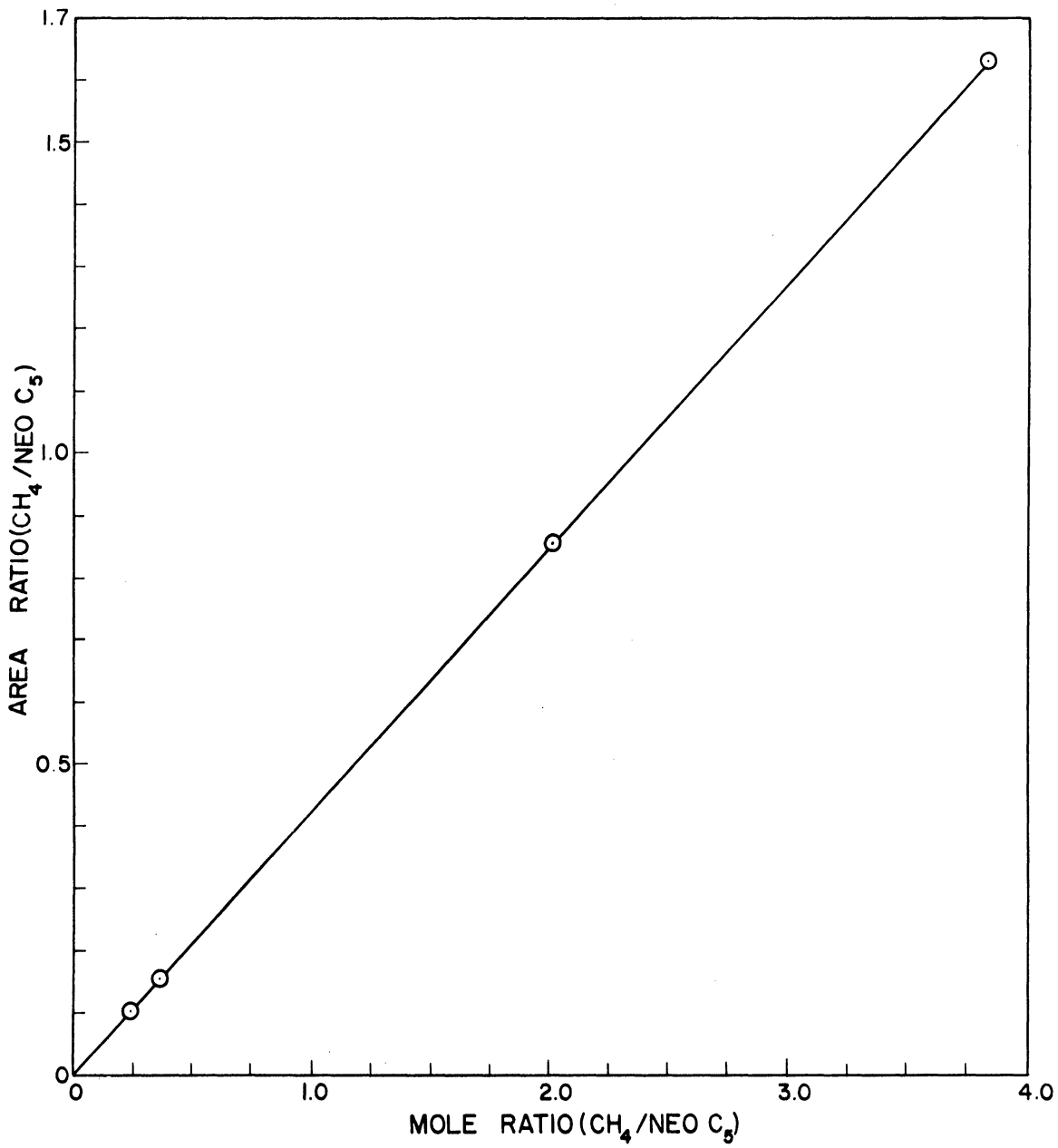

Figure 27. Gas Chromatograph Calibration for Methane-Neopentane System on a Neopentane Basis.

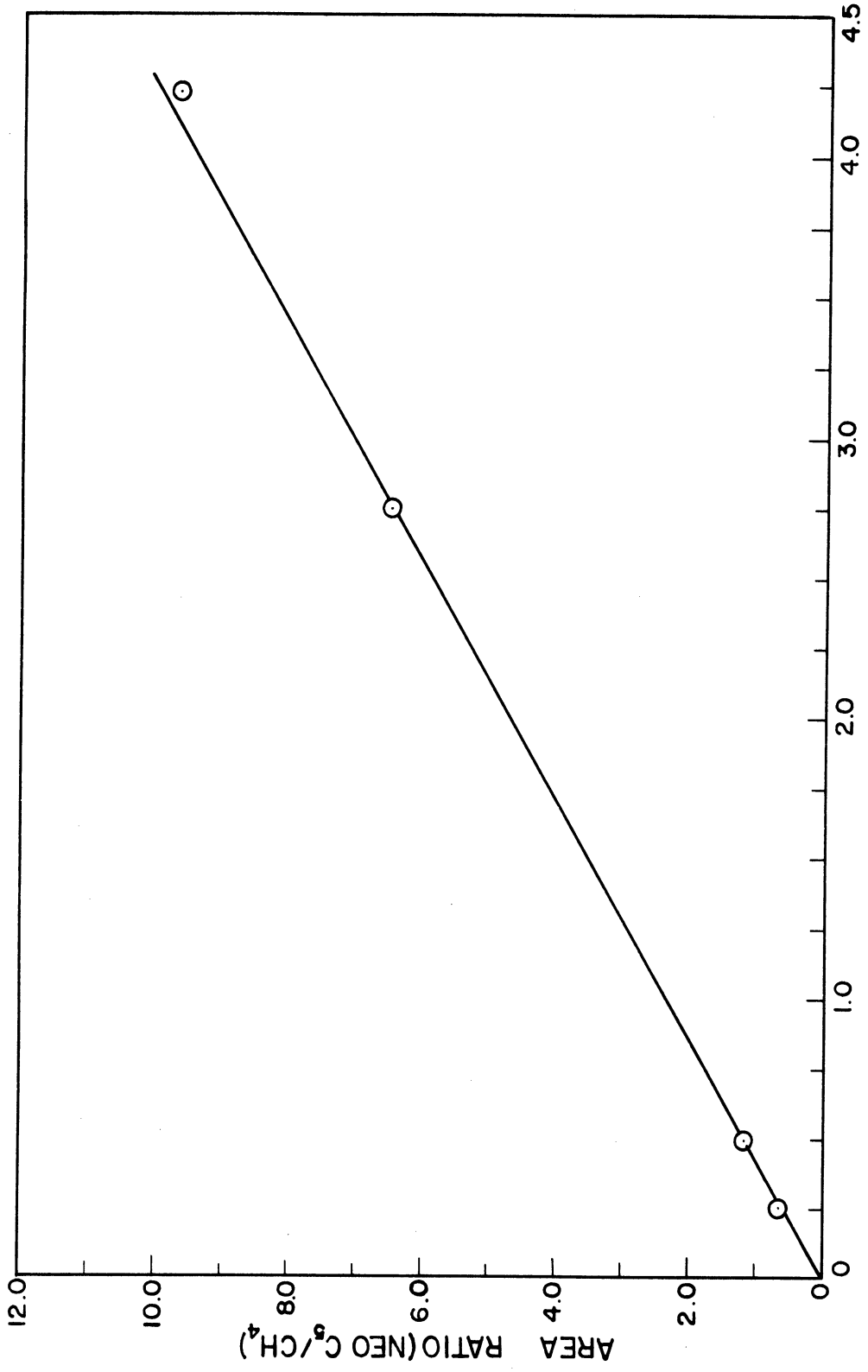

Figure 28. Gas Chromatograph Calibration for Methane-Neopentane System on a Methane Basis.

binary mixtures:

$$y_1 = \frac{A_1}{A_1 + cA_2}$$

An equation of the following form was used for composition determination of ternary mixtures:

$$y_1 = \frac{A_1}{A_1 + cA_2 + c'A_3}$$

where A_1 is the peak area for methane, and A_2 and A_3 are the peak areas for the pentane isomers. The symbols c and c' are the relative response factors established from the slope of the calibration curves. These response factors correct for the difference of thermal conductivity of the components.

Table XXX compares the methane composition as determined from the analytical technique with the known mole fraction for the three prepared mixtures of methane-n-pentane. Several analyses were made for each mixture.

Table XXXI compares the sample composition determined by chromotography with the known composition for four prepared methane-isopentane mixtures.

Table XXXII compares chromatographic composition determinations with known methane-neopentane mixtures.

Included in Tables XXX, XXXI, and XXXII are analyses of three mixtures determined with the aid of a mass spectrometer. Only one mixture of each of the three binary systems was subjected to mass spectrometer analysis.

TABLE XXX

COMPARISON OF ANALYSES FOR METHANE-N-PENTANE MIXTURES

Blend	Actual Composition mole % CH_4	Actual Composition mole % $n\text{-}C_5$		G.C. Analyses mole % CH_4	G.C. Analyses mole % $n\text{-}C_5$	M.S. Analyses mole % CH_4	M.S. Analyses mole % $n\text{-}C_5$
1	19.43	80.57		19.41	80.59	19.88	80.12
				19.49	80.51	19.50	80.50
				19.53	80.47	19.25	80.75
			Avg.	19.48	80.52	19.54	80.46
2	80.1	19.9		80.0	20.0		
				80.1	19.9		
				80.1	19.9		
			Avg.	80.1	19.9		
3	56.1	43.9		56.0	44.0		
				56.1	43.9		
				56.2	43.8		
				55.8	44.2		
			Avg.	56.0	44.0		

TABLE XXXI

COMPARISON OF ANALYSES FOR METHANE-ISOPENTANE MIXTURES

	Actual Composition mole %		G.C. Analyses mole %		M.S. Analyses mole %	
Blend	CH_4	i-C_5	CH_4	i-C_5	CH_4	i-C_5
1	30.4	69.6	30.5	69.5		
			30.5	69.5		
			30.4	69.6		
			Avg. 30.5	69.5		
2	34.4	65.6	34.4	65.6	35.14	64.86
			34.7	65.3	35.01	64.99
			34.4	65.6	33.84	66.16
			Avg. 34.5	65.5	34.67	65.33
3	52.1	47.9	51.9	48.1		
			52.0	48.0		
			52.6	47.4		
			52.1	47.9		
			Avg. 52.2	47.8		
4	79.7	20.3	79.8	20.2		
			79.6	20.4		
			79.8	20.2		
			79.7	20.3		
			Avg. 79.7	70.3		
5	23.4	76.6	23.8	76.2		
			23.6	76.4		
			23.7	76.3		
			23.3	76.7		
			23.7	76.3		
			Avg. 23.6	76.4		

TABLE XXXII

COMPARISON OF ANALYSES FOR METHANE-NEOPENTANE MIXTURES

Blend	Actual Composition mole % CH_4	neo C_5		G.C. Analyses mole % CH_4	neo C_5	M.S. Analyses mole % CH_4	neo C_5
1	19.14	80.86		19.49	80.51		
				19.47	80.53		
				19.57	80.43		
			Avg.	19.51	80.49		
2	26.8	73.2		26.7	73.3	26.51	73.49
				26.7	73.3	26.27	73.73
				26.3	73.7	26.47	73.53
				26.5	73.5		
			Avg.	26.5	73.5	26.41	73.59
3	79.2	20.8		79.2	20.8		
				79.1	20.9		
				79.5	20.5		
				79.3	20.7		
			Avg.	79.4	20.6		
4	66.7	33.3		66.8	33.2		
				66.6	33.4		
				66.7	33.3		
				66.8	33.2		
				66.8	33.2		
			Avg.	66.8	33.2		

APPENDIX D

GRAPHICAL COMPARISONS OF CALCULATED K-VALUES WITH OBSERVED K-VALUES

Figures 29 through 38 present comparisons of the calculated equilibrium vaporization ratios with the observed equilibrium vaporization ratios as a function of pressure. The experimental or observed K-values, are represented by a solid curve and the calculated values, as presented in Table XXV, are represented by a dashed curve.

Visual inspection of Figures 29 through 38 indicate that the analytical expressions does not adequately represent the phase behavior of methane in enopentane at high temperatures.(see Figure 34.)

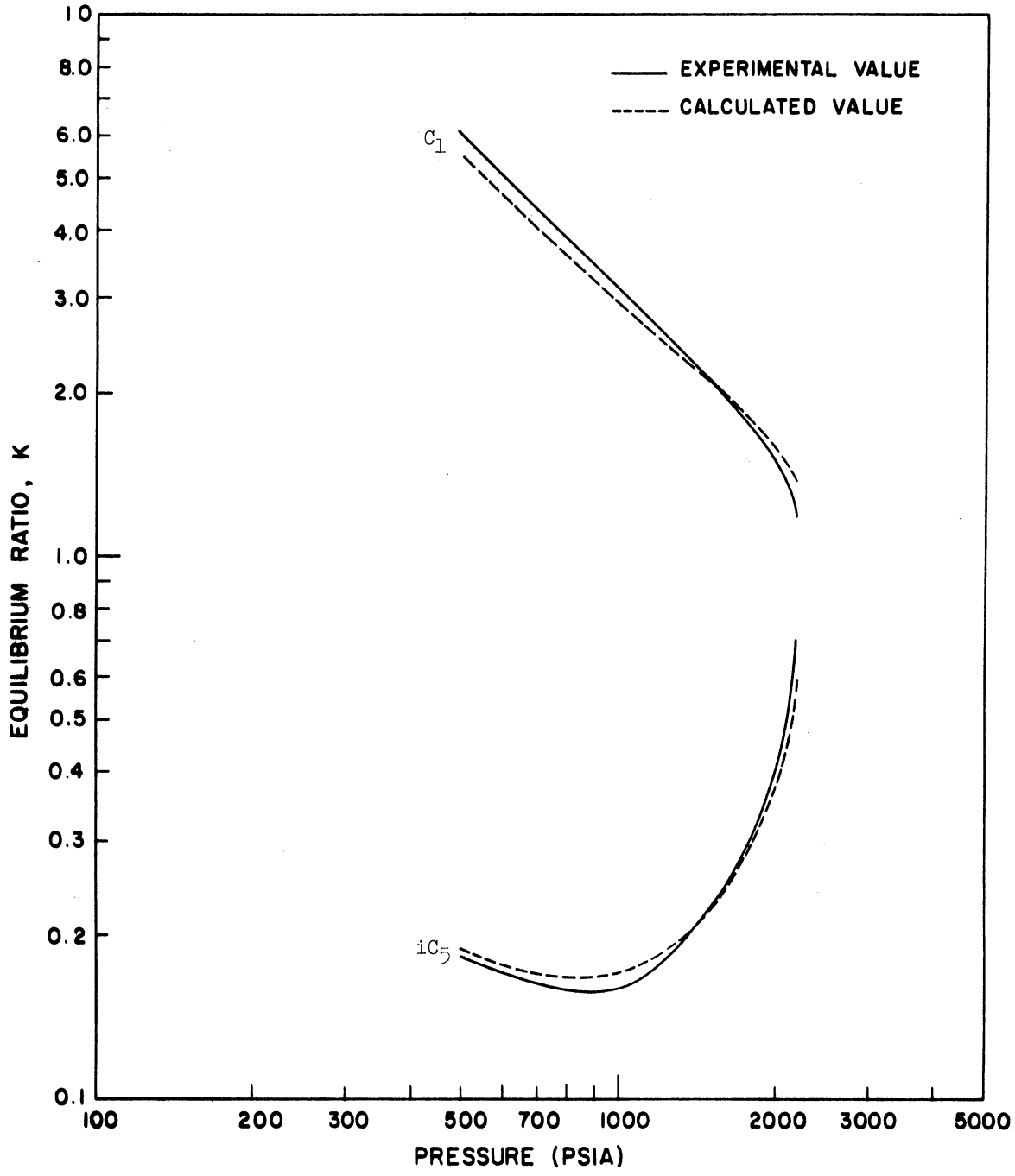

Figure 29. Comparison of Calculated K with Observed K for Methane-Isopentane Binary at 160°F.

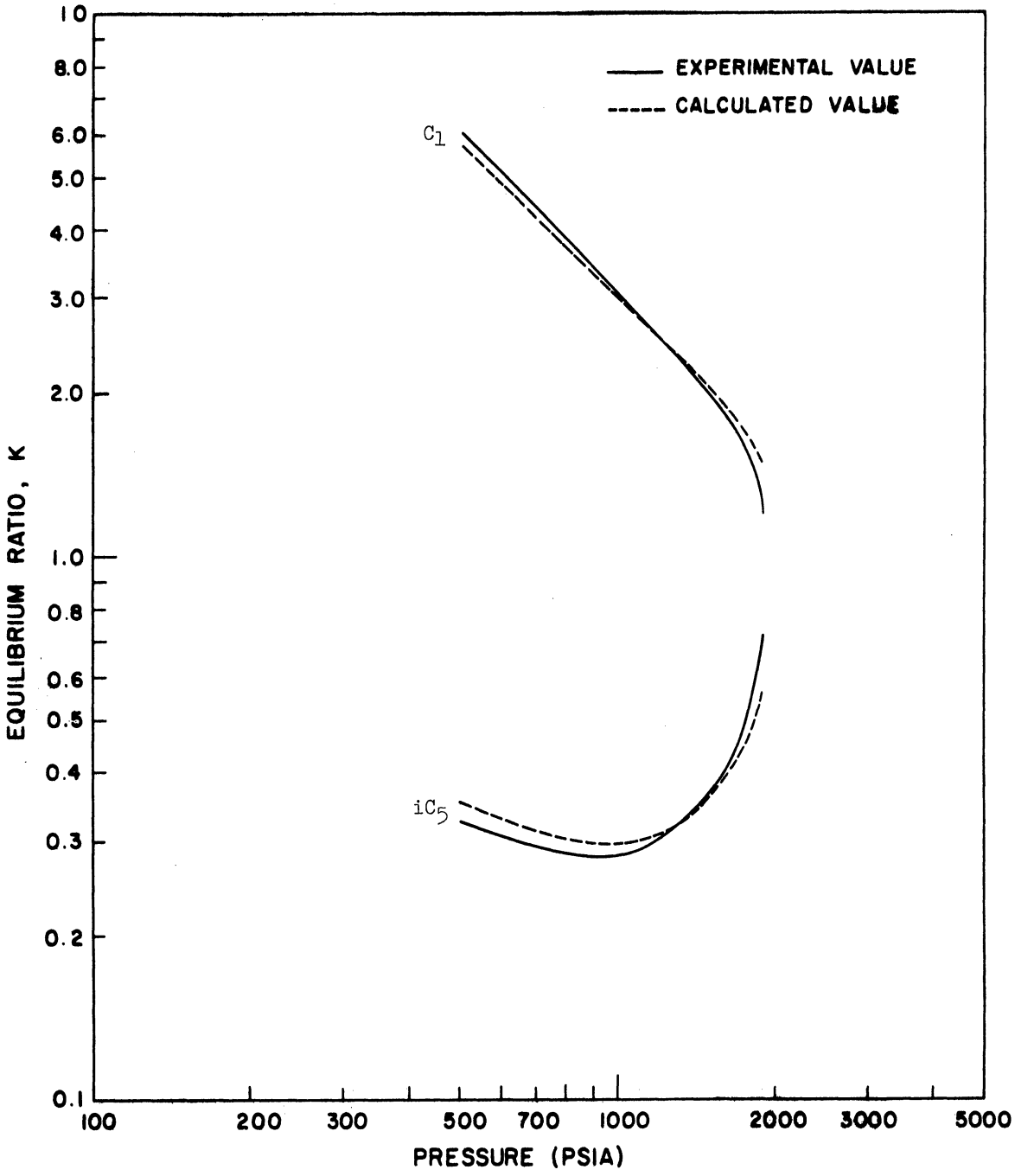

Figure 30. Comparison of Calculated K with Observed K for Methane-Isopentane Binary at 220°F.

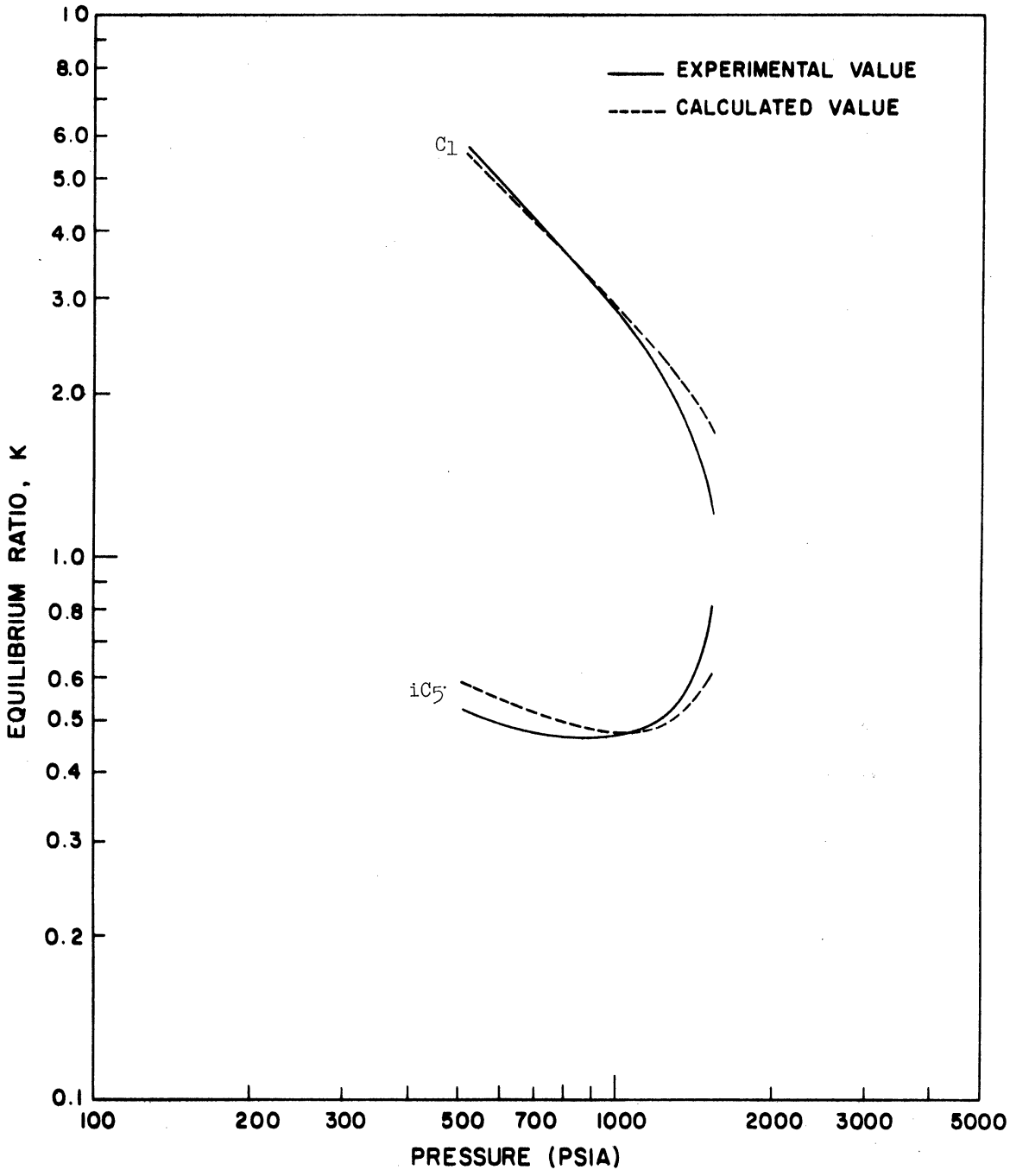

Figure 31. Comparison of Calculated K with Observed K for Methane-Isopentane Binary at 280°F.

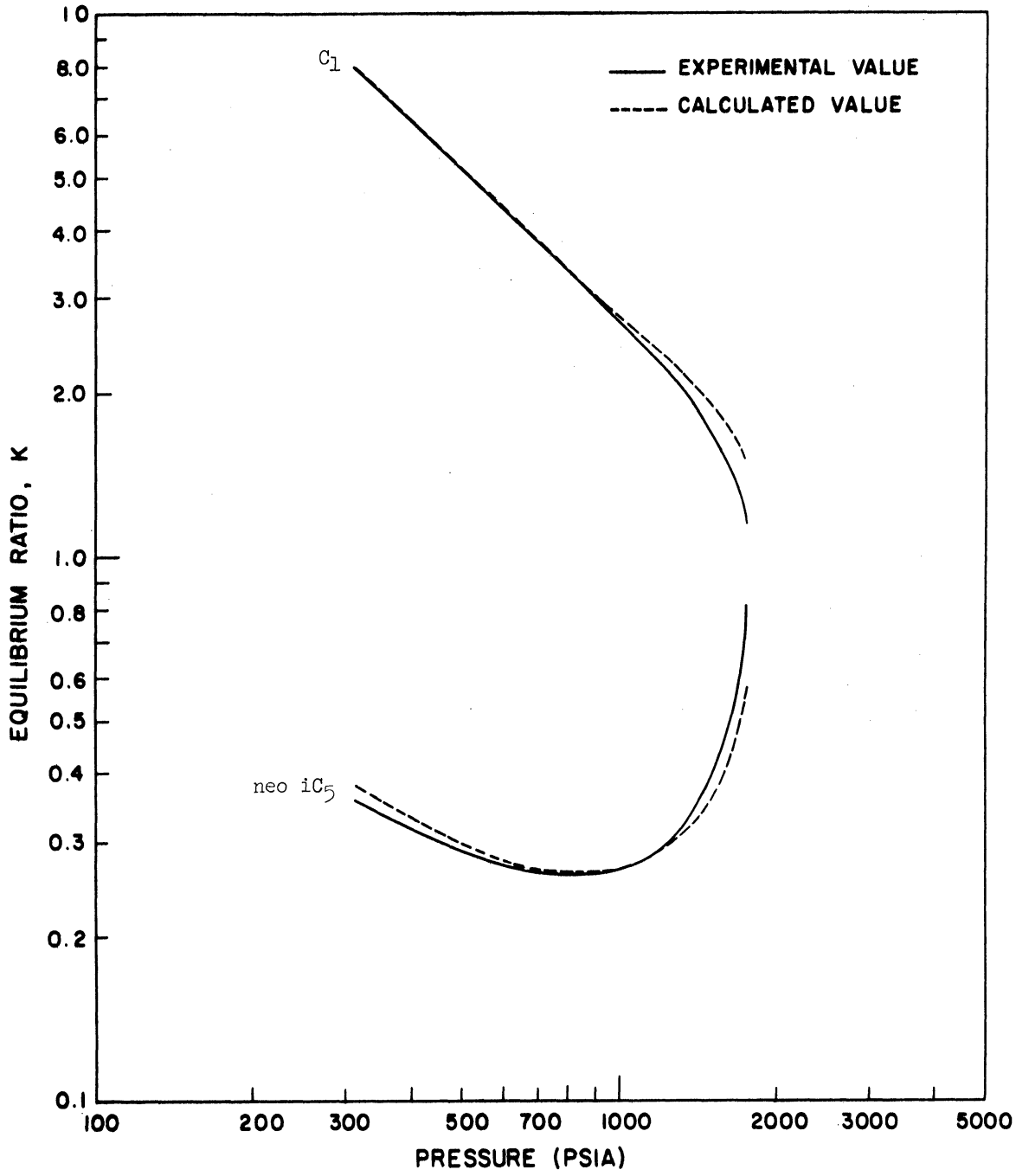

Figure 32. Comparison of Calculated K with Observed K for Methane-Neopentane Binary at 160°F.

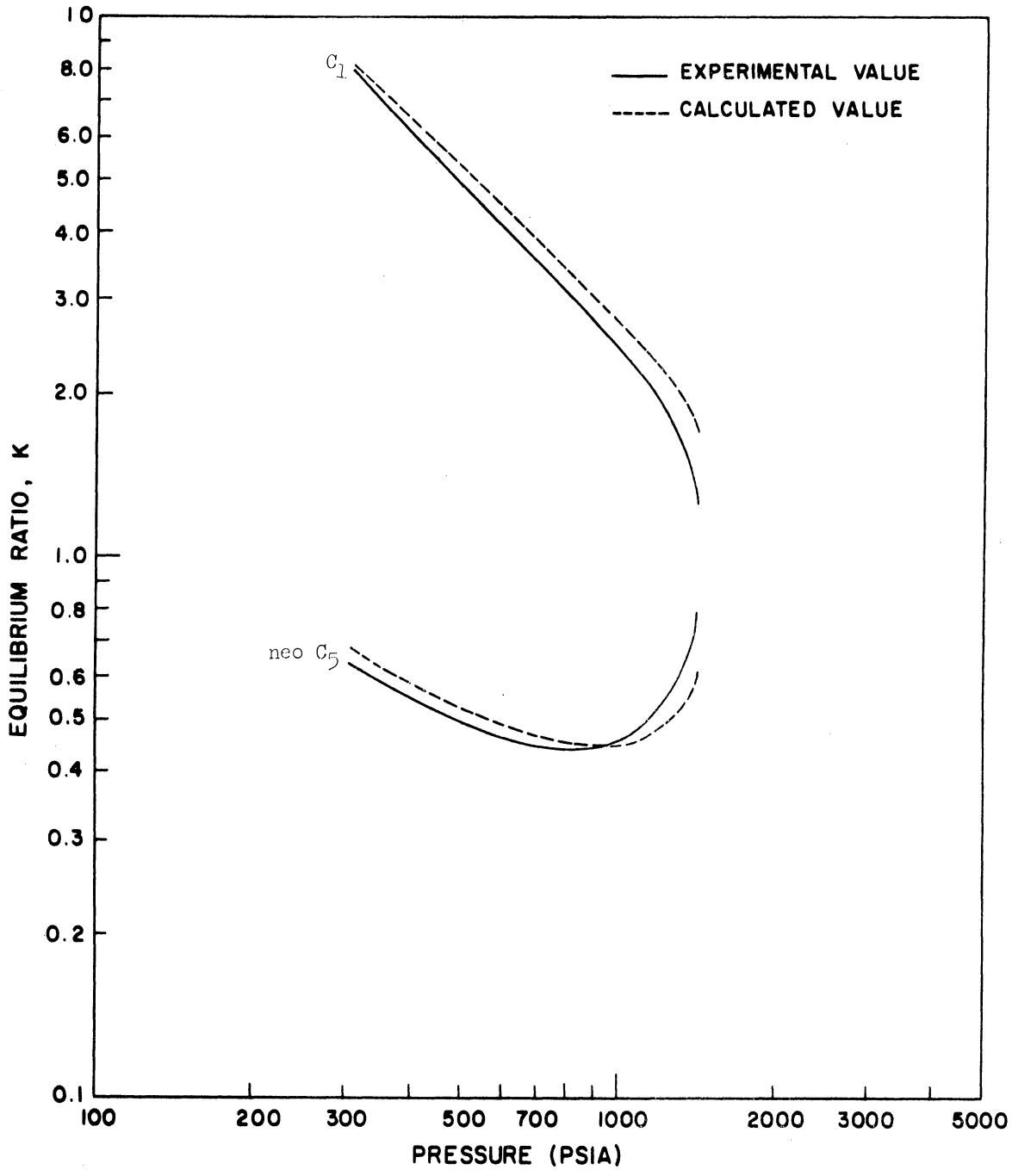

Figure 33. Comparison of Calculated K with Observed K for Methane-Neopentane Binary at 220°F.

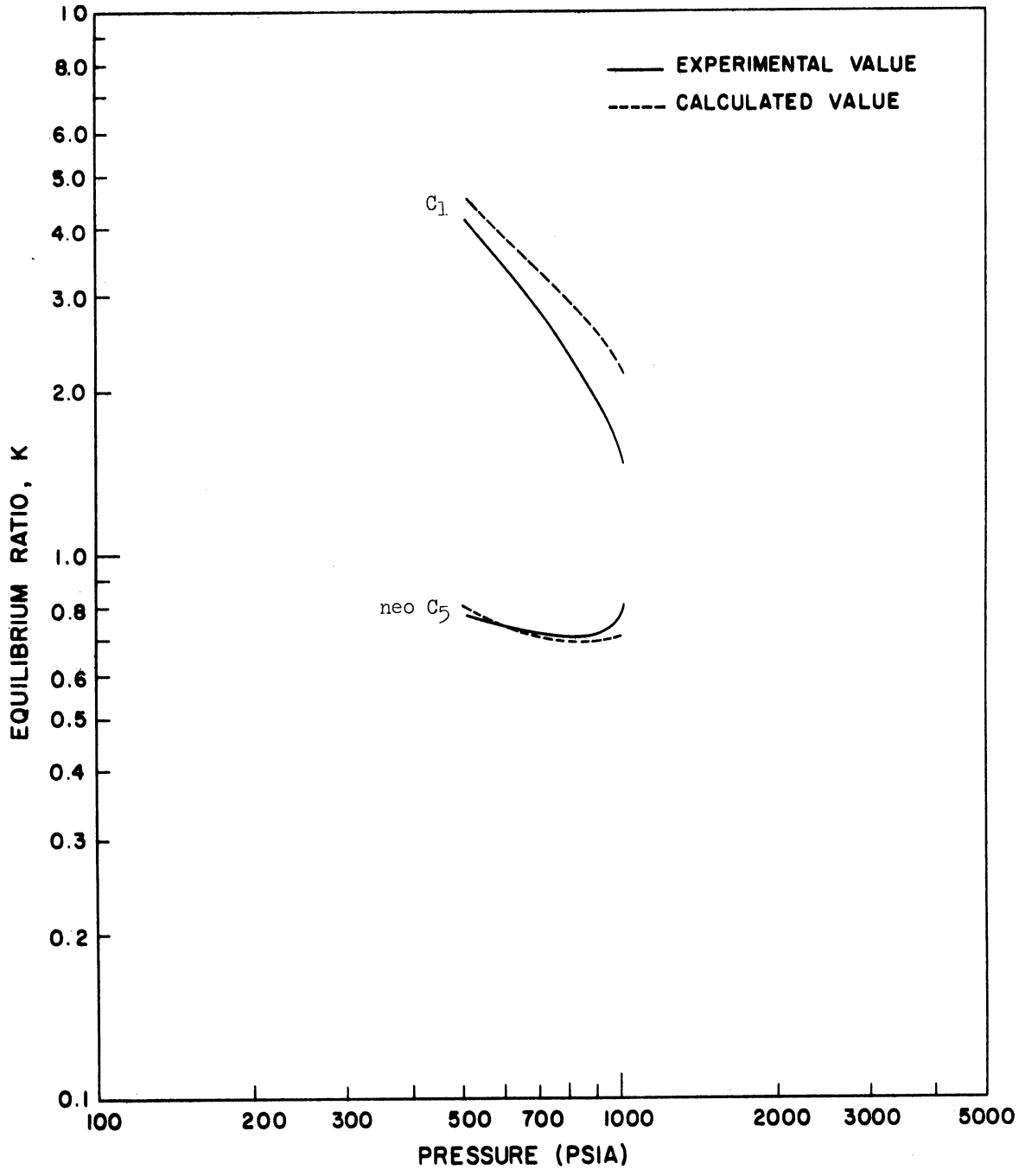

Figure 34. Comparison of Calculated K with Observed K for Methane-Neopentane Binary at 280°F.

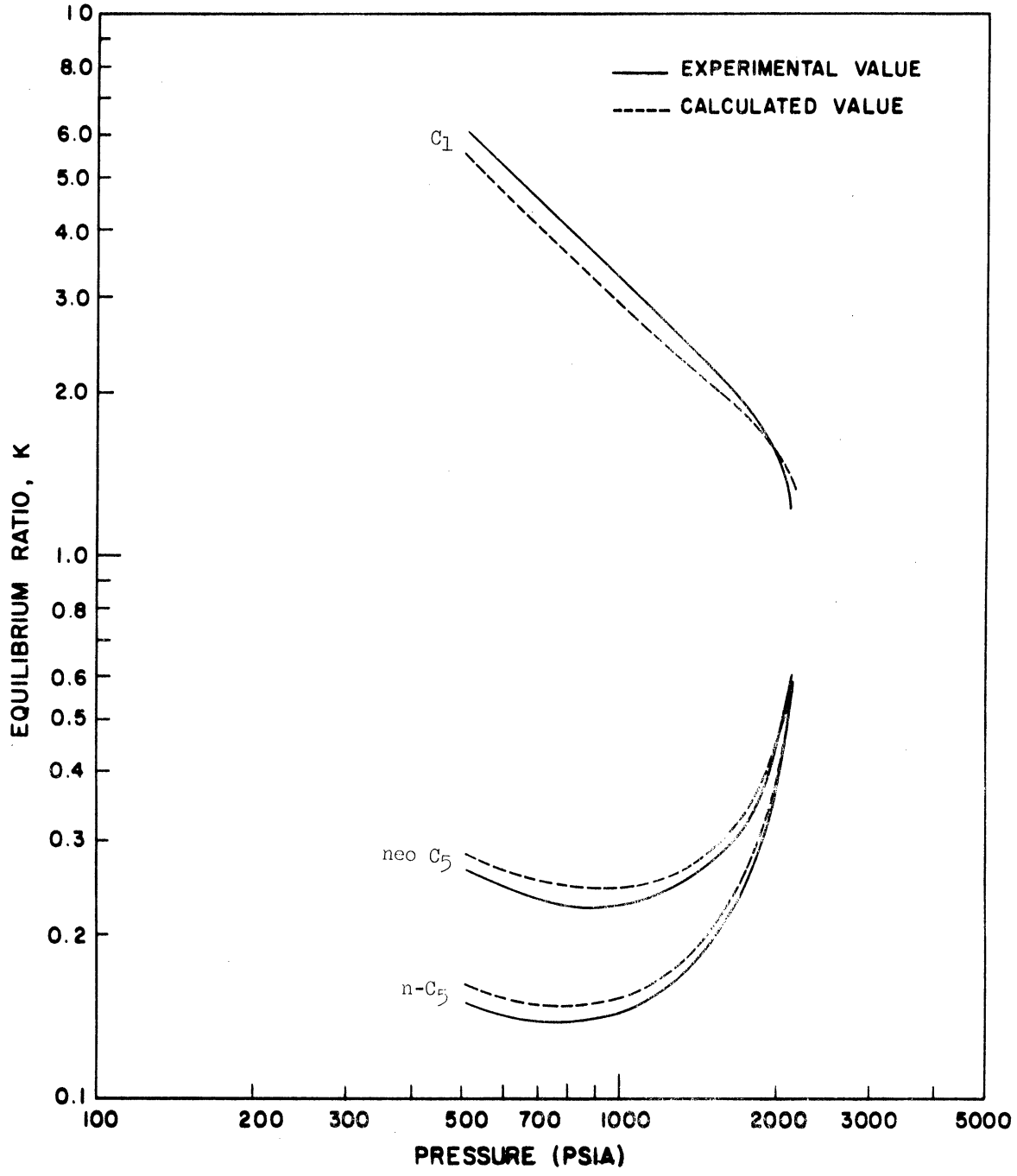

Figure 35. Comparison of Calculated K with Observed K for Methane-Neopentane-Normal Pentane Ternary at 160°F.

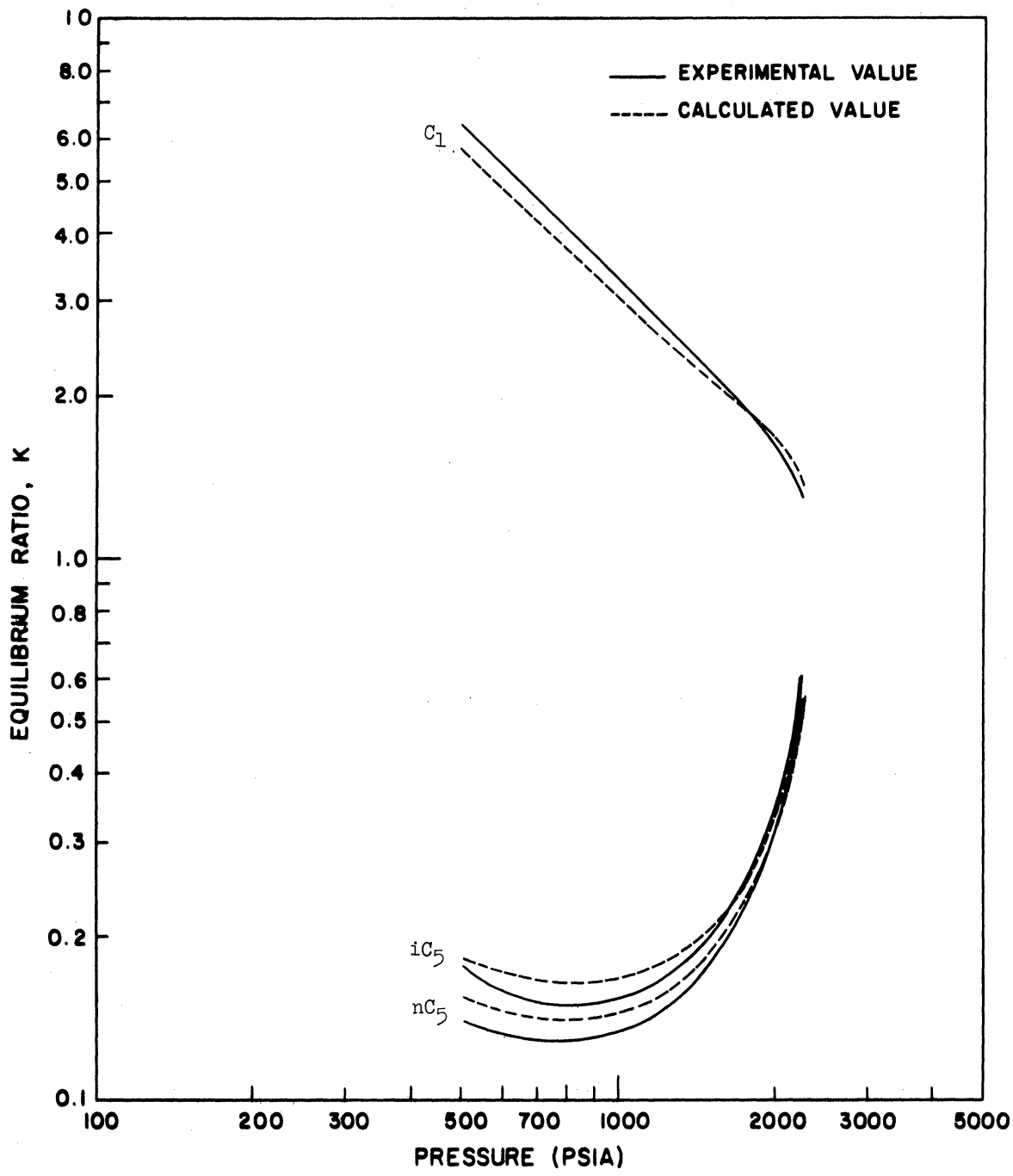

Figure 36. Comparison of Calculated K with Observed K for Methane-Isopentane-Normal Pentane Ternary at 160°F.

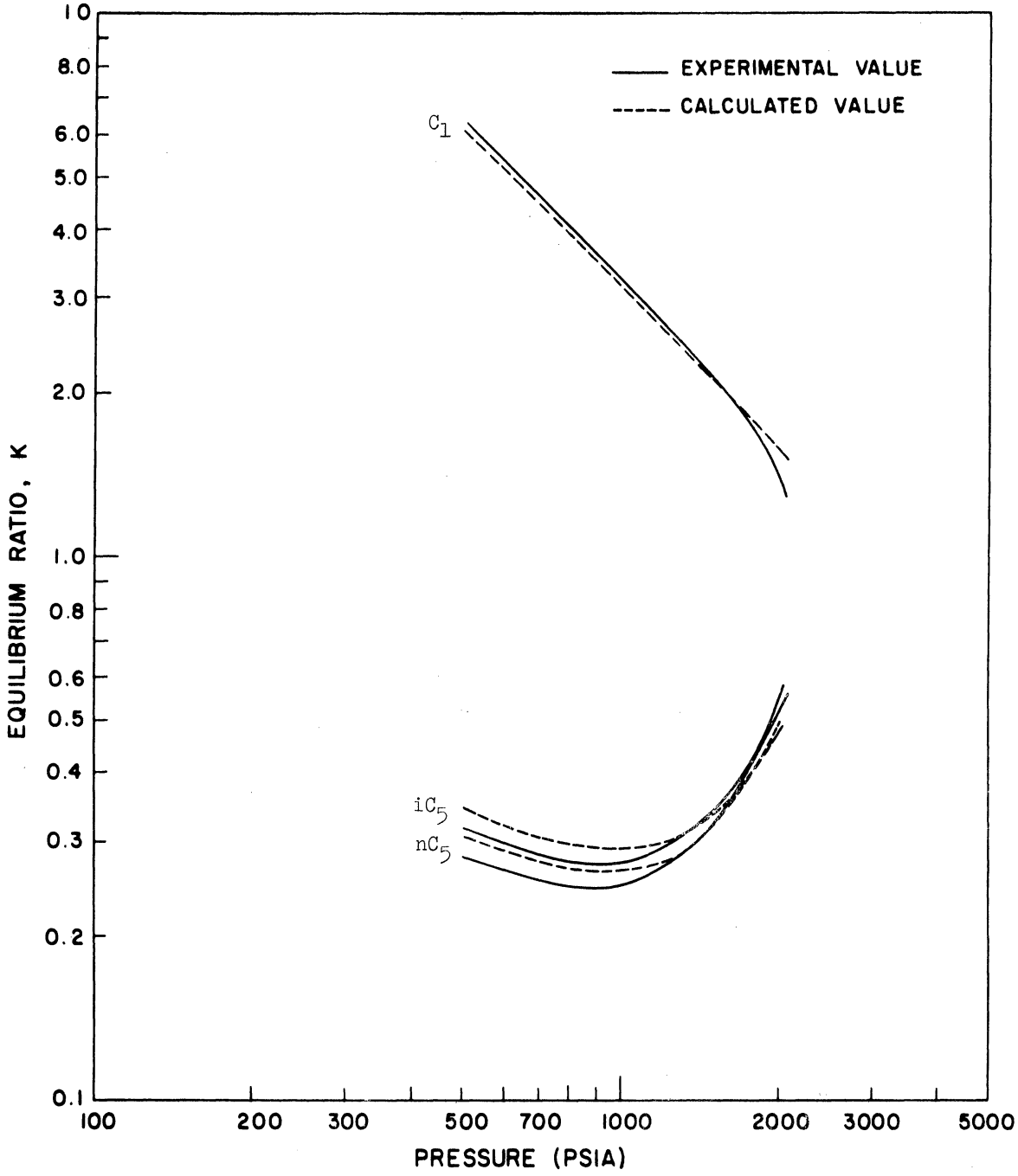

Figure 37. Comparison of Calculated K with Observed K for Methane-Isopentane-Normal Pentane Ternary at 220°F.

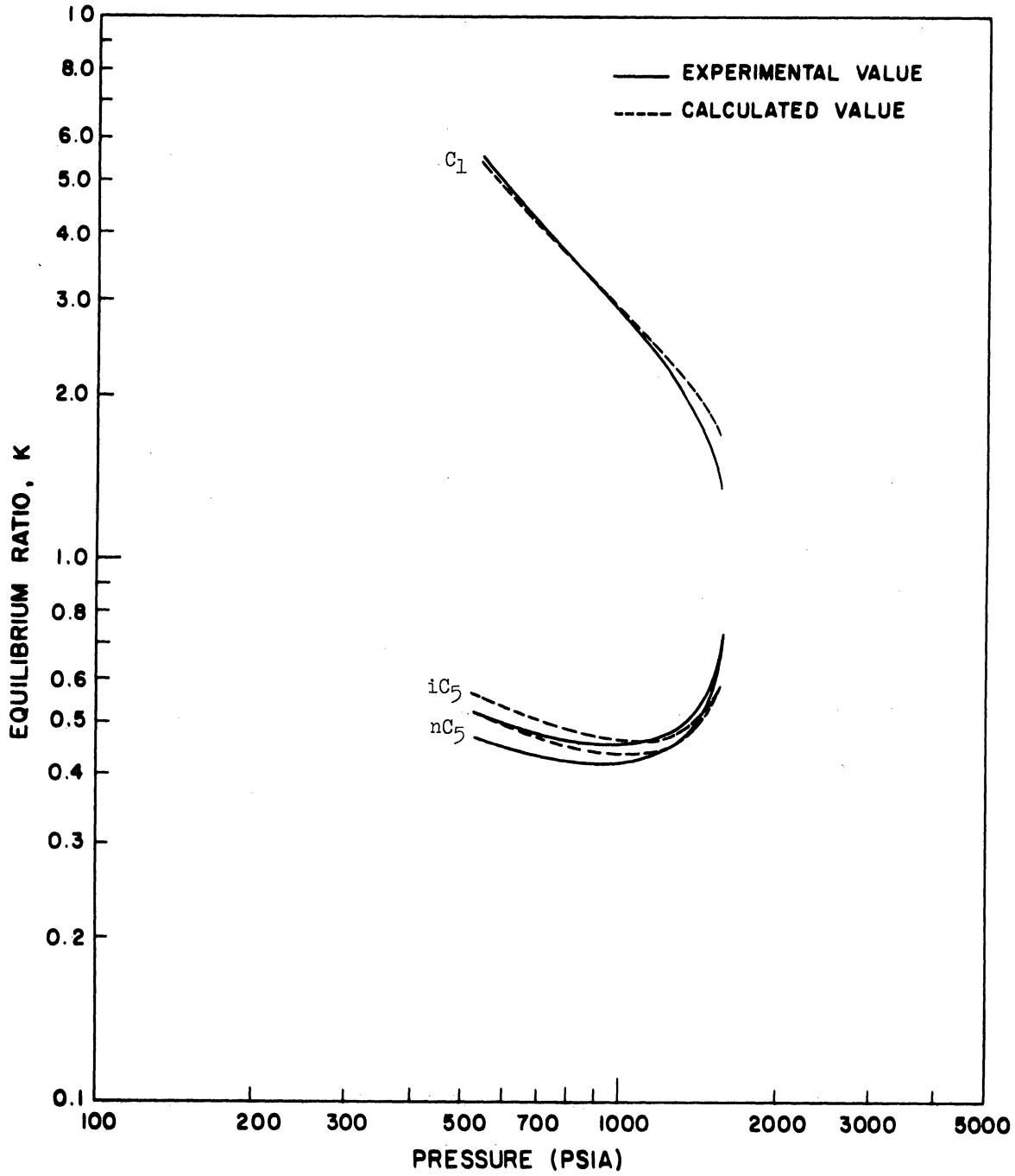

Figure 38. Comparison of Calculated K with Observed K for Methane-Isopentane-Normal Pentane Ternary at 280°F.